Title
Empirical Essays on Natural Resource Exploitation

Author
Englander, Aaron Gabriel

Publication Date
2021

Peer reviewed|Thesis/dissertation

Empirical Essays on Natural Resource Exploitation

by

Aaron Gabriel Englander

A dissertation submitted in partial satisfaction of the

requirements for the degree of

Doctor of Philosophy

in

Agricultural and Resource Economics

in the

Graduate Division

of the

University of California, Berkeley

Committee in charge:

Professor Maximilian Auffhammer, Chair
Professor Solomon Hsiang
Associate Professor Joseph Shapiro

Spring 2021

Empirical Essays on Natural Resource Exploitation

Abstract

Empirical Essays on Natural Resource Exploitation

by

Aaron Gabriel Englander

Doctor of Philosophy in Agricultural and Resource Economics

University of California, Berkeley

Professor Maximilian Auffhammer, Chair

Failures to conserve wildlife do not typically arise from an absence of conservation policies; they occur when existing policies are ineffective. From national laws prohibiting the killing of African elephants to international agreements governing the exploitation of marine animals, behavioral responses and enforcement capacity shape the extent to which conservation policies improve or worsen conservation outcomes. Causal estimates of the effects of conservation policies and their underlying mechanisms are largely unavailable, limiting the extent to which declines in wildlife abundance and biodiversity can be reduced and reversed. In this dissertation, I use causal inference econometrics, high-resolution data, and economic theory to begin to fill this knowledge gap. In its three chapters, I uncover how a conservation policy backfires when it implicitly communicates valuable information to firms, how deterrence is possible even when enforcement is difficult, and how exogenous shocks can increase illegal behavior.

First, I establish that regulations aimed at mitigating common-pool extraction externalities in the world's largest fishery backfire substantially and exacerbate inefficiencies. The most important biological externality in Peru's anchoveta fishery is the harvesting of juvenile anchoveta. To reduce juvenile catch, the regulator temporarily closes areas where the share of juvenile catch is high. By combining administrative microdata with biologically richer data from fishing firms, I isolate variation in closures that is due to the regulator's lower resolution data. I estimate substantial temporal and spatial spillovers from closures. Closures *increase* total juvenile catch by 50% because closure announcements implicitly signal that fishing before, just outside, and after closures is high productivity.

Second, managing global marine resources by assigning property rights could align economic and conservation incentives, but only if unauthorized resource use is deterred. Exclusive Economic Zones (EEZs) are country-level property rights to marine resources, covering approximately 39% of the ocean's surface and accounting for more than 95% of global marine fish catch. However, EEZs might not be respected by unauthorized resource users because

the cost of monitoring and enforcing such large areas may be prohibitive. Here I provide the first evidence that EEZs are in fact respected by unauthorized resource users. Using global, high-resolution fishing effort datasets and the ecologically arbitrary boundaries between EEZs and the high seas, I find that unauthorized foreign fishing is 81% lower just inside EEZs compared to just outside. Consistent with the high cost of enforcing EEZ boundaries, this deterrence effect is concentrated in EEZs that are most valuable near their boundaries. These results suggest that property rights institutions can enable effective governance of global marine resource use.

Finally, poaching is the greatest threat to the survival of elephants and other commercially valuable species. There are many hypothesized drivers of wildlife poaching, but few empirical estimates of their causal effects on poaching levels. In this paper, I provide the first causal estimates of a spatially-varying driver of wildlife poaching. Using elephant poaching and armed conflict data spanning 13 years and 77 sites in 39 countries across Africa and Asia, I find that the onset of a new conflict near elephant populations significantly increases contemporaneous elephant poaching levels by 12-22%. I leverage a variety of econometric methods to show that these estimates are plausibly causal and robust to alternative specifications and different measures of conflict and poaching. I estimate that conflict accounts for the illegal killing of 80,000 elephants between 2002 and 2014. To protect elephants, governments and NGOs should increase support to affected areas when conflicts begin.

Contents

List of Figures

List of Tables

Acknowledgments

Peter Berck was my first dissertation chair. He was the first person to believe in me as a researcher and he always made time for me when I needed him. Maximilian Auffhammer volunteered to become my dissertation chair when Peter died in 2018, which allowed me to grieve for Peter without worrying about how his death would affect my career. Max is my model for how I want to treat people in my professional life. He always gave me constructive and actionable advice, and his consistent encouragement made me leave his office feeling happier than when I entered. Max taught me how to write an economics paper.

Solomon Hsiang was an intense and sincere advisor who pushed me to brainstorm new research questions and to interrogate the choices I made in my research projects. Sol taught me how to write a paper for a scientific journal. James Sallee listened, understood, and offered insightful feedback the first time he heard a new idea. Reed Walker taught me the strategic aspects of research and proved that it is possible to be both an academic researcher and an organized person. Dale Squires was an energetic and generous mentor, who shared fisheries knowledge, professional contacts, and funding opportunities with me.

Larry Karp, Elisabeth Sadoulet, Michael Anderson, and Sofia Villas-Boas also had significant impacts on my development as a researcher. Carmen Karahalios and Diana Lazo helped me navigate Berkeley's fearsome bureaucracy.

The support and friendship of my wife, Paula Ochiel, and my ARE cohort-mates are why these six years at Berkeley have been such happy ones. The generosity of my grandmother, Harriet Englander, freed me from financial stress.

My parents, Hayley and Shepard Englander, taught me to love learning. They read to me at night, helped me with my homework, and pushed me to take challenging classes. I am incredibly fortunate to be their son.

I acknowledge generous financial support from the Giannini Foundation, the National Science Foundation, and NOAA grant No. NA18OAR4170326, California Sea Grant College Program Project No. E/MRE-9.

Chapter 1

Information and spillovers from targeting policy in Peru's anchoveta fishery

1.1 Introduction

Managing common-pool resource extraction is complicated because extraction causes multiple externalities (Smith, 1969). The most well-known is the stock externality: extraction by one agent harms other agents by reducing the amount of resource available to them (Gordon, 1954). Some regulators have been able to mitigate this market failure by setting a cap on total extraction and assigning quasi-property rights to the resource by dividing the cap among agents (Costello et al., 2008; Isaksen & Richter, 2019). But there are many other production externalities that property rights-like instruments do not address, including externalities related to the timing of extraction, the location of extraction, and biological and environmental characteristics of the resource (Smith, 2012).

I study the effects of a policy that is targeted to reduce the most important biological externality in the world's largest fishery: the capture of juvenile anchoveta in Peru (Paredes, 2014; Salvatteci & Mendo, 2005). I find that the policy reduces juvenile catch in the areas and time periods to which it applies (direct effect). But the policy also has the unintended consequence of increasing juvenile catch in nearby areas and during time periods in which the policy does not apply. These spatial and temporal spillovers more than offset the direct effect of the policy. The policy backfires, *increasing* juvenile catch by 50% on net, because the policy implicitly reveals that nearby areas and time periods are high-productivity fishing grounds. These information spillovers are valuable because finding quality fishing locations is a key challenge for fishermen (Asriyan et al., 2017; Joo et al., 2015).

Peru's anchoveta fishery is the world's largest, accounting for 8% of global marine fish catch, and it contributes nearly $2 billion dollars in export revenues for Peru each year (FAO, 2018; PRODUCE, 2018a). The regulator restricts fishing to allow the anchoveta stock to

grow quickly, enabling large, sustainable harvests (Pikitch et al., 2012). One important variable for the growth of the anchoveta stock is the level of juvenile catch. Catching juvenile anchoveta reduces the future anchoveta stock more than catching adult anchoveta, in part because juveniles have lower reproductive capacity than adults (Salvatteci & Mendo, 2005). Fishermen do not account for this biological externality because they are paid according to the tons they catch and the international price of fishmeal, not the composition of juveniles and adults they catch (Fréon et al., 2014; Hansman et al., 2020; SUPNEP, 2017). Taxing juvenile catch is the first-best solution, but the fishing industry opposes such a policy (Instituto Humboldt et al., 2018). Instead, the regulator attempts to reduce juvenile catch by implementing temporary spatial closures in areas where it believes juveniles are abundant.

I analyze the regulator's temporary spatial closures policy in this paper, accounting for other regulations that also affect fishing behavior. I use administrative microdata and data from fishing firms, which together contain the location, time, and number of juvenile anchoveta each vessel catches each time it sets its net in the water. These data comprise hundreds of thousands of vessel-level fishing operations. Fishermen report the percentage juvenile they catch to the regulator in real-time.[1] When percentage juvenile values in an area are high, the regulator temporarily bans fishing in that area for three to five days. Fishermen are not allowed to fish inside actively closed areas. But they are allowed to fish inside closed areas between the announcement and the beginning of closure periods, just outside closed areas during closure periods, and inside closed areas after the end of closure periods. Between 2017 and 2019, the regulator implemented 410 temporary spatial closures, each covering a different area of ocean and time period.

Due to other regulations in the fishery, reducing search costs is the primary margin by which fishermen can increase profits within a fishing season. Vessels spend more than 20% of their time on fishing trips searching for anchoveta, and fuel comprises one-third of variable costs (Joo et al., 2015; Kroetz et al., 2016). Closures might help fishermen reduce search costs because closures implicitly signal high-productivity fishing locations: the regulator implements closures in response to real-time anchoveta catch data from all vessels, and there is only anchoveta catch in an area if anchoveta are sufficiently abundant. This information is potentially valuable because there is zero anchoveta catch in most areas, but strong correlations in anchoveta catch over time and space.[2] I develop a simple game theoretic model to show that total juvenile catch can increase as a result of the closures policy given two conditions: (1) closures announcements are a sufficiently large positive signal of fishing productivity near closures (before, just outside, and after closures) and (2) productivity and

[1] In my regressions, I correct for misreporting to the regulator by matching fishermen-reported data to percentage juvenile measured by third-party inspectors. Third-party inspector data is not used by the regulator to determine closures.

[2] The daily probability any vessel catches anchoveta in a given .1° grid cell (∼11 by 11 km) during the fishing season is 0.5%. However, conditional on at least one vessel catching anchoveta in a .1° grid cell yesterday, the probability of positive anchoveta catch today in the same grid cell is 31% (temporal correlation). Conditional on at least one vessel catching anchoveta in a .1° grid cell today, the probability of positive anchoveta catch in at least one adjacent grid cell on the same day is 92% (spatial correlation).

relative juvenile abundance near closures are sufficiently high.

Estimating the causal effect of the temporary spatial closures policy requires counterfactual areas and times that could have been closed and are comparable to closures declared by the regulator. To address this challenge, I generate "potential closures" by creating an algorithm that mimics the regulator's closure rule and takes as its input the same data the regulator uses to determine closures. I intersect potential closures with the closures declared by the regulator, yielding treatment units (potential closures that get closed) and control units (potential closures that do not get closed). I estimate whether juvenile catch is different inside treated potential closures compared to control potential closures—the direct effect of the policy—as well as whether juvenile catch is different before, just outside, and after treated potential closures compared to control potential closures—the temporal and spatial spillover effects of the policy.

Treatment variation occurs because the regulator declares closures based on one sample statistic: the percentage juvenile measured by fishermen. I obtained biologically richer data from fishing firms which contains the distributions that percentage juvenile values are drawn from.[3] This data is not available to the regulator when it is making closure decisions. By controlling for this distribution (rather than the percentage juvenile values themselves), the identifying variation comes from comparing potential closures that by chance had higher percentage juvenile draws (so were declared actual closures by the regulator) to potential closures that by chance had lower percentage juvenile draws (so were not declared closures by the regulator). I also flexibly control for location, time, and fishing productivity. Identification occurs from comparing potential closures that are equally desirable fishing locations and contain similar concentrations of juveniles, but which the regulator believes are different because the data available to the regulator are lower resolution.

I test three hypotheses. The first concerns measuring the causal effect of the policy and the second and third relate to testing a potential mechanism. First, do temporary spatial closures reduce total juvenile catch when accounting for temporal spillovers, spatial spillovers, and other regulations that affect fishing? Second, does the policy communicate information about the value of fishing before, just outside, and after closures? Third, does this information mechanism increase spillovers?

To test the first hypothesis I empirically estimate direct, temporal spillover, and spatial spillover effects of the policy. I find that the policy reduces juvenile catch inside closed areas during closure periods (direct effect). But the policy also causes large spillovers that more

[3]To estimate percentage juvenile, fishermen measure the length of 200 anchoveta out of the several million individual anchoveta caught per set of the fishing net (an individual fishing operation). Fishermen record the length distribution of these 200 anchoveta—the number of measured anchoveta in each half-cm length interval—and report this data to their firm but not to the regulator. My regressions control for the average length distribution of the sets that generate each potential closure. Percentage juvenile from each set is one sample statistic from this distribution: the percentage of measured individuals that are less than 12 cm (juveniles are anchoveta less than 12 cm). Each percentage juvenile value reported to the regulator is a "draw" from this distribution because sets that generate the same potential closure are fishing from the same local anchoveta population. I account for misreporting to the regulator or to fishing firms with an additional dataset from third-party inspectors.

than offset the direct effect of the policy. I estimate that the policy increases juvenile catch inside closed areas between the announcement and the beginning of closure periods (temporal spillover), it increases juvenile catch just outside closed areas during closure periods (spatial spillover), and it increases juvenile catch inside closed areas after the end of closure periods (temporal spillover). These areas and time periods are not targeted by the policy; the regulator only intends to change juvenile catch inside closed areas during closure periods. Summing the direct, temporal spillover, and spatial spillover effects, I estimate that the policy increases total juvenile catch by 50% despite a second regulation which sets binding limits on total catch (juveniles and adults). The closures policy backfires—worsening its target outcome on net—because closures cause vessels to reallocate fishing to areas where the share of juveniles is higher.

Second, I posit that closures backfire because they implicitly provide information about the value of fishing near closures. If information is the key mechanism, then it must be the case that fishing near closures is more productive than fishing elsewhere, absent vessels' responses to the information. However, this need not be true in equilibrium because of congestion: the more vessels that fish in the same location, the less each vessel catches per unit of fishing effort (Huang & Smith, 2014; Smith, 1969). I support these predictions from my game theoretic model with the following empirical evidence. I estimate that vessels that fish near *potential* closures (before, just outside, or after potential closures) catch 9% more tons of anchoveta per unit of fishing effort than if they fished elsewhere. However, I also estimate that vessels that fish near *actual* closures declared by the regulator do not catch more tons of anchoveta per unit of fishing effort. Indeed, the policy increases total tons caught near closures by 35%, but this increase is shared across a larger number of vessels and a higher degree of fishing effort (congestion). Together, the result using potential closures suggests that closures do provide valuable information, but the result using actual closures suggests that the *ex post* value of this information is competed away by vessels in the equilibrium. These results illustrate one benefit of the identification strategy in this paper. The component of information that is valuable in closures declared by the regulator is also contained in potential closures; they are both correlated with anchoveta abundance. But because potential closures are unobservable to fishermen, the value of this information cannot be competed away, making it observable econometrically.

Finally, I estimate whether the information provided by closures increases spillovers. If information is a mechanism underlying the policy's spillover effects, then vessels that receive larger information shocks from closure announcements should have larger treatment effects. I test this model prediction by dividing vessels into those that did or did not fish inside a given potential closure the day before closure announcement would occur (if the potential closure is declared an actual closure by the regulator). Juvenile catch increases by 87% for vessels that did not fish inside a given potential closure the day before closure announcement. But for vessels that already had information about the productivity of fishing near a potential closure because they fished there the day before closure announcement, there is no treatment effect. This information mechanism also operates at the firm-level. Among firms that own multiple fishing vessels, the response to closures is driven by vessels in firms with less information

about an area before closure announcement. Juvenile catch increases by 78% for vessels that had no other member of their firm fish inside a given potential closure the day before closure announcement would occur. But for vessels that already had information about the productivity of fishing near a potential closure because a different vessel in their firm fished there the day before closure announcement, the increase in juvenile catch because of the policy is only 19%.

The primary contributions of this paper are to the literature on targeted policies. Because governments have finite capacity to solve market failures, policymakers often attempt to reduce an externality by targeting only the highest marginal damage places, time periods, or firms (Gray & Shimshack, 2011; Greenstone & Jack, 2015). Whether targeted policies succeed in reducing externalities depends on their direct effects on targeted units and their spillover effects on non-targeted units. Previous papers have estimated spatial or temporal spillovers from a targeted policy (in addition to the direct effect), such as spatial spillovers from a hot-spot policing intervention in Colombia (Blattman et al., 2019), temporal spillover from the US Endangered Species Act's critical habitat provision (List et al., 2006), and spatial spillovers from blacklisting high-deforestation municipalities in Brazil (Assunção et al., 2019). However, estimating the total effect of a targeted policy (direct, temporal spillover, and spatial spillover effects) is rare.[4] Additionally, while previous papers have estimated spillovers that partially offset or augment the direct effect of a targeted policy, it is uncommon to find spillovers so large they reverse the sign of the policy's effect. Finally, I provide evidence for an information mechanism underlying the large spillovers I estimate. Because the direction and magnitude of spillovers are context-dependent, identifying the mechanisms through which targeting causes spillovers is necessary for yielding generalizable lessons for targeted policy design (Pfaff & Robalino, 2017).

The information mechanism I uncover in this paper is most similar to the concept of "information spillovers" in financial economics. In Asriyan et al. (2017), information spillovers occur because sellers' private asset values are correlated, so a trade by one agent is a signal of the value of other agents' assets. In this paper, information spillovers occur through the policy, which communicates information about non-targeted units (the value of fishing near closures), which in turn changes the outcomes of non-targeted units. Policy-induced information spillovers likely operate in a range of other contexts as well. For example, rationing the consumption of some goods to reduce stockpiling could increase stockpiling of non-rationed goods if the policy causes consumers to believe shortages of non-rationed goods are more likely (Erdem et al., 2003; Keane & Neal, 2020). Alternatively, targeting infectious disease tests to priority groups could increase social activity and disease transmission among non-targeted people if the policy causes them to lower their subjective probability of infection (Acemoglu et al., 2020). Though policy-induced information spillovers are probably

[4]Estimating direct, temporal spillover, and spatial spillover effects requires substantial treatment variation. Two other papers that estimate these effects are Ladino et al. (2019), which studies Colombia's illegal crop substitution program, and Gibson and Carnovale (2015), which evaluates driver responses to road pricing.

common, I know of no prior research that empirically shows that information spillovers can undermine the intended goals of a second-best externality mitigation policy.

Most economics research on common-pool resources since the seminal works of Gordon (1954) and Scott (1955) has focused on alleviating the stock externality by assigning quasi-property rights to the resource. But rights-based instruments defined in terms of tons, as in Peru and in the vast majority of fisheries with rights-based instruments, do not account for age-specific differences in reproduction, growth, and mortality (Quaas et al., 2013; Smith, 2012). I contribute to the literature on common-pool resource extraction by estimating the extent to which a new type of place-based policy, known as "dynamic ocean management", succeeds in reducing the most important biological externality in the world's largest fishery (Dunn et al., 2016; Hazen et al., 2018).

In Section 1.2 I describe fishermen's economic incentives, the temporary spatial closures policy, and the structure of the anchoveta industry. I present my game theoretic model in Section 1.3, data in Section 1.4, and empirical strategy in Section 1.5. I test my three hypotheses in Sections 1.6, 1.7, and 1.8 and discuss policy alternatives in Section 1.9.

1.2 Institutional context

Fishermen's economic incentives and the temporary spatial closures policy and broader regulatory environment inform my game theoretic model and empirical strategy. This contextual information is also necessary for understanding the data I use and my empirical results.

Globally, capture fisheries generate revenues of $130 billion per year, provide 17% of animal protein directly consumed by humans, and directly employ 40.3 million people (FAO, 2018). Of these, the Peruvian anchoveta fishery is the largest, accounting for 8% of tons caught between 2005 and 2016 (FAO, 2018). Peruvian anchoveta (*Engraulis ringens*) are a species of anchovy. 97% of anchoveta tons are processed into fishmeal and fish oil, which are primarily used for aquaculture and livestock feed (PRODUCE, 2018a). There are two Peruvian anchoveta stocks (populations): the North-Central stock, which occurs entirely within Peruvian jurisdiction, and the Southern stock, which is shared with Chile. I limit my analysis to the North-Central stock, which accounts for 95% of tons landed during my study period, the six fishing seasons of 2017, 2018, and 2019. "Landing" refers to the point of landing, when a vessel transfers its catch to a processing plant.

Fishermen incentives

In most industries, firms choose output and input quantities to maximize profits. Depending on market structure, firms' choices may also affect output and input prices. In the Peruvian anchoveta fishery, policy and contracts constrain fishermen's ability to adjust most of these variables. First, as described in the immediately following subsection, individual vessel quotas limit the tons of anchoveta that vessels can land each season. This constraint on output quantity is typically binding. Second, output price is exogenous because fishermen

are paid a fixed percentage of the international price of fishmeal for each ton of anchoveta they land.[5] Individual fishermen or fishing vessels cannot affect the international price of fishmeal. Input prices are also not affected by fishermen's decisions. The price of fuel is exogenous and wages equal a fixed percentage of the international price of fishmeal.

Given these constraints on output quantity, output price, and input prices, input quantities are the main margin fishermen can adjust to increase profits within a fishing season. In particular, fishermen can increase profits by reducing the quantities of labor and fuel they spend searching for anchoveta. Examining the potential effects of temporary spatial closures on search costs can therefore guide predictions of how the policy might change fishermen behavior.

Vessels spend more than 20% of their time on fishing trips searching for anchoveta; fuel comprises about one-third of variable costs; and maintenance is about one-fifth of total costs (Joo et al., 2015; Kroetz et al., 2016). Fishermen who do not pay fuel costs or maintenance costs directly (because they work for a large fishing company) still incur an opportunity cost of their time that could be reduced by finding anchoveta more quickly. Closures might help fishermen reduce search costs because closures implicitly signal high-productivity fishing locations: the regulator implements closures in response to real-time anchoveta catch data from all vessels, and there is only anchoveta catch in an area if anchoveta are sufficiently abundant.[6]

This information is potentially valuable because there is zero anchoveta catch in most areas; the daily probability any vessel catches anchoveta in a given $.1^\circ$ grid cell ($\sim$11 by 11 km) during the fishing season is 0.5%. However, anchoveta catch is highly correlated over time and space. Conditional on at least one vessel catching anchoveta in a $.1^\circ$ grid cell yesterday, the probability of positive anchoveta catch today in the same grid cell is 31% (temporal correlation). Conditional on at least one vessel catching anchoveta in a $.1^\circ$ grid cell today, the probability of positive anchoveta catch in at least one adjacent grid cell on the same day is 92% (spatial correlation).

Fishing near closures (just before, outside, or after closures) could also reduce costs by increasing average tons caught per set of the fishing net (an individual fishing operation).

[5]Fishermen are paid per ton of anchoveta they land. The price per ton is a fixed percentage of the average monthly free-on-board (FOB) price of fishmeal in Hamburg (Fréon et al., 2014). According to a collective bargaining agreement with companies that account for more than 33% of landings, fishermen that land anchoveta that will be processed into fishmeal and fish oil receive 1.792% of the FOB price per ton of anchoveta (SUPNEP, 2017). Under this agreement, crews divide revenue amongst themselves in fixed proportions: the captain receives "two parts" (twice as much as a regular fisherman), the second-in-command and first engineer receive one and a half parts, and regular fishermen recieve one part (SUPNEP, 2017). Interviews and analysis conducted by Hansman et al. (2020) indicate that fishermen not covered by this agreement are also paid a fixed percentage of the FOB price of fishmeal.

[6]There is also a positive correlation between percentage juvenile reported to the regulator and tons caught: a one percentage point increase in percentage juvenile predicts 1.8% more tons caught. While my game theoretic model and main empirical result can accommodate both explanations of why vessels fish more near closures—because of information on anchoveta presence or because high percentage juvenile areas are especially desirable fishing grounds—the results in Section 1.7 support the former explanation.

Tons caught per set is a measure of fishing productivity conditional on finding anchoveta because fishermen only perform a set when they see anchoveta in the water.[7] The average fishing trip lasts 20.3 hours and features 2.2 sets (medians are 17.2 and 2). An increase in tons caught per set would be valuable to fishermen because each set requires about one and a half hours of physically demanding labor and increases the cost of maintaining the net (e.g. by causing wear and tear). Moreover, an increase in tons per set would be indirect evidence that closures reduce search costs. In this case, vessels need fewer sets to reach their quota for the season, which suggests lower time and fuel costs from searching for anchoveta in order to perform sets.

The percentage or number of juveniles that fishermen catch does not affect profits during my study period.[8] Fishermen are paid per ton, not by the composition of juveniles and adults they catch. Moreover, the regulator eliminated penalties for catching juveniles in 2016 (PRODUCE, 2016a).[9] Though juvenile anchoveta are relatively more abundant near closures, as one would expect given that the regulator closes areas where the share of juvenile catch is high, fishermen do not have an economic incentive to avoid catching juvenile anchoveta. If fishing near closures reduces search costs or increases tons caught per set, profit-maximizing fishermen will fish more near closures, potentially increasing total juvenile catch.

Temporary spatial closures and other relevant regulations

The anchoveta fishery is subject to a suite of regulations designed to promote economically profitable and biologically sustainable fishing. For this paper, the three most important regulations are an industry-wide catch limit for each fishing season, individual vessel quotas, and the temporary spatial closures policy.

The regulator (PRODUCE) sets an industry-wide limit on the total tons that can be landed during each fishing season, called the Total Allowable Catch (TAC). Population estimates before the beginning of the fishing season from IMARPE, Peru's marine science agency, guide this decision (IMARPE, 2019). The regulator sets the TAC such that the remaining biomass of adult (sexually mature) anchoveta at the end of the fishing season will exceed 4 to 5 million tons, depending on environmental conditions. The regulator and scientific agency do not want adult biomass to fall below 4 million tons because when this occurred in the past the stock grew more slowly than usual, reducing the tons of anchoveta that could be caught in the next season and in future seasons (Pikitch et al., 2012). While

[7]For example, an executive at a large fishing company told me in an interview that tons per set is the primary performance metric his company uses to evaluate the captains of their fishing vessels.

[8]Very small juveniles can get stuck in the holes in the net, increasing the time fishermen need to spend cleaning the net before they can resume fishing. But these events are rare (Instituto Humboldt et al., 2018).

[9]This regulatory change was motivated by concerns that fishermen were discarding catch with a high percentage of juveniles at sea to avoid being penalized, as well as complaints from the fishing industry that fishermen have limited control over juvenile catch because fishermen cannot predict percentage juvenile before performing a set (Instituto Humboldt et al., 2018; Paredes, 2014). Discarding juveniles is wasteful because juveniles can be processed into fishmeal and fish oil.

TAC prevents biological overexploitation, it does not by itself prevent the dissipation of economic rents if new vessels can enter the fishery, existing vessels can upgrade their capacity, or fishermen "race to fish" before the TAC is reached (Homans & Wilen, 1997, 2005; Huang & Smith, 2014; Reimer & Wilen, 2013; Smith, 1969). There are two fishing seasons per year in the North-Central zone. The first season is typically between April and July and the second season is typically between November and January. The season ends at the scheduled end date or when the TAC is reached, whichever comes first. The season can also be cancelled preemptively due to biological or oceanographic conditions. In the second season of 2017 and 2019, the season was cancelled when only 44% and 36% of the TAC had been reached.[10] In the second season of 2018 and the first season of 2017, 2018, and 2019, tons landed were 99%, 85%, 98%, and 96% of the TAC.

The second important regulation is individual vessel quotas (IVQs). The regulator assigned IVQs in 2009 and they are defined as a percentage of the TAC (Kroetz et al., 2019; Tveteras et al., 2011). Vessels have the same IVQ each season. For example, the IVQ for the vessel with the unique identifier CE-4122-PM is 0.22858% of each season's TAC. In the first season of 2017, when the TAC was 2.8 million tons, this vessel was entitled to land $\backsim$6,400 tons. IVQs are only transferrable within-firm. To transfer an IVQ across firms, the vessel itself must be sold (Natividad, 2016). By limiting entry and reducing the race to fish, the implementation of IVQs in the Peruvian anchoveta fishery increased firms' profits (Kroetz et al., 2019; Natividad, 2016; Tveteras et al., 2011). IVQs belong to a larger class of (property) "rights-based instruments".[11] In addition to improving economic outcomes, rights-based instruments increase biomass (size of a stock in tons) and reduce the probability of fisheries "collapse" (Costello et al., 2008; Costello et al., 2016; Isaksen & Richter, 2019). But rights-based instruments defined in terms of tons, as in Peru and in the vast majority of fisheries with rights-based instruments, do not account for age-specific differences in reproduction, growth, and mortality (Quaas et al., 2013; Smith, 2012).

The third important regulation, temporary spatial closures, attempts to address this age externality. The regulator's goal in implementing temporary spatial closures is to reduce the capture of juvenile anchoveta. The purpose of this paper is to analyze the extent to which temporary spatial closures achieve this objective.

The excess capture of juvenile fish was a leading explanation for decreased catch in many European fisheries in the late 1800s. The debate over the effects of juvenile catch was partly responsible for the beginnings of fish biology research (Smith, 1994, p. 70-76). If fish are not allowed to reach maturity and reproduce, the stock will diminish. Larger fish also tend to be

[10]The second season of 2017 was cancelled because IMARPE detected significant spawning activity (IMARPE, 2018). The second season of 2019 was cancelled because oceanographic conditions led schools of juveniles to inhabit the same areas as schools of adults (PRODUCE, 2020b). The co-occurrence of juveniles and adults led to high rates of juvenile catch because fishermen have limited ability to predict whether anchoveta in the water are juveniles or adults (IMARPE, 2019; Paredes, 2014).

[11]IVQs and other rights-based instruments are not formal property rights because they entitle fishermen to a flow from the resource (e.g., a percentage of the TAC), but do not typically confer ownership of the stock itself (the state retains ownership of the stock) (Reimer & Wilen, 2013)

more valuable. These two consequences of excessive juvenile catch are known as "recruitment overfishing" and "growth overfishing", respectively (Quaas et al., 2013). It is now a common goal of fisheries management to allow most fish in a stock to spawn at least once in their life (Paredes, 2014; Wallace & Fletcher, 1997).

The regulator began implementing temporary spatial closures, called Suspensiones Preventivas, in the first fishing season of 2014.[12] The regulator can temporarily close an area of ocean when the percentage of individuals caught in that area that are juvenile exceeds 10%. The 10% juvenile threshold is not strictly applied in practice; many instances of percentage juvenile greater than 10% do not lead to closures. Juvenile anchoveta are anchoveta smaller than 12 cm. Percentage juvenile therefore refers to the percentage of individual anchoveta that are less than 12 cm long.

Between 2014 and 2016, the data used to determine closures came from third-party inspectors sampling anchoveta at the point of landing. When a vessel landed anchoveta with a high percentage of juveniles, the regulator could determine where the vessel had fished by asking the captain and reviewing the vessel's locations and movement patterns. Each vessel's location, heading, and speed is transmitted live to the regulator through an on-board GPS transponder, referred to as a "vessel monitoring system" (VMS).[13] In the first year of the policy, the regulator was required to announce closures at least 24 hours before the start of closure periods. In August 2015, the announcement period was shortened to its current form (PRODUCE, 2015). Closures that begin at midnight (93% of all closures) must be announced by 3 PM (9 hours in advance). Closures announced between 3 and 6 PM begin at 6 AM the next day (announcement is at least 12 hours in advance).

I analyze the effects of the policy during the six fishing seasons of 2017, 2018, and 2019, when the use of "electronic logbooks" further enhanced the regulator's ability to target high-juvenile areas. Electronic logbooks refer to software fishermen use to record ("log") their catch at sea. Beginning with the first fishing season of 2017, the regulator required vessels to report to the regulator the location, estimated tons caught, and estimated percentage juvenile caught immediately after each set (an individual fishing operation). Since estimating percentage juvenile at point of landing typically measures anchoveta from several sets, hours after they were caught at sea, electronic logbook data are both higher-resolution and timelier. For my empirical analysis, I calculate juvenile catch by matching electronic logbook data with third-party inspector landings data, which preserves the resolution of the electronic logbook data while eliminating the bias that would occur if I only used the fishermen-reported electronic logbook data (Section 1.4).

The regulator determines closures as follows.[14] An official monitors the electronic logbook data in real-time, which appear as points on a digital map. Each point is a set and the color of each point is the set's percentage juvenile value. When the official decides that the

[12]The regulation allowing the regulator to declare temporary spatial closures was published in 2012 (PRODUCE, 2012).

[13]The acronym used in Peru is SISESAT.

[14]The government officials tasked with determining closures demonstrated their process to me in a December 2019 interview in their Lima office.

percentage juvenile values for a group of sets are too high, he selects that group of sets by drawing a rectangle around them with his mouse. Based on the points selected by the official, a computer algorithm calculates the boundary and number of days for the resulting closure. The computer algorithm is not publicly available, but government officials have described it in workshops and personal conversations. Closure area increases in the total tons caught by the group of sets (Instituto Humboldt & SNP, 2017; Instituto Humboldt et al., 2018). Closures last three, four, or five days.[15] Higher percentage juvenile values result in longer closures. The official can make manual adjustments to the closure generated by the computer algorithm, for example to ensure the closure covers all the sets selected by the official (Instituto Humboldt & SNP, 2017; Instituto Humboldt et al., 2018).

Vessels are not allowed to fish inside active closures (inside closed areas during the three-to-five-day closure periods). However, vessels are allowed to fish inside closed areas after the announcement but before the beginning of closure periods, outside closed areas during closure periods, and inside closed areas after the end of closure periods.

The regulator uses real-time VMS data to monitor fishing inside active closures. The regulator defines fishing as moving slower than two knots at a non-constant heading for more than one hour and penalizes vessels that move in this way inside an active closure (PRODUCE, 2016a).[16] VMS transponders can be physically disabled but not manipulated; the transponder is inside a closed, metal box and it transmits data to the regulator automatically every 10 minutes. The vessel owner is penalized if the vessel's transponder does not transmit data to the regulator for more than two hours for any reason (e.g., PRODUCE, 2017b). To the extent that vessels are able to conceal fishing inside active closures, this detection avoidance would accentuate my main result that the policy increases total juvenile catch.

The regulator announces closures on their website and by sending emails and WhatsApp messages to firms (PRODUCE, 2020c). Firms then communicate closures to vessels at sea using radio, and fishermen enter the coordinates of closed areas into their on-board electronic navigation systems. Some fishing companies also monitor the locations of their vessels in relation to active closed areas and call vessels on the radio when they are near an active closure. 43% of closure announcements create multiple closures; the average announcement creates 1.58 closures.

I downloaded all temporary spatial closures announcements from the regulator's website. The regulator declared 410 closures in the North-Central zone during my study period (Figure 1.1). The smallest and largest closures are 170 and 12,512 km^2. The mean and median closures are 1,328 and 1,211 km^2 (about twice as large as New York City). The share of closures that last three, four, and five days is 48%, 15%, and 36%. There are 0.73 active

[15] I estimate the effects of closures declared by the regulator, PRODUCE. The scientific agency, IMARPE, can declare closures of up to 10 days. These closures can apply to all fishing grounds (i.e., Peru's entire Exclusive Economic Zone). IMARPE also has the power to end a fishing season before the scheduled end date and before vessels have reached the TAC.

[16] All fishing in the Peruvian anchoveta fishery is "purse seine fishing", which involves dragging a net in a circle around a group of anchoveta.

Figure 1.1: Temporary spatial closures in the North-Central zone by fishing season

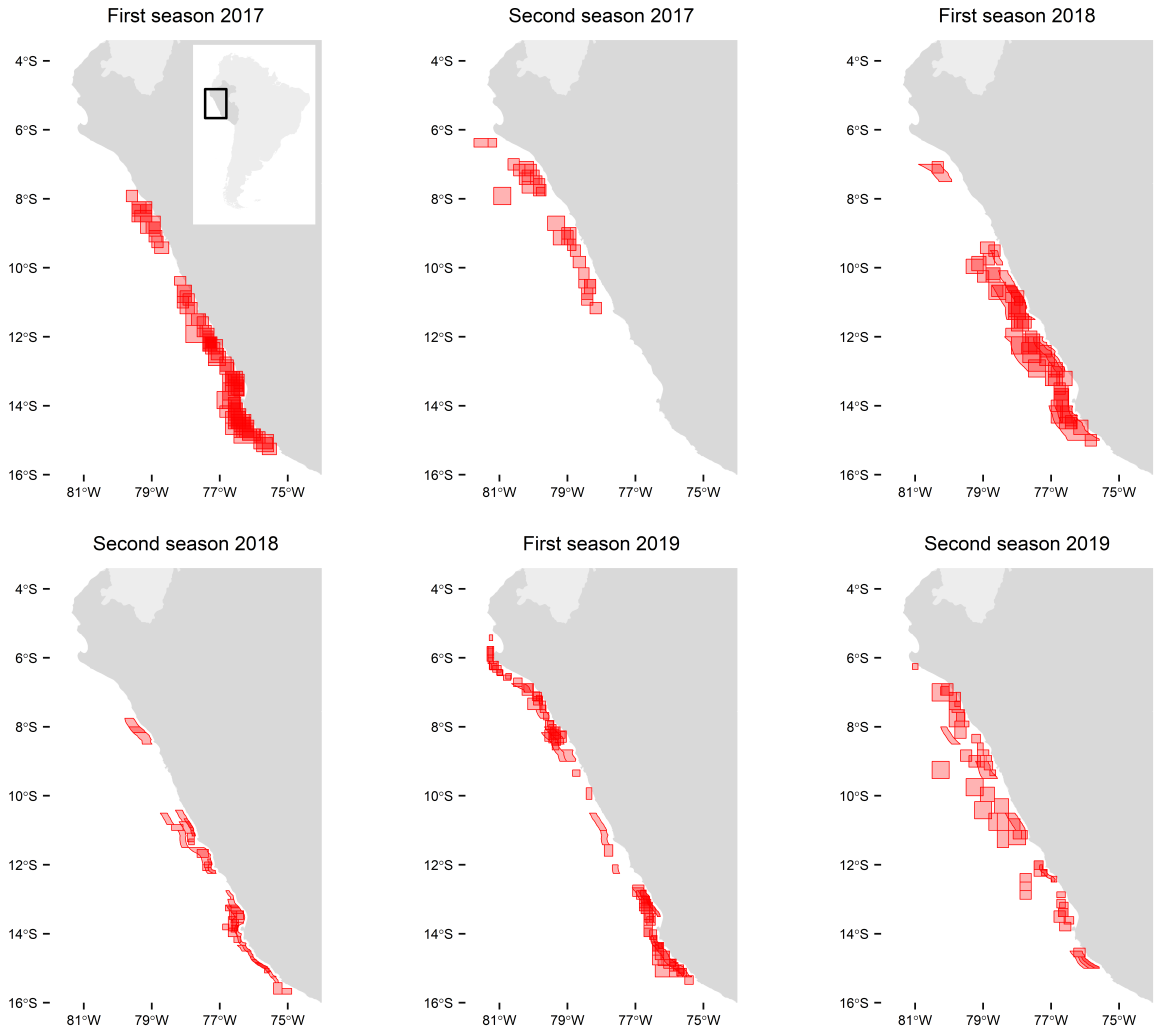

Notes: Each red polygon represents a closure. Closures last three, four, or five days. The average closure is 1,328 km^2. The regulator declared 410 closures in the North-Central zone during the six fishing seasons of 2017, 2018, and 2019. There are 0.73 active closures on an average day during the fishing season. The inset map in the top, left panel shows South America (light grey), Peru (dark grey), and the North-Central zone (black rectangle).

closures on an average day during the fishing season. Closures are spatially correlated: 26% of closures border or intersect a closure created by the regulator's next closure announcement. On average, the minimum distance between closures created by successive announcements is 178 km.

Temporary spatial closures are a type of "dynamic ocean management" in that they vary

over space and time and are updated by the regulator in response to real-time data (Lewison et al., 2015; Maxwell et al., 2015). Dynamic ocean management is different from more traditional management approaches, like marine protected areas, which are time-invariant, and seasonal closures of an entire fishery, which are space-invariant. Dynamic ocean management is designed to reduce fishing in the areas and times where fishing is likely to cause ecologically undesirable outcomes. But it does not need to cover as much space-time as more traditional management approaches because it only targets relevant areas and times. For these reasons, simulations of dynamic ocean management find it can achieve the same ecological objectives as more traditional management approaches at a lower economic cost (Dunn et al., 2016; Hazen et al., 2018). The same win-win idea motivates temporary spatial closures. By allowing fishing to continue in most places, temporary spatial closures could reduce total juvenile catch while minimizing the cost of the policy to fishermen.

Temporary spatial closures could reduce total juvenile catch by causing fishermen to search for new fishing grounds. In this case, closures would reduce total juvenile catch if the share of juveniles is lower in the new fishing grounds. There is substantial variation in relative juvenile abundance across space because schools of fish tend to be age-segregated (i.e., each school of anchoveta contains mostly juveniles or mostly adults).

The fishing industry opposes penalties on juvenile catch because of fishermen's limited ability to predict percentage juvenile before performing a set (Instituto Humboldt et al., 2018). In interviews I conducted in Peru in December 2019, fishing industry employees and stakeholders argued that a tax on juvenile catch would be "unfair" for this reason. Temporary spatial closures do not suffer from this political economy constraint because fishermen are able to entirely control their compliance with closures (Paredes, 2014).

The regulator believes the temporary spatial closures policy reduces total juvenile catch. For example, they calculated that the 174 closures during the first and second season of 2017 and the first season of 2018 protected 1,049,411 tons of juvenile anchoveta (PRODUCE, 2017a, 2018b, 2018c). The regulator does not describe how they calculate this number, nor do they define the meaning of "protected" in this context. The regulator also implements temporary spatial closures to protect juvenile horse mackerel and may expand the policy to cover additional fish species in the future (PRODUCE, 2020a).

Industry structure

There is an average of 730 vessels active each fishing season. IVQs preclude entry of new vessels into the fishery. Vessels are made of steel or wood (40% and 60%). On average, steel vessels are longer than wood vessels (37.5 m compared to 17.5 m), have greater storage capacity (354 m^3 compared to 72.5 m^3), and have more powerful engines (797 horsepower compared to 339 horsepower). Steel vessels also have larger crews than wood vessels (about 20 people compared to 12 people on wood vessels) and are more likely to belong to a firm that owns multiple fishing vessels (92% compared to 41% of wood vessels).

All vessels are privately owned. Seven large firms own at least 19 vessels each, which together account for 60.3% of landings (Table A.4). All seven large firms are vertically

integrated in that they also own fishmeal processing plants (Hansman et al., 2020). 271 vessels are "singletons": they belong to a firm that owns only one vessel. Singleton vessels account for 12.8% of landings. Finally, there are medium firms that each own 2 to 10 vessels. Vessels that belong to medium firms account for 26.8% of landings. The level of market concentration in Peru's anchoveta fishery is similar to other fisheries with rights-based instruments. For example, the top 10 largest firms in Iceland own quotas equal to 50.5% of annual landings (Agnarsson et al., 2016).

1.3 Model

I present a simple game theoretic model to interpret my empirical result that the temporary spatial closures policy increases total juvenile catch. The proposed mechanism is that closure announcements are a positive signal of fishing productivity near closures. This mechanism implies an auxiliary prediction regarding treatment effect heterogeneity, which I also test empirically. Namely, vessels that receive a positive information shock from closure announcements will have larger treatment effects than vessels who already had the signal.

I vessels simultaneously choose where to fish in order to maximize expected profits, which depend on the state variable C.[17] When $C = 0$, there is no closure and vessels choose from two possible fishing locations: g and k. Each vessel i chooses exactly one of the two available fishing locations. When $C = 1$, part of location g is closed to fishing, but $h \subset g$ remains open to fishing (Figure 1.2). Vessels choose whether to fish in h or k when $C = 1$.[18] Location h represents areas and times that are near closures, such as before, just outside, and after closures. I derive testable predictions from this model by comparing outcomes across the two values of the state variable C, such as whether the closures policy reduces total juvenile catch (i.e., whether total juvenile catch is lower when $C = 1$ than when $C = 0$).

Let ℓ denote a generic fishing location. Profit π decreases in the number of other vessels who make the same location choice, $I_{-i,\ell}$, due to congestion (Huang & Smith, 2014; Smith, 1969). Profit increases in the productivity (e.g. tons per set) of the fishing location, which is summarized by the scalar μ_ℓ. Vessels know that draws of μ_ℓ are independent across locations conditional on C. But vessels do not observe the vector of true productivity $\vec{\mu}$ in the possible fishing locations before making their location choice. For the base case suppose that vessels are identical and that they have the same beliefs $\tilde{\vec{\mu}}$ regarding mean productivity of each location (e.g., the value of $\tilde{\mu_k}$ is the same across vessels).

There are two differences when $C = 1$ compared to when $C = 0$. First, the closure announcement is a positive signal to vessels: $\tilde{\mu_h} > \tilde{\mu_g}$. The closure announcement does not change vessels' beliefs regarding mean productivity of location k ($\tilde{\mu}_{k|C=1} = \tilde{\mu}_{k|C=0}$). Second,

[17] This model abstracts away from important institutional details, such as heterogeneity among vessels and dynamic decision-making. Its purpose is to provide a simple, single framework for understanding the three main empirical results of this paper.

[18] Suppose the expected fine from fishing in the closed part of location g is sufficiently large such that expected profit from fishing in h or k is always greater.

Figure 1.2: Illustration of model

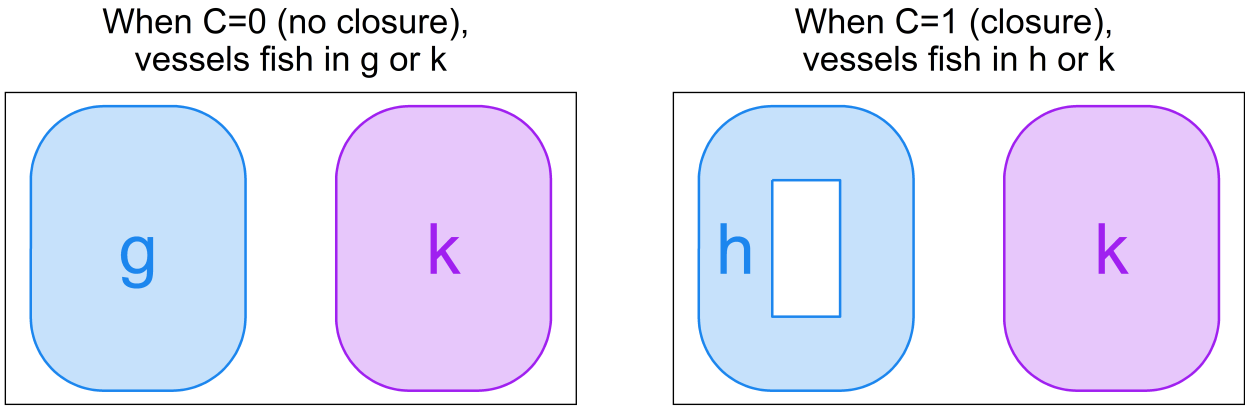

Notes: When $C = 0$ (no closure), vessels choose to fish in location g or in location k. When $C = 1$, part of location g is closed to fishing. Vessels choose to fish in location h (the part of g that remains open to fishing) or in location k.

since location h covers less area than g, marginal congestion costs are higher in h than in g ($|\pi_{i,h}(\cdot)I_{-i,h}| > |\pi_{i,g}(\cdot)I_{-i,g}|$).

When there is no closure, vessel i's objective is

$$\max_{\ell \in \{g,k\}} \quad \mathrm{E}[\pi_{i,\ell}(\mu_\ell, I_{-i,\ell})|\tilde{\mu_g}, \tilde{\mu_k}, C = 0].$$

Vessel i chooses to fish in g if the expected profit from doing so exceeds the expected profit from fishing in k; $\mathrm{E}[\pi_{i,g}(\mu_g, I_{-i,g})|\tilde{\mu_g}, \tilde{\mu_k}, C = 0] > \mathrm{E}[\pi_{i,k}(\mu_k, I_{-i,k})|\tilde{\mu_g}, \tilde{\mu_k}, C = 0]$. When part of location g is closed ($C = 1$), vessels choose between h and k to maximize their expected profit, yielding a similar decision rule. Let I_ℓ denote the number of vessels who choose location ℓ and let $TotJuv(C)$ denote total juvenile catch given the value of C. Suppose total juvenile catch is the product of the number of vessels who fish in each location, productivity, and percentage juvenile, summed over locations.[19] Then $TotJuv(C = 0)$ equals $\gamma(I_g\mu_g\rho_g + I_k\mu_k\rho_k)$ and $TotJuv(C = 1)$ equals $\gamma(I_h\mu_h\rho_h + I_k\mu_k\rho_k)$, where γ is a constant and ρ_ℓ is percentage juvenile.

There exists unique Bayes-Nash equilibria (I_g^*, I_k^*) and (I_h^*, I_k^*) such that:

[19] In reality, I calculate the number of juvenile anchoveta caught by each set in Section 1.4, which forms the main outcome variable of interest in my regressions (Section 1.5).

Proposition 1. If (1) the closure announcement is a sufficiently large positive signal relative to congestion costs and (2) productivity and percentage juvenile are sufficiently high in location h relative to locations g and k, then the closures policy increases total juvenile catch; $TotJuv(C=1) > TotJuv(C=0)$.

Proposition 2a. When there is no closure, the expected profit from fishing in location g equals the expected profit from fishing in location k; $\mathrm{E}[\pi_{i,g}(\mu_g, I_{-i,g})|\tilde{\mu_g}, \tilde{\mu_k}, C=0] = \mathrm{E}[\pi_{i,k}(\mu_k, I_{-i,k})|\tilde{\mu_g}, \tilde{\mu_k}, C=0]\ \forall i$. The same is true when $C=1$; $\mathrm{E}[\pi_{i,h}(\mu_h, I_{-i,h})|\tilde{\mu_h}, \tilde{\mu_k}, C=1] = \mathrm{E}[\pi_{i,k}(\mu_k, I_{-i,k})|\tilde{\mu_h}, \tilde{\mu_k}, C=1]\ \forall i$.

Proposition 2b. However, profit from fishing in g exceeds profit from fishing in k if true, unobservable productivity is higher in g than in k ($\mu_g > \mu_k$) and vessels believe mean productivity is the same in both locations ($\tilde{\mu_g} = \tilde{\mu_k}$); $\pi_{i,g}(\mu_g, I_{-i,g}) > \pi_{i,k}(\mu_k, I_{-i,k})\ \forall i$.

The proofs are in Appendix A.4. Figure 1.3 displays the equilibria when $\mathrm{E}[\pi_{i,\ell}(\mu_\ell, I_{-i,\ell})|\tilde{\vec{\mu}}, C] = \tilde{\mu_\ell} - \alpha_\ell I_{-i,\ell}$, where α_ℓ is the cost to vessel i from one additional vessel fishing in location ℓ. Vessel i's expected profit (y-axis) depends on its choice (lines) and the choices of the other I_{-i} vessels (x-axis). Consider Proposition 2a first. When $C=0$, the equilibrium (I_g^*, I_k^*) is given by the intersection of the two black lines, which represent vessel i's expected profit from fishing in g and expected profit from fishing in k. At this point, no vessel can increase their expected profit by changing their location choice. Similarly, when $C=1$ the equilibrium (I_h^*, I_k^*) is given by the intersection of the red line (expected profit from fishing in location h) and the upward-sloping black line (expected profit from fishing in location k).

Now consider Proposition 1 as illustrated in Figure 1.3. Expected profit from fishing in h has a higher intercept than for g, because the closure announcement is a positive signal of productivity, but it also has a steeper slope, because marginal congestion costs are higher ($\alpha_h > \alpha_g$). Figure 1.3 displays the case where the positive signal is sufficiently large relative to congestion costs, such that more vessels choose to fish in h in equilibrium than in g ($I_h^* > I_g^*$), even though h is a subset of g. In order for this increase in fishing near closures to translate into an increase in total juvenile catch, it must also be the case that productivity and percentage juvenile in h are sufficiently high relative to productivity and percentage juvenile in g and k. Because I is fixed, $I_h^* > I_g^* \Rightarrow I_{k|C=1}^* < I_{k|C=0}^*$. If productivity and percentage juvenile are the same across locations, the closures policy will not increase total juvenile catch because the vessels who switch from k to h catch the same quantity of juveniles in both locations.[20] Whether the temporary spatial closures policy increases total juvenile catch is therefore an empirical question. This outcome is possible, but only if (1) closure announcements are a sufficiently large positive signal relative to congestion costs and (2) productivity and percentage juvenile near closures are sufficiently high.

For Proposition 2b, note that fishing location decisions depend on vessels' beliefs re-

[20] Fixed I in the model is similar to the role that the total allowable catch limit plays in mediating the effect of the closures policy: if the closures policy increases tons caught near closures, then tons caught elsewhere in the same season must fall by an offsetting amount (Section 1.6).

Figure 1.3: Illustration of Propositions 1 and 2a

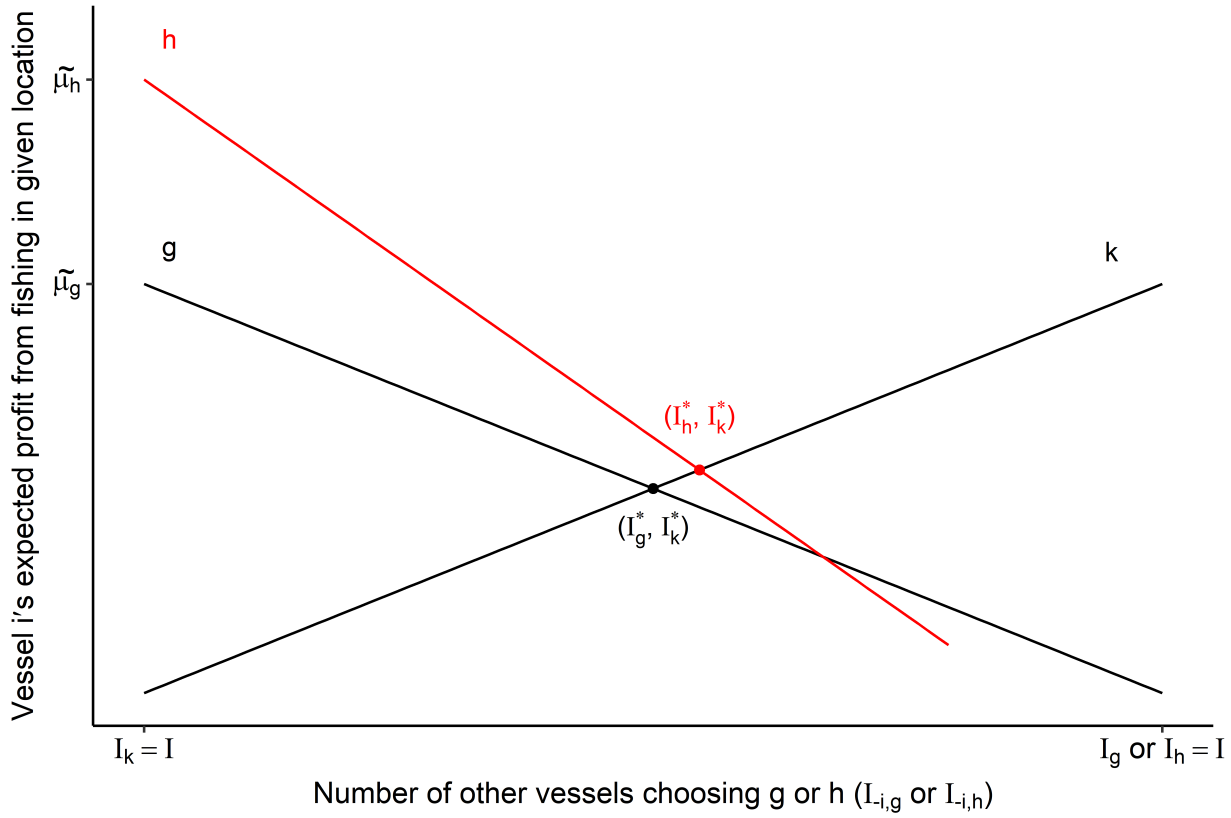

Notes: The y-axis is vessel i's expected profit when $\mathrm{E}[\pi_{i,\ell}(\mu_\ell, I_{-i,\ell})|\tilde{\vec{\mu}}, C] = \tilde{\mu}_\ell - \alpha_\ell I_{-i,\ell}$. The x-axis is the number of other vessels who choose g when $C = 0$ and the number of other vessels who choose h when $C = 1$. The black and red lines indicate vessel i's expected profit from fishing in a given location. The black point is the Nash equilibrium when $C = 0$ and the red point is the Nash equilibrium when $C = 1$. In this parametric example, $I_h^* > I_g^*$ because the closure announcement is a sufficiently large positive signal (difference in intercepts) relative to congestion costs (difference in slopes of lines).

garding mean productivity in each location ($\tilde{\vec{\mu}}$), but not true productivity $\vec{\mu}$ because $\vec{\mu}$ is unobserved. Then $\pi_{i,g}(\mu_g, I_{-i,g}) > \pi_{i,k}(\mu_k, I_{-i,k}) \ \forall i$ because vessels are identical and profit is increasing in true productivity. If the closure announcement contains valuable information in that it informs vessels that the true productivity of g is higher than k, then vessels that happen to fish in g when $C = 0$ have higher profits because there is no closure announcement that vessels can use to change their fishing location decisions.

The information mechanism proposed in this model also implies a prediction regarding treatment effect heterogeneity. Instead of assuming identical vessels, now suppose there are

two types of vessels. When $C = 0$, type a vessels already have the signal regarding location g, but type $-a$ vessels do not: $\tilde{\mu_{g,a}} > \tilde{\mu_{g,-a}}$. When $C = 1$, both types receive the positive signal from the closure announcement, so $\tilde{\mu_{h,a}} = \tilde{\mu_{h,-a}}$. The closures policy treatment effect τ equals $TotJuv(C = 1) - TotJuv(C = 0)$ and the treatment effect as a percentage of the number of type a vessels is $\frac{\tau_a}{I_a}$. Because type $-a$ vessels receive a positive information shock from the closure announcement and type a vessels do not, the percentage treatment effect for type $-a$ vessels will be larger than the percentage treatment effect for type a vessels.

Proposition 3. Consider two types of vessels, indicated by the subscript a. Suppose $\tilde{\mu_{g,a}} > \tilde{\mu_{g,-a}}$ when $C = 0$, $\tilde{\mu_{h,a}} = \tilde{\mu_{h,-a}}$ when $C = 1$, juvenile catch per vessel is higher in location g than in location k ($\mu_g \rho_g > \mu_k \rho_k$), and an interior Bayes-Nash equilibrium when $C = 0$ ($I_g^*, I_k^* > 0$) and when $C = 1$ ($I_h^*, I_k^* > 0$). Then type $-a$ vessels have a larger percentage treatment effect than type a vessels; $\frac{\tau_{-a}}{I_{-a}} > \frac{\tau_a}{I_a}$.

The proof is in Appendix A.4. If some vessels receive a positive information shock from the closure announcement and others do not, total juvenile catch will increase by a larger percentage among vessels that receive the information shock.

1.4 Data

The recent emergence of vessel-level GPS data has enabled researchers to predict when and where vessels are fishing at a global scale (Kroodsma et al., 2018). These new data, made publicly available by the organization Global Fishing Watch, have expanded the set of answerable research questions (Englander, 2019; Sala et al., 2018), but they do not measure the most important outcomes caused by fishing: the quantities and types of fish that vessels catch. As a result of fieldwork I conducted in Peru, I obtained two administrative datasets that contain these variables from Peru's Ministry of Production (PRODUCE) in March 2020. Both datasets contain the tons of anchoveta and the percentage juvenile caught by all vessels in the North-Central zone during the six fishing seasons of 2017, 2018, and 2019. However, they differ in important ways which allow me to accurately calculate the number of juvenile anchoveta each vessel catches each time it sets its net (an individual fishing operation).

The first dataset is *electronic logbook data*. Fishermen report to the regulator when a fishing trip begins, when a fishing trip ends, and the location, time, tons caught, and percentage juvenile caught from each set during a fishing trip. Fishermen record this information on a smartphone or tablet application, which transmits data in real-time to the regulator through the vessel's on-board GPS transponder. Fishermen perform sets once they have located anchoveta in the water. They encircle the anchoveta with a large net (a "purse seine"), close the net, and transfer the anchoveta from the net into the vessel's hold. As fishermen transfer anchoveta from the net into the hold, a trained fisherman estimates the percentage of juveniles by taking three samples using a standardized bucket: once during the first 30% of transference and two more times during the remaining 70% (PRODUCE, 2016b). The fisherman measures each fish in the sample in half-cm intervals, producing data on the length

distribution of anchoveta caught by that set (e.g., 10 individuals between 11 and 11.5 cm, 17 individuals between 11.5 and 12 cm, etc.). Out of the several million individual anchoveta caught in a typical set, approximately 200 are measured. The percentage juvenile for the set is the percentage of measured individuals that are less than 12 cm long. Percentage juvenile is reported to the regulator but the length distribution is not. I obtained a supplementary electronic logbook dataset for a group of vessels that report length distribution data to their owners. These vessels represent 56% of tons landed and I imputed the length distribution for sets by other vessels given sets' location, time, and percentage juvenile (see Appendix A.3).

The second dataset is *landings data*. When vessels finish fishing, they return to shore and transfer ("land") the anchoveta they caught on their trip to a fishmeal and fish oil processing plant. Each time a vessel lands its catch at a processing plant, a third-party inspector measures percentage juvenile and tons landed and reports this data to the regulator. The third-party inspector follows the same procedure described above, taking three samples and measuring approximately 200 individuals in total. The landings data are lower resolution than the electronic logbook data because third-party inspectors measure percentage juvenile from the sum of anchoveta caught by all sets on a fishing trip (average number of sets per trip is 2.2), whereas fishermen measure percentage juvenile after each set in the electronic logbook data. However, unlike fishermen in the electronic logbook data, the closures policy does not give third-party inspectors an incentive to misreport percentage juvenile because the regulator does not use landings data to determine closures during my study period. Third-party inspectors are from one of three international firms and tend to have more rigorous technical training in measurement and sampling than fishermen (PRODUCE, 2018d).

I match sets in the electronic logbook data to landings in the landings data at the vessel-trip level and use the percentage juvenile measured by third-party inspectors and length distribution data to calculate the number of juvenile anchoveta caught by each set in the electronic logbook data (Appendix A.3). I also use the percentage juvenile measured by third-party inspectors to calculate corrected length distribution for each set. If I did not have landings data, I would mismeasure juvenile catch because fishermen seem to underreport percentage juvenile in the electronic logbook data. The weighted average percentage juvenile is 40% lower in the electronic logbook data than in the landings data (11% compared to 18.3%).[21] Fishermen might underreport percentage juvenile to avoid triggering a closure in the area they are fishing.[22] This phenomen also occurs in other settings where agents may be regulated as a consequence of the data they report, such as industrial plants in India and car owners in Mexico (Duflo et al., 2013; Oliva, 2015). Matching the electronic logbook and landings data preserves the resolution of the electronic logbook data while ensuring that the outcome variable in my main regression—juvenile catch at a given location and time—is not systematically manipulated.

[21] Weights are the number of individual anchoveta caught by each set or landed in each landing event.

[22] Closures provide valuable information to fishermen regarding the location of anchoveta, but only to fishermen who did not recently fish in that area (Section 1.8).

Figure 1.4: Electronic logbook data, 2017 to 2019

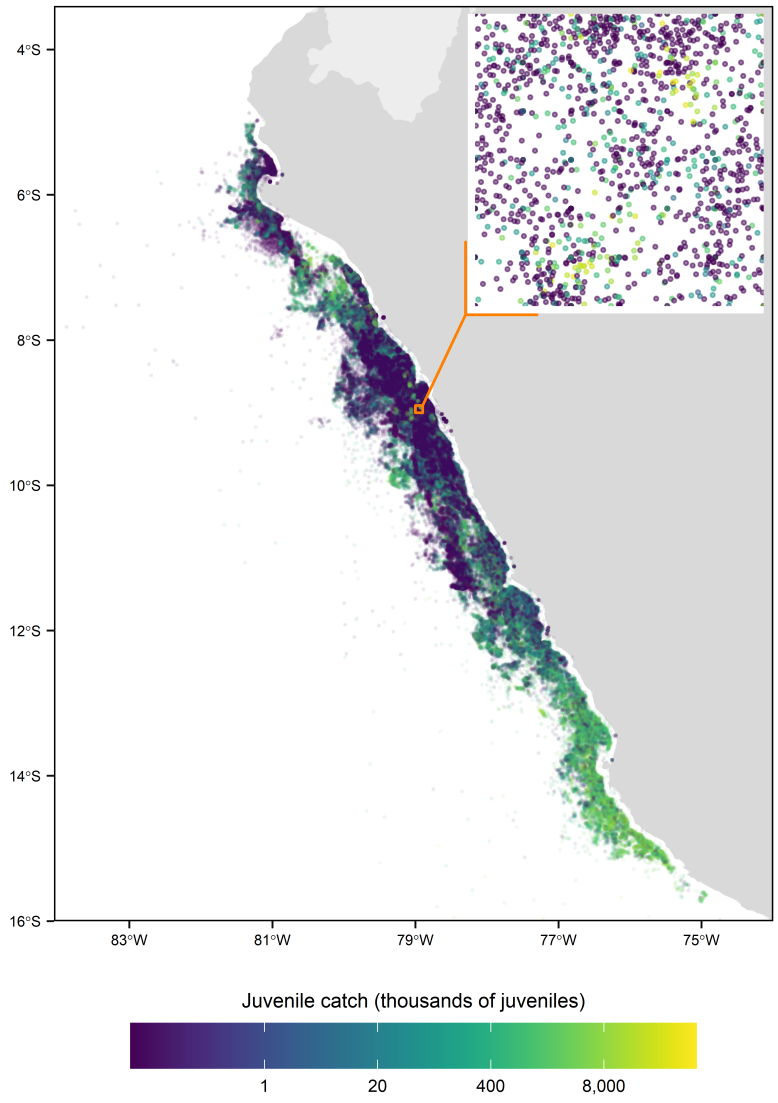

Notes: Each point is a set (vessel-level fishing operation). The color of each point is the number of juvenile anchoveta caught by that set, which I calculate by matching sets to landing events and using the percentage juvenile measured by third-party inspectors at landing. There are 246,914 sets reported by 806 unique vessels in the electronic logbook data. All vessels are prohibited from fishing within 5 nautical miles (9.3 km) of the coast. There are 572 sets per day on average during a fishing season. The average set catches 570,103 juvenile anchoveta. The inset map in the top, right panel magnifies the sets that occur inside the orange rectangle.

There are 246,914 sets reported by 806 unique vessels in the electronic logbook data. 95% of sets occur within 80 km of the coast (Figure 1.4). During a fishing season there are 572 sets per day on average. The average set catches 570,103 juvenile anchoveta and 2,508,788 adult anchoveta, which together weigh 50.2 tons. Fishermen do not underestimate tons caught in the electronic logbook data, perhaps because this variable has little effect on whether a closure is declared (Section 1.2).[23] The median anchoveta caught is between 13 and 13.5 cm long (Figure A.14).

As discussed in Section 1.2, I downloaded all closures announcements from the regulator's website. Closure announcements are pdf documents containing the areas and time periods vessels are not allowed to fish. I geo-coded closure boundaries and recorded the time each closure begins and ends, creating a complete digital record of the 410 temporary spatial closures during my study period. In the next section, I will detail how I use the electronic logbook data to construct "potential closures". I use potential closures to identify the effect of the temporary spatial closures policy on juvenile catch, to test whether the policy implicitly provides valuable information to fishermen, and to estimate whether this information is a mechanism underlying the policy's effects on juvenile catch.

1.5 Empirical strategy

This paper first seeks to quantity the total effect of the temporary spatial closures policy on juvenile catch, including the policy's direct, temporal spillover, and spatial spillover effects. After doing so in Section 1.6, I explore a mechanism underlying the policy's effects in Sections 1.7 and 1.8.

As a consequence of the data processing described in the previous section, I observe juvenile catch inside and near closures declared by the regulator, but I do not observe what juvenile catch would have been in those same places and times in the absence of closures (Holland, 1986). If the regulator randomly assigned closures, I could estimate the effect of the policy by comparing juvenile catch in treated areas to control areas. In reality, the variables that affect the probability of closure—percentage juvenile caught by vessels before closure announcements—are correlated with the main outcome variable of interest—the number of juveniles caught after closure announcements. I solve this causal inference challenge by creating a "potential closures" algorithm that mimics the regulator's closure rule and takes as its input the same data the regulator uses to determine closures. I intersect potential closures with the closures declared by the regulator, yielding treatment units (potential closures that get closed) and control units (potential closures that do not get closed). Potential closures

[23] 8% more tons are reported in the electronic logbook data than are measured at landing. This difference is within the range at which fish can degrade or be lost between being caught at sea and landed (Getu et al., 2015). Fishermen have little incentive to bias their estimates of tons caught in the electronic logbook data. Tons measured at landing, rather than tons estimated by fishermen in the electronic logbook data, are the data used by processing plants to pay fishermen and by the regulator to determine when a vessel has reached its quota for the season.

are the unit of observation. I estimate whether juvenile catch is different inside treated potential closures compared to control potential closures—the direct effect of the policy—as well as whether juvenile catch is different before, just outside, and after treated potential closures compared to control potential closures—the temporal and spatial spillover effects of the policy.

The unconditional difference in juvenile catch from comparing treated potential closures to control potential closures is likely biased upward relative to the causal effect of the policy because potential closures that would have had high juvenile catch independent of treatment are more likely to be treated. For example, pre-period juvenile catch is 26% higher inside treated potential closures compared to control potential closures. As discussed below, I adjust for the systematic differences between treated and control potential closures by including potential closure-level control variables and flexible fixed effects in my regressions, which balance treated and control potential closures on pre-period juvenile catch levels, pre-period juvenile catch trends, and observable measures of fishing productivity. Identification occurs from comparing potential closures that are equally desirable fishing locations and contain similar concentrations of juveniles, but which the regulator believes are different because the data available to the regulator is lower resolution.

I also estimate the effect of the closures policy with a more standard approach, where the unit of observation is a .05° grid cell by three-hour period of time (Appendix A.1). In this model, any .05° grid cell by three-hour period of time has the potential to be treated. The results from this regression using rasterized data display the same pattern of treatment effects as my estimates using potential closures, but potential closures offer three advantages. First, potential closures make the valuable information provided by closures observable econometrically (Section 1.7). In the regression using rasterized data, vessels can compete away the *ex post* value of information provided by public closure announcements. This limitation applies to any estimation approach that does not explicitly include counterfactual closures (areas that could have been but were not declared closures by the regulator). Second, potential closures collapse the data to the policy-relevant unit of observation; the regulator is choosing to close an area of ocean for three to five days, not an individual grid cell. Finally, collapsing the data eases data processing and analysis because the rasterized data contain nearly 100 million observations.

Potential closures

As detailed in Section 1.2, the regulator uses real-time electronic logbook data to determine closures. When a government official wants to create a closure, they draw a rectangle around a group of sets that occurred near each other during the same time period. A computer algorithm then calculates the exact boundaries and number of days the resulting closure will last. The first step of my empirical strategy is to develop an algorithm that mimics the first stage of the closure rule, when the official selects a group of sets (vessel-level fishing observations) on their computer. I cluster sets in the electronic logbook data that occur near each other and record the bounding box around each cluster. The resulting rectangles

are "potential closures". Unlike the regulator, I create potential closures from *every* cluster of sets. I do not attempt to reproduce the second stage of the closure rule, when the computer algorithm determines the exact boundaries and time length of a closure, because this algorithm depends on variables endogenous to my outcome of interest, such as the percentage juvenile values in the cluster of sets reported to the regulator.

First, I use the single-linkage clustering algorithm to group sets that occur within 5 nautical miles of each other on the same day between midnight and 3 PM (R Core Team, 2019). I choose this time period because closures that begin at midnight (91% of closures during my study period) must be announced by 3 PM (9 hours in advance). The remaining 9% of closures begin at 6 AM and must be announced by 6 PM of the previous day. I use a 5 nautical mile threshold in the single-linkage clustering algorithm because the regulator's second-stage algorithm rounds the boundaries of rectangular closures to the nearest 5 nautical mile interval (Instituto Humboldt & SNP, 2017). Then for each cluster containing more than three sets, I draw a rectangle to cover its convex hull (the smallest convex polygon that encloses the cluster), rounded up to the nearest 5 nautical mile interval. I drop all potential closures that are smaller than the smallest closure declared by the regulator that season.

As an illustrative example, Figure 1.5 displays sets from the electronic logbook data in one region of the fishery between midnight and 3 pm on April 28, 2019. The single-linkage clustering algorithm creates two clusters from these sets (Figure 1.5a). Figure 1.5b displays the potential closures that result from these clusters.

I assume all potential closures last for three days, which is the modal length of closures declared by the regulator (the regulator can also declare closures that last four or five days). Since a closure cannot be declared in the same place and time as an already-existing closure, I loop forward in time and subtract areas of potential closures that overlap with already-existing potential closures. I drop potential closures that have become non-convex or smaller than that season's smallest closure after this procedure.

My potential closures algorithm generates 970 potential closures in total, compared to 410 actual closures declared by the regulator during my study period. 89 percent of actual closures have positive overlap with a potential closure (intersect in space at the same time). The average potential closure is smaller than the average actual closure (957 km^2 compared to 1,328 km^2). Figure 1.6 displays the potential closures in each fishing season. My results are robust to a variety of alternative specifications, such as assuming potential closures last for four days instead of three days, assuming potential closures last for five days, and making potential closures 40% larger so that they are the same average size as actual closures (Appendix A.1). My results are also robust to estimating the effect of the policy via synthetic controls, where actual closures (treatment units) are matched to potential closures (control units) (Appendix A.1).

Outcome, treatment, control variables, and identifying variation

The main outcome of interest is juvenile catch inside potential closures. In Figure 1.5, juvenile catch is the number of juvenile anchoveta that are caught inside each blue rectangle

Figure 1.5: Creation of potential closures example

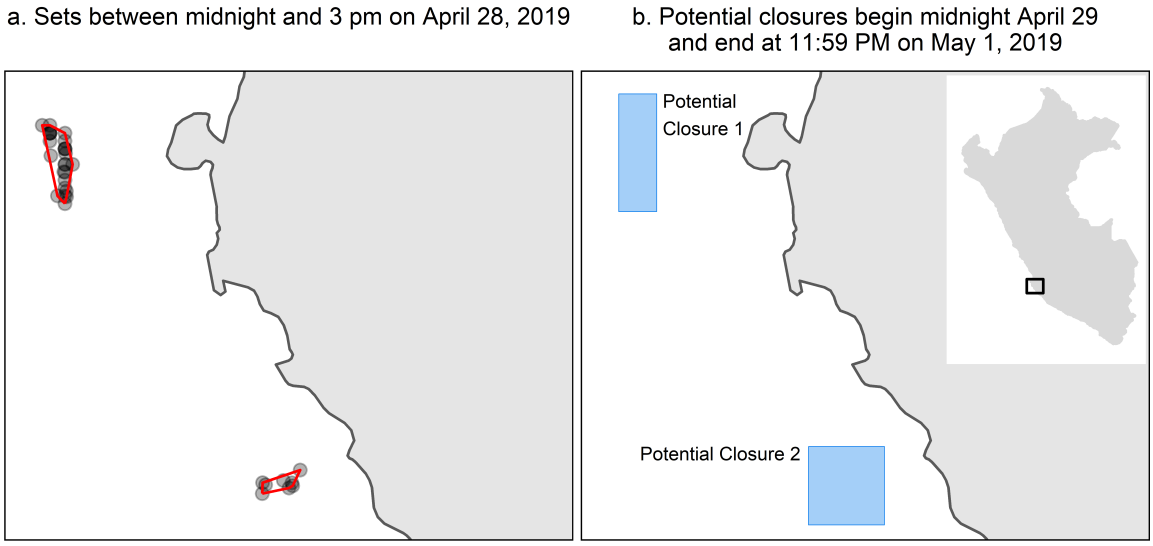

Notes: (a) Sets that occur between midnight and 3 pm on April 28, 2019 in one region of the North-Central zone are displayed as points. The single-linkage clustering algorithm groups these sets into two clusters. The red polygons enclosing each cluster are the clusters' convex hulls. (b) Potential closures are rectangles covering clusters' convex hulls, rounded up to the nearest 5 nautical mile interval. Rectangular closures declared by the regulator are also rounded to the nearest 5 nautical mile interval. These potential closures begin at midnight on April 29, 2019 and last for three days. The inset map in the upper right corner shows Peru (grey) and the region these potential closures occur in (black rectangle).

from midnight on April 29, 2019 until 11:59 PM on May 1, 2019. I filter sets to those that occur inside a potential closure during these three days. Then I sum juvenile catch over sets that occur inside the same potential closure. For example, suppose there are two sets that each catch 1 million juveniles inside Potential Closure 1 between midnight on April 29, 2019 and 11:59 PM on May 1, 2019. Then juvenile catch for Potential Closure 1 is 2 million juveniles. Note that the three days of Potential Closure 1 occur after the sets that generated Potential Closure 1 (midnight to 3 PM on April 28, 2019). They represent the time period that Potential Closure 1 would be closed if the regulator decides to create an actual closure based on the sets that occurred between midnight and 3 PM on April 28, 2019.

I define treatment by the intersection of potential closures with actual closures declared by the regulator. Specifically, I compute the average spatial and temporal overlap between potential closures and actual closures. For example, a potential closure that shares 60% of its area and is active for two of the three same days as an actual closure would have

Figure 1.6: Potential closures in the North-Central zone by fishing season

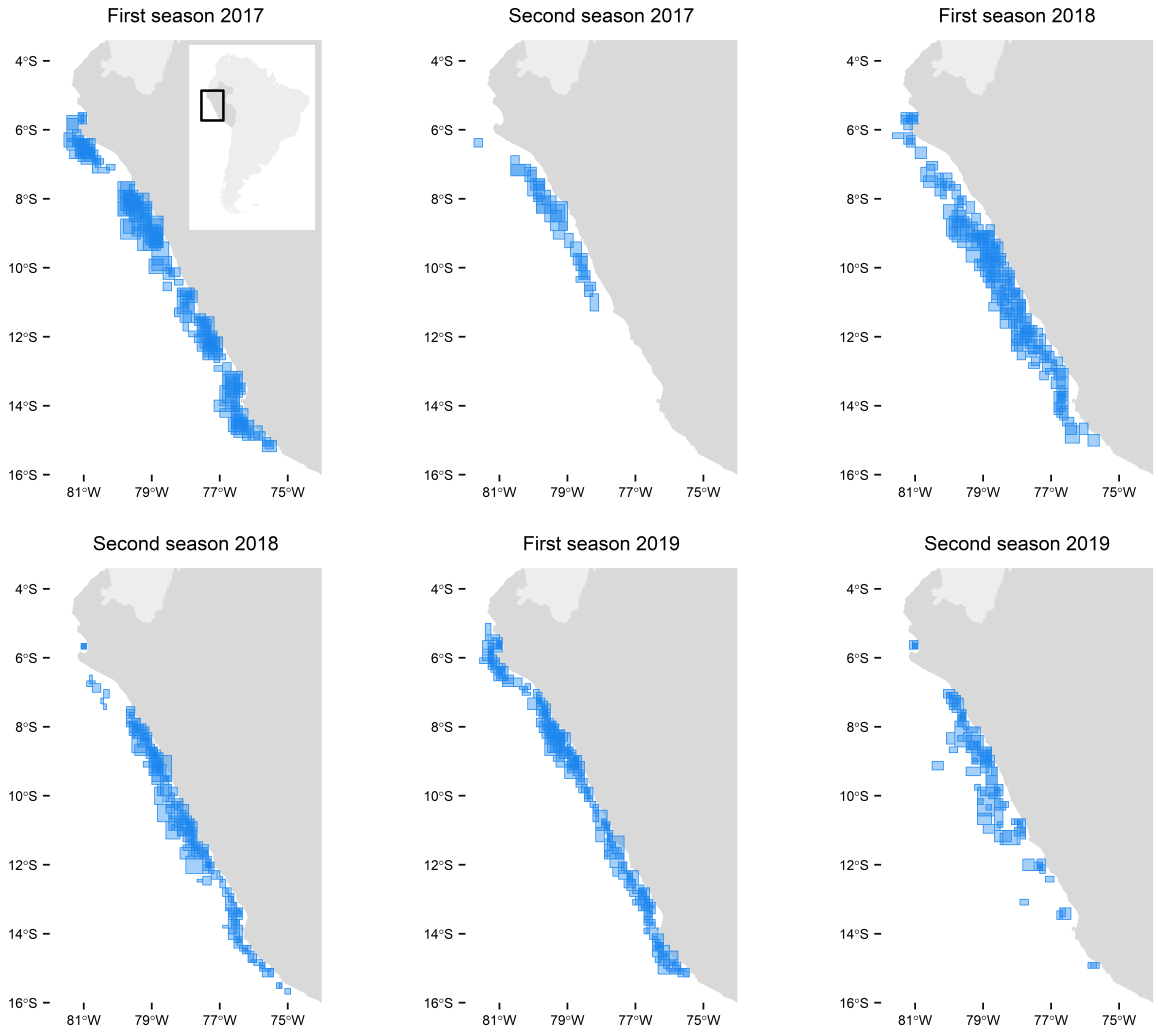

Notes: Blue polygons are potential closures. Potential closures last three days by assumption. The average potential closure is 957 km^2. My potential closures algorithm generates 970 potential closures in the North-Central zone during the six fishing seasons of 2017, 2018, and 2019, compared with 410 actual closures declared by the regulator (Figure 1.1). There are 1.72 active potential closures on an average day during the fishing season. The inset map in the top, left panel shows South America (light grey), Peru (dark grey), and the North-Central zone (black rectangle).

a treatment fraction of .4 (60% spatial overlap $\times$ two-thirds temporal overlap = .4). If a potential closure intersects multiple actual closures, I compute the treatment fraction with each actual closure and record the sum of treatment fractions. The average treatment fraction for potential closures is 0.2.

The most important control variables in my regressions are the length distribution of anchoveta caught by the sets that generate potential closures (e.g. 1% of individuals caught were between 10 and 10.5 cm, 1.4% caught were between 10.5 and 11 cm, etc.). Controlling for the length distribution is akin to controlling for the probability distribution function from which percentage juvenile values for those sets are drawn because percentage juvenile is a statistic of the length distribution (fraction of individuals smaller than 12 cm). Sets that generate the same potential closure are "drawing" percentage juvenile values from the same length distribution because they occur near each other during the same 15 hour time period; they are fishing from the same local anchoveta population. The percentage juvenile values reported to the regulator affect the probability a potential closure is declared an actual closure; length distribution does not because fishermen do not report length distribution to the regulator (Section 1.4). I do not control for the percentage juvenile values reported to the regulator in order to preserve treatment variation. By instead controlling for length distribution, the identifying variation comes from comparing potential closures that by chance had higher percentage juvenile draws (so were declared closures by the regulator) to potential closures that by chance had lower percentage juvenile draws (so were not declared closures by the regulator). There is variation in percentage juvenile draws conditional on potential closure-level length distribution because of the sampling procedure discussed in Section 1.4, wherein fishermen estimate percentage juvenile by measuring 200 anchoveta out of the several million anchoveta caught in a typical set. One way to quantify this variation is by regressing set-level percentage juvenile values reported to the regulator on potential closure-level length distribution, for the subset of sets that generate potential closures. The R^2 from this regression is 0.24, indicating ample identifying variation.

I control for length distribution by calculating the weighted-average proportion of anchoveta individuals in each half-cm length interval among the sets that generate potential closures, where the weights are the total number of anchoveta individuals caught by each set. Recall that these sets occur before potential closures begin. For example, the weighted-average proportion of anchoveta in each length interval for potential closures in Figure 1.5b is calculated from sets that occur between midnight and 3 pm on April 28, 2019 (Figure 1.5a).

In Appendix A.3 I detail how given sets' location, time, and percentage juvenile, I impute the length distribution for sets from vessels that do not report length distribution to their owners. I use percentage juvenile measured by third-party inspectors to calculate corrected length distributions for all sets. I control for corrected length distributions in my regressions so that potential misreporting to vessel owners does not bias my results.[24] My regressions thus compare potential closures whose true anchoveta populations are similar, but which the regulator believes are different because the regulator does not use length distribution or third-party inspector data when making closure decisions.

Controlling for the length distribution adjusts for differences in the size-structure of an-

[24]I also use the corrected number of individuals caught by each set in calculating the average length distribution for each potential closure.

choveta populations across potential closures, but not for differences in fishing productivity or fishing costs across potential closures. If treated potential closures are more desirable fishing locations, either because anchoveta are more abundant or because fishing costs are lower, juvenile catch would be higher (all else equal) in treated potential closures independent of treatment because total catch would be higher. I avoid bias due to differences in fishing productivity and fishing costs by controlling for the number of sets that generate each potential closure, the total tons caught by the sets that generate each potential closure, the size of each potential closure in km^2, the distance of each potential closure's centroid to Peru's coast in km, tons caught per set among the sets that generate each potential closure, and tons caught per km^2 among the sets that generate each potential closure. The number of sets, tons caught, and potential closure area are measures of anchoveta abundance, distance to the coast is a proxy for fishing costs, and tons per set and tons per km^2 are proxies for fishing productivity.

Finally, I include in my regressions two-week-of-sample by two-degree grid cell fixed effects and day-of-sample fixed effects (defined by the centroid or date a potential closure begins). The first set of fixed effects ensure identification comes from comparing potential closures that occur near each other during a similar time period. On average, there are 4.4 potential closures per two-week-of-sample by two-degree grid cell. The day-of-sample fixed effects control for the following possible confounders: the number of actual closures that are active that day and the area they cover; aggregate juvenile catch and fishing productivity that day; and the international price of fishmeal.

The fixed effects and control variables described in this section balance treated and control potential closures on pre-period juvenile catch levels, pre-period juvenile catch trends, and observable measures of fishing productivity (Appendix A.1).

Spatial and temporal spillover bins

The temporary spatial closures policy may reduce juvenile catch inside closed areas during the active closure period (direct effect). But it could also cause spillovers over space or time: changes in juvenile catch because of the policy outside the closed area or outside the closure period. Estimating these spatial and temporal spillovers in addition to the direct effect of the policy is critical because both vessels and anchoveta move. Instead of fishing inside active closures, vessels could fish inside closed areas after closure announcements but before the beginning of closure periods, just outside closed areas during closure periods, or inside closed areas after closure periods have ended. All of these types of fishing reallocation do not violate the policy. Moreover, closures need not merely reallocate fishing. If closures are a sufficiently large positive signal of fishing productivity, they could also increase the total quantity of fishing that occurs near closures (Section 1.3).

The "treatment window" over which I allow the policy to affect juvenile catch is from nine hours before a potential closure begins until four days after a potential closure has ended, within 50 km of the potential closure. I chose this treatment window empirically: it is large enough to observe the effect of the closures policy dissipate over both space and

Figure 1.7: Treatment window over which the closures policy can affect juvenile catch

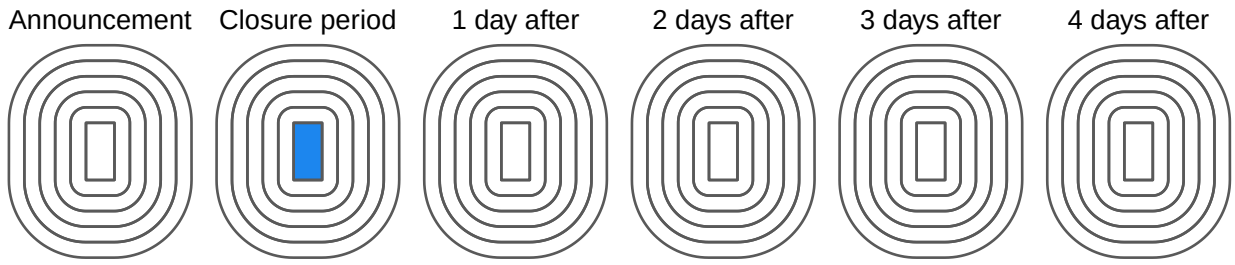

Notes: The original potential closure is the closure period, inside the potential closure treatment bin (blue). The other 35 treatment bins in the treatment window are white.

time (Section 1.6). There are six time periods of interest for each potential closure: nine hours before the potential closure begins ("Announcement" in Figure 1.7), the three-day period in which the potential closure is active ("Closure period"), and one, two, three, and four days after the potential closure has ended. For each time period, there are 6 spatial units of interest: inside the potential closure, 0 to 10 km outside the potential closure, 10 to 20 km outside the potential closure, 20 to 30 km outside the potential closure, 30 to 40 km outside the potential closure, and 40 to 50 km outside the potential closure. There are thus 36 "treatment bins" of interest (6 time periods $\times$ 6 spatial units). Since there are 970 potential closures, there are 34,920 potential closure-treatment bin observations. Figure 1.7 visualizes the 36 treatment bins in the treatment window. I refer to the spatial units outside the potential closure as "rings". For example, the 10 km ring is the 0 to 10 km outside the potential closure unit.

The original potential closure is the three-day closure period, inside the potential closure treatment bin. I calculate treatment fraction and juvenile catch for the other 35 treatment bins in the same way that I calculate them for this treatment bin (see immediately preceding subsection). To calculate treatment fraction, I create the same spatial and temporal leads and lags for each actual closure declared by the regulator. Then I compute the treatment fraction of each potential closure-treatment bin with the same treatment bin of actual closures.[25] I calculate juvenile catch inside each potential closure-treatment bin by summing juvenile

[25]Some potential closure-treatment bins partially overlap with each other (cover the same area during the same time period). However, this overlap is uncorrelated with treatment fraction, both unconditionally and conditional on the control variables and fixed effects in Equation 3.1. This non-correlation indicates that overlap between potential closure-treatment bins does not bias my estimated treatment effects.

catch over sets that occur inside the same potential closure-treatment bin.[26] Finally, the control variables are defined at the level of a potential closure; their values are the same for all treatment bins for a given potential closure.[27]

Estimating equation

I estimate the effect of the temporary spatial closures policy on juvenile catch with the following ordinary least squares regression:

$$\begin{aligned} JuvenileCatch_{ist} = \alpha_{st} + \beta_{st} TreatFraction_{ist} + \sum_{\ell=[3,3.5)}^{[18.5,19)} \xi_\ell Prop_{i\ell} \\ + \gamma_1 Sets_i + \gamma_2 Tons_i + \gamma_3 Area_i + \gamma_4 DistToCoast_i \\ + \gamma_5 TonsPerSet_i + \gamma_6 TonsPerArea_i + \sigma_{wg} + \delta_d + \epsilon_{ist} \end{aligned} \tag{1.1}$$

where i = potential closure, s = spatial unit, t = time period, ℓ = half-cm length interval, w = two-week-of-sample, g = two-degree grid cell, and d = day-of-sample. I defined the construction of the data and all variables in this equation in the immediately preceding subsections.

The outcome variable is the inverse hyperbolic sine of millions of juveniles caught in each potential closure-treatment bin. The inverse hyperbolic sine transformation allows coefficients to be interpreted in elasticity terms, but unlike a logarithmic transformation allows zero values (Bellemare & Wichman, 2020). The $Prop_{i\ell}$ terms are the proportion of anchoveta individuals in each half-cm length interval ℓ that are caught by the sets that generate potential closure i. Recall that these sets, from which $Sets_i$, $Tons_i$, $Area_i$, $DistToCoast_i$, $TonsPerSet_i$, and $TonsPerArea_i$ are also defined, occur before the treatment window for potential closure i begins.

The coefficients of interest are β_{st}, which measure the effects of the closures policy on juvenile catch. The identifying variation is across potential closures, within the same treatment bin and conditional on the fixed effects and potential closure-level controls. For example, comparing 10 km-wide rings around potential closures that begin on the same day within the same two-week-of-sample by two-degree grid cell and conditional on potential-level controls, $\beta_{s=10,t=closure\ period}$ captures the change in juvenile catch 10 km outside closures during the closure period that is due to treatment. Potential closures are balanced on pre-period juvenile catch (levels and trends) and on observable measures of fishing productivity, conditional on fixed effects and potential closure-level controls (Appendix A.1). Identification occurs from comparing potential closures that are equally desirable fishing locations and contain similar concentrations of juveniles, but which the regulator believes are different because the data available to the regulator are lower resolution.

[26] Some sets occur inside multiple potential closure-treatment bins. I correct for this "double-counting" when estimating the effect of the closures policy on juvenile catch (detailed in Footnote 28).

[27] However, the fixed effects are specific to each potential closure-treatment bin.

I cluster standard errors at the level of two-week-of-sample by two-degree grid cell. I cluster at this level because it is greater than the level at which treatment is assigned: the 50 km ring around the largest closure (potential or actual) is smaller than a two-degree grid cell and the maximum temporal window over which closures affect juvenile catch is less than two weeks (Abadie et al., 2017). I drop 21 potential closures that do not have length distribution data because there were no sets from vessels that report length distribution data to their owner in the same two-week-of-sample by two-degree grid cell (Appendix A.3). There are 255 clusters and 34,164 observations when I estimate Equation 3.1 (949 potential closures $\times$ 36 treatment bins).

1.6 Do closures reduce total juvenile catch?

I estimate the effect of the temporary spatial closures policy on juvenile catch with Equation 3.1, convert the treatment coefficients into levels, and compute standard errors using the delta method.[28] Figure 1.8 shows the main result of this paper. The y-axis is the change in the number of juveniles caught because of the policy and the x-axis is the treatment bin. I estimate the effect of the policy with a single regression (Equation 3.1) but plot the results in six separate subfigures, with one subfigure for each of the six time periods in my treatment window.

After the announcement of closures but before the beginning of closure periods (Figure 1.8a), juvenile catch increases by 1.2 billion inside soon-to-be closed areas (temporal spillover). There is no change in juvenile catch outside closed areas before the beginning of closure periods. Vessels catch more juveniles in the places where fishing will soon be temporarily banned (inside closed areas), but they do not catch more juveniles in the places where fishing will be allowed to continue (outside closed areas).

During closure periods, juvenile catch decreases by 2.2 billion inside closed areas. This effect is not statistically significant. Outside closed areas during closure periods, there are large, statistically significant increases in juvenile catch. In total, spatial spillovers during the closure period sum to a 44.5 billion increase in juvenile catch.

The hollow, red triangles in Figure 1.8 are the level estimates (black points) normalized by the area inside potential closures. This area normalization accounts for the fact that each subsequent spatial ring covers a larger area (see Figure 1.7 for a representative illustration).

[28] Figure A.2 displays the treatment coefficients (the β_{st} terms in Equation 3.1). I convert the treatment coefficients into levels as follows. First, I convert the treatment coefficients into percent changes with the transformation $exp(\beta_{st}) - 1$. The percentage change in juvenile catch in treatment bin st equals $(ObservedJuvenileCatch_{st} - CounterfactualJuvenileCatch_{st})$ divided by $CounterfactualJuvenileCatch_{st}$. $ObservedJuvenileCatch_{st}$ is the total juvenile catch that occurs in the data in bin st, multiplied by the ratio of total juvenile catch observed anywhere to $ObservedJuvenileCatch_{st}$ summed over all treatment bins. This ratio is .394; many potential closure-bins are overlapping so I rescale $ObservedJuvenileCatch_{st}$ to avoid artificially inflating observed juvenile catch. Then I re-arrange terms and calculate $CounterfactualJuvenileCatch_{st} = \frac{ObservedJuvenileCatch_{st}}{exp(\beta_{st})}$. Then the change in juvenile catch in bin st in levels is $ObservedJuvenileCatch_{st} - CounterfactualJuvenileCatch_{st}$.

Figure 1.8: Change in billions of juveniles caught because of the closures policy

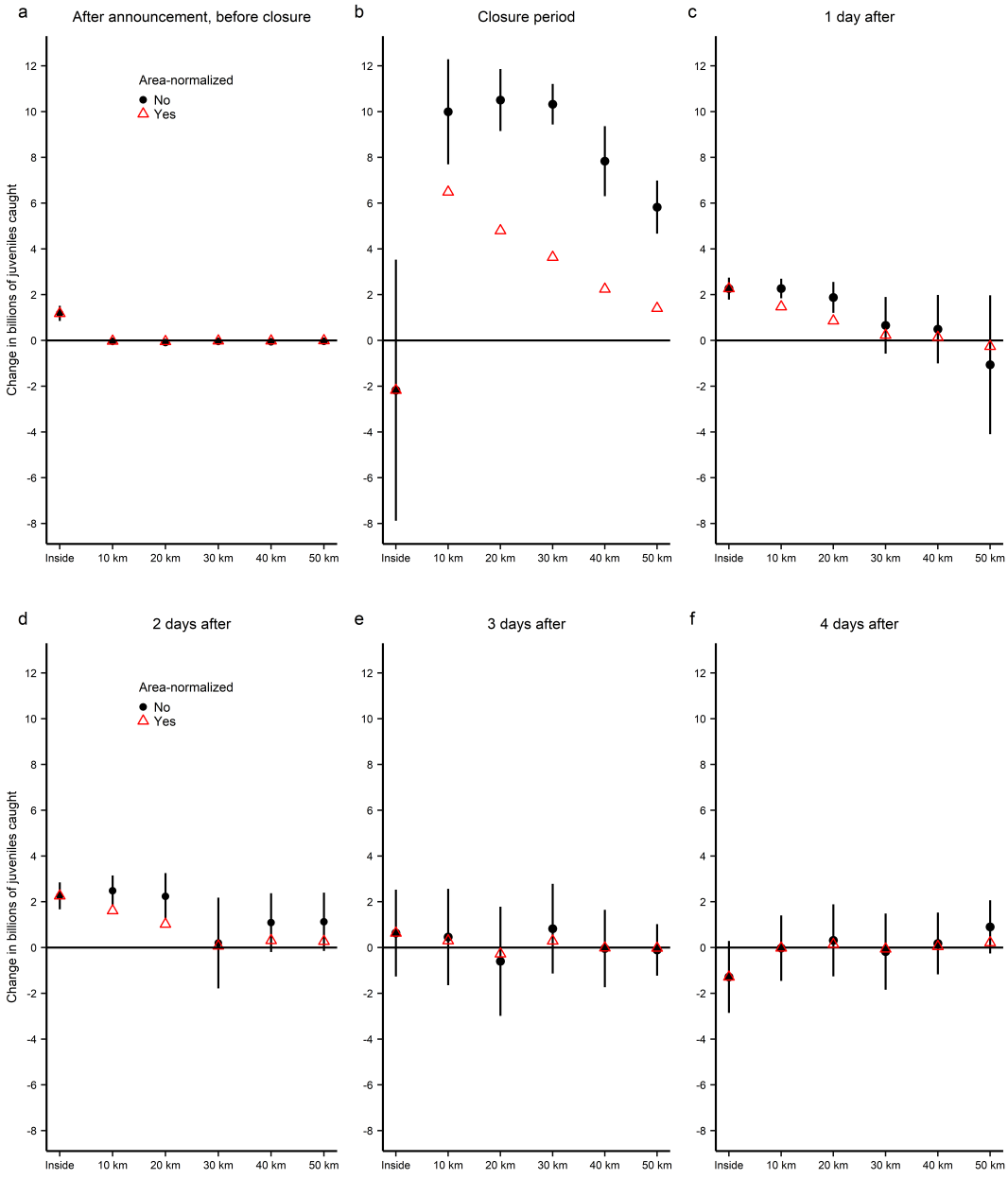

Notes: The six subfigures (a to f) correspond to the six time periods in my treatment window. In each time period, there are six spatial units of interest (x-axis). The black points are the treatment effects in levels and the black whiskers are 95% confidence intervals. The hollow, red triangles are normalized by the area inside potential closures because larger spatial rings cover more area. N = 34,164. Standard errors clustered at level of two-week-of-sample by two-degree grid cell.

There is a mechanical increase in the level estimates in larger spatial rings for this reason. The area-normalized estimates reveal intuitive spatial decay. The increase in juvenile catch because of the policy during closure periods is largest just outside closed areas, and the effect of the policy diminishes farther from closed areas.

The policy also increases juvenile catch in the first two days after the end of closure periods (Figures 1.8c and 1.8d). Juvenile catch increases by 2.3 billion inside closed areas in the first 24 hours after the end of closure periods (temporal spillover). Juvenile catch is also significantly higher 10 and 20 km outside closed areas, but the effect of the policy is insignificant in the 30, 40, and 50 km rings. This pattern also occurs in the second day after the end of closure periods. However, by the third and fourth day after the end of closure periods, the effect of the policy on juvenile catch attenuates to 0, both inside and outside closed areas.

Summing the level estimates over treatment bins implies that the total effect of the temporary spatial closures policy is an increase in the number of juveniles caught by 60 billion, or 75%. However, this approach is naïve because it ignores the total allowable catch limit the regulator sets each season (Section 1.2). When I use tons as the dependent variable in Equation 3.1, I estimate that the closures policy increases tons caught by 35% on average across the 36 treatment bins. But total tons caught cannot increase in the four (of six) fishing seasons during my study period in which the total allowable catch limit was binding. In those seasons, though there was an increase in tons caught within the treatment window, tons caught necessarily decreased by the same amount outside the treatment window. When I account for this mechanical re-allocation, the total effect of the closures policy is an increase in the number of juveniles caught by 47 billion, or 50% (delta method standard errors are 5.1 billion and 5.5%). This 50% increase in juvenile catch is my preferred estimate of the total effect of the closures policy. This result is robust to alternative specifications and estimation approaches (Appendix A.1).

The regulator's total allowable catch limit, enforced through individual vessel quotas, reduces the backfire caused by the closures policy because without it, closures would increase juvenile catch by an even greater amount. The increase in juvenile catch because of closures remains substantial even after accounting for the reallocation in tons caught due to the total allowable catch limit because relative juvenile abundance is much higher near closures declared by the regulator (the second condition in Proposition 1 from Section 1.3). Average percentage juvenile among sets within the treatment window of actual closures is 25%, compared to 9% outside the treatment window (Figure A.15).

1.7 Do closures provide valuable information?

Why does the temporary spatial closures policy increase total juvenile catch? Closures might provide valuable information regarding the location of anchoveta because the regulator declares closures in response to real-time anchoveta catch data from all vessels, and there is only anchoveta catch in an area if anchoveta are sufficiently abundant in the area. If

vessels respond to closures because closures provide valuable information, one might expect vessels who fish near closures to reap the value of that information by catching more tons of anchoveta per set (Section 1.2). On the other hand, since closures are publicly announced, the *ex post* value of this information might be competed away due to congestion; there are diminishing marginal returns when more vessels fish from the same local, exhaustible anchoveta population (Huang & Smith, 2014; Smith, 1969). It is even possible that vessels could overreact to closures, such that tons per set near closures is lower.

Proposition 2a in Section 1.3 states that in the Bayes-Nash equilibrium, vessels fish near closures until the profit from doing so equals the profit from fishing elsewhere. Using the electronic logbook data, I test whether observed vessel response to closures is consistent with the Bayes-Nash equilibrium by estimating the difference in tons caught per set near closures compared to tons caught per set elsewhere, conditional on the distance of the set to the coast, vessel by season fixed effects, day-of-sample fixed effects, and two-degree grid cell by season fixed effects. I estimate the following ordinary least squares regression in Column 2 of Table 1.1:

$$Tons_{vjk} = \beta_1 \mathbb{1}\{Near\}_{vjk} + \beta_2 DistToCoast_{vjk} + \delta_{vj} + \gamma_d + \alpha_{jg} + \epsilon_{vjk} \tag{1.2}$$

where v = vessel, j = season, k = set, d = day-of-sample, and g = two-degree grid cell.

The outcome variable is the inverse hyperbolic sine of the tons caught by a given set.[29] The explanatory variable $\mathbb{1}\{Near\}_{vjk}$ equals 1 for sets that occurred inside a treatment bin in which there was a statistically significant change in juvenile catch (see Figure 1.8) and equals 0 otherwise. I define $\mathbb{1}\{Near\}_{vjk}$ in this way because I am interested in whether the large spillover effects I estimated in Section 1.6 can be explained by the closures policy communicating information about the value of fishing in those places and times. In this regression, treatment bins are defined relative to closures declared by the regulator. The coefficient of interest is β_1, which measures the difference in tons caught by sets near closures declared by the regulator. I include fixed effects and the distance of each set to the coast in order to partially control for differences in the cost of each set (e.g., sets farther from shore require more fuel, all else equal). Day-of-sample fixed effects also control for the international price of fishmeal, which determines the price fishermen receive per ton of anchoveta they land. Therefore, the change in tons per set captured by β_1 represents the change in revenue per set from fishing near closures declared by the regulator. To the extent that the fixed effects and the distance of each set to the coast control for cost per set, β_1 can also be interpreted as the change in profit per set from fishing near closures declared by the regulator.

Without fixed effects, sets near closures declared by the regulator catch 36% more tons (Column 1 in Table 1.1). However, including fixed effects reduces β_1 by an order of magnitude and makes it statistically insignificant: sets near closures declared by the regulator do not catch more tons of anchoveta (Column 2). While this null result suggests that vessels' response to closures is consistent with the Bayes-Nash equilibrium, the same null result would also occur if closures do not provide valuable information.

[29] Fishermen report catching 0 tons for 11% of sets in the electronic logbook data.

Table 1.1: Closures provide valuable information, but the value of this information is competed away

	Dependent variable: asinh(tons)			
	Actual closures		Potential closures	
	(1)	(2)	(3)	(4)
$\mathbb{1}\{\text{Near}\}$	0.310	-0.022	0.177	0.082
	(0.080)	(0.033)	(0.073)	(0.026)
Distance to shore (km)	0.011	0.004	0.011	0.004
	(0.002)	(0.001)	(0.002)	(0.001)
Constant	3.306		3.289	
	(0.082)		(0.101)	
Fixed effects		X		X

All regressions have 246,914 observations. $\mathbb{1}\{\text{Near}\}$ is an indicator for whether the set occurred inside a treatment bin in which there is a significant change in juvenile catch because of the temporary spatial closures policy. In Columns 1 and 2, Near is defined relative to actual closures declared by the regulator (mean of this indicator equals .391). In Columns 3 and 4, Near is defined relative to potential closures (mean of this indicator is .799). Electronic logbook data is for all vessels from April 2017 to January 2020. Regressions in Columns 2 and 4 include vessel by season fixed effects, day-of-sample fixed effects, and two-degree grid cell by season fixed effects. Standard errors clustered at level of two-week-of-sample by two-degree grid cell.

I use potential closures to test whether actual closures declared by the regulator provide valuable information. In Section 1.5, I described how I generate potential closures from the same electronic logbook data the regulator uses to determine actual closures. If they were announced, potential closures would communicate similar information to fishermen as actual closures: fishing occurred recently in the area, so anchoveta are likely abundant nearby. But because potential closures and the electronic logbook data they are based on are not public, potential closures enable a test of whether actual closures provide valuable information that is unconfounded by vessels' response to this information (Proposition 2b in Section 1.3).

I now estimate the same regression as Equation 3.2, except the Near indicator is defined relative to potential closures rather than actual closures. Without fixed effects, sets near potential closures catch 19% more tons (Column 3 in Table 1.1). Including fixed effects in Column 4 reduces β_1 by half, but the difference in tons caught per set near potential closures remains statistically significant (t-statistic > 3). Sets near potential closures catch

9% more tons on average. Taken together, these results suggest closures do provide valuable information (second testable hypothesis from introduction), but the *ex post* value of this information is competed away.

1.8 Does the information provided by closures increase spillovers?

In Section 1.7, I presented evidence that closures implicitly provide information to fishermen about the value of fishing before, just outside, and after closures. I now test explicitly whether the information provided by closures is a mechanism underlying the policy's large spillover effects.

Proposition 3 in Section 1.3 states that vessels that receive a larger positive information shock from closure announcements will have larger treatment effects. Vessels experience a larger information shock from closure announcements if they have less information about an area before closure announcement. I test Proposition 3 using the same potential closures I generated to estimate the effect of the policy on juvenile catch, except I now calculate juvenile catch inside a potential closure-treatment bin separately for two types of vessels: vessels with more information about a potential closure and vessels with less information about a potential closure. I consider two ways in which vessels can acquire information about a potential closure before closure announcement would occur (if the potential closure is declared an actual closure by the regulator). First, vessels have more information about a potential closure if they fished inside the potential closure the day before closure announcement would occur. Second, vessels have more information about a potential closure if another vessel in their firm fished inside the potential closure the day before closure announcement would occur. I estimate the following equation by ordinary least squares regression:

$$\begin{aligned} JuvenileCatch_{isth} =& \alpha_{sth} + \beta_{sth} TreatFraction_{ist} + \sum_{\ell=[3,3.5)}^{[18.5,19)} \xi_\ell Prop_{i\ell} + \\ & \gamma_1 Sets_i + \gamma_2 Tons_i + \gamma_3 Area_i + \gamma_4 DistToCoast_i + \\ & \gamma_5 TonsPerSet_i + \gamma_6 TonsPerArea_i + \sigma_{wg} + \delta_d + \epsilon_{isth} \end{aligned} \tag{1.3}$$

where h indicates heterogeneity (in information) category and all other variables and subscripts are as defined for Equation 3.1.

Note that Equation 1.3 is identical to Equation 3.1 except there are now twice as many treatment coefficients of interest (two heterogeneity categories for each treatment bin). There are also twice as many observations in this regression because I calculate juvenile catch in the potential closure-treatment bin among vessels with less information and among vessels with more information. Figure 1.9 presents the result when I categorize vessels by whether they personally fished inside the potential closure the day before closure announcement would occur, and Figure 1.10 displays the result when I categorize vessels by whether a vessel in

their firm fished inside the potential closure the day before closure announcement would occur.[30] Unlike in Figure 1.8, I present the results in percent changes rather than changes in levels because more vessels belong to the lower information group.

Vessels that fished inside a potential closure the day before closure announcement have a much smaller total treatment effect (0.7% increase in total juvenile catch) than vessels that did not (87.5% increase in total juvenile catch).[31] The treatment effect for vessels that fished inside a potential closure the day before closure announcement is not different from zero (delta method standard error is 3.2%), whereas the treatment effect for vessels that did not fish inside a potential closure the day before closure announcement is highly statistically significant (standard error is 5.5%). The difference in treatment effects between the two information groups is also statistically significant (difference is 86.8% with a standard error of 6.4%).[32]

The information mechanism also operates at the firm-level. Vessels who had a different member of their firm fish inside a potential closure the day before closure announcement would occur have a much smaller treatment effect (19.1% increase in juvenile catch) than vessels who did not (77.9% increase in juvenile catch). Both treatment effects are different from zero (standard errors are 3.7% and 5.1%), as is the difference in treatment effects (difference is 58.8% with a standard error of 6.3%).

The results in this section support Proposition 3 that vessels that receive a larger information shock from closures have larger treatment effects. The information provided by closures is a mechanism underlying the policy's large spillover effects. The vessel-level result in Figure 1.9 also provides an explanation of why fishermen underreport percentage juvenile in the raw electronic logbook data (Section 1.4) even though closures provide valuable information (Section 1.7). Closures only provide information to fishermen who were not already fishing in the area, so fishermen might underreport percentage juvenile to avoid triggering a closure in the area they are already fishing.[33]

1.9 Discussion

Peru's temporary spatial closures policy is targeted to reduce juvenile catch by temporarily banning fishing in the places with the highest relative abundance of juvenile anchoveta.

[30] I leave out own-fishing in the firm-level categorization, so that vessels are coded as having had a member of their firm fish inside a potential closure the day before closure announcement would occur only if a different vessel in their firm did so.

[31] I calculate the percentage change in total juvenile catch for both groups and both categorizations in the same way as in Section 1.6, converting the treatment coefficients into changes in levels and accounting for the reallocation in tons caught in the four fishing seasons the total allowable catch limit was binding.

[32] Note that this result does not reflect mean reversion because estimation is across potential closures. The treatment effect for vessels that fished inside a potential closure the day before closure announcement would occur is estimated by comparing juvenile catch by these vessels near potential closures that get closed to juvenile catch by this same group of vessels near potential closures that do not get closed.

[33] Recall that underreporting by fishermen does not bias my estimates because I calculate my regressions' outcome variable and control variables using third-party inspector data.

Figure 1.9: Percent change in juvenile catch because of the closures policy by whether vessels fished in the potential closure the day before closure announcement

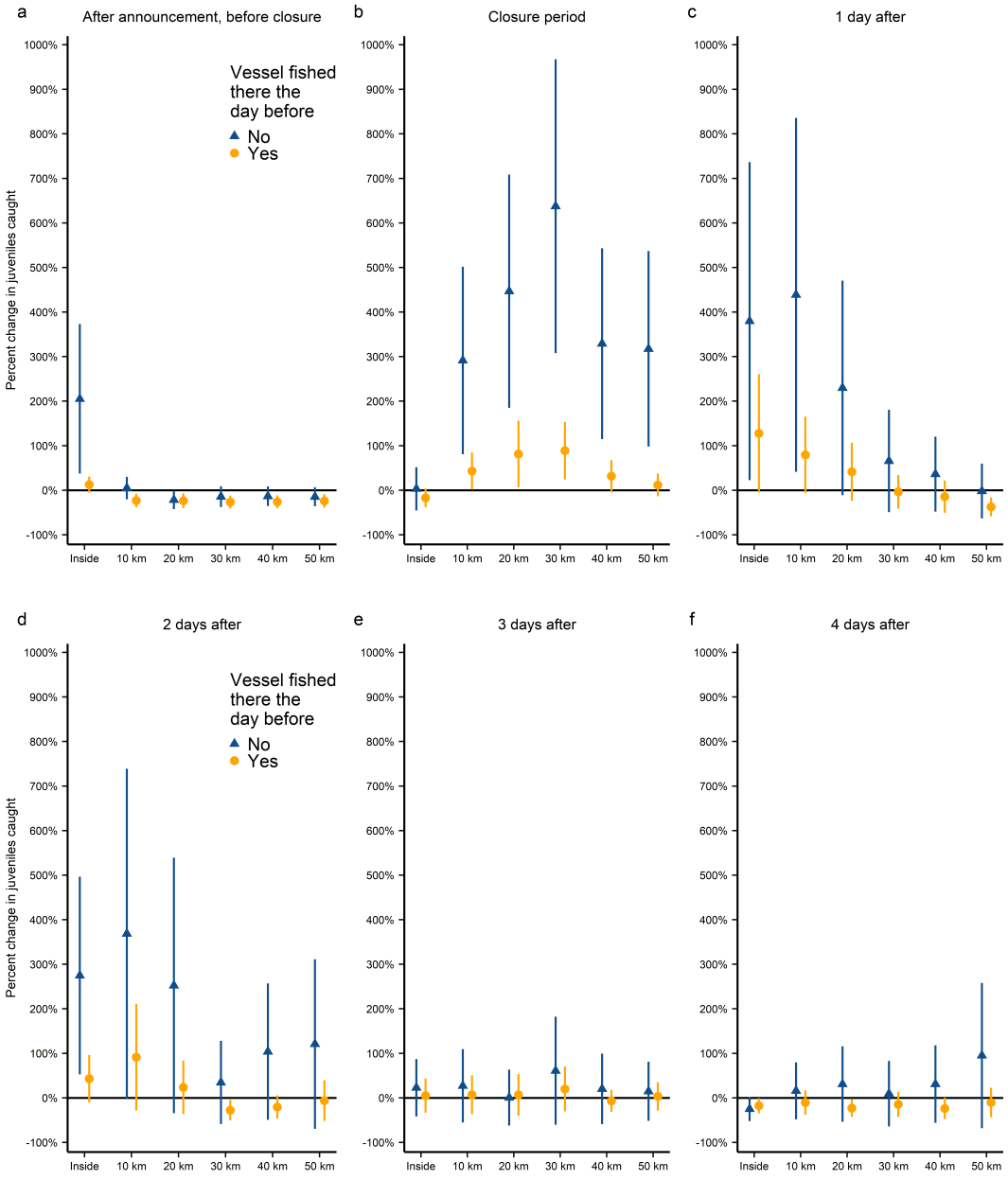

Notes: The six subfigures (a to f) correspond to the six time periods in my treatment window. In each time period, there are six spatial units of interest (x-axis). The points are the treatment effects in percentages and the whiskers are 95% confidence intervals. N = 68,328. Standard errors clustered at level of two-week-of-sample by two-degree grid cell.

Figure 1.10: Percent change in juvenile catch because of the closures policy by whether vessels had a different member of their firm fish in the potential closure the day before closure announcement

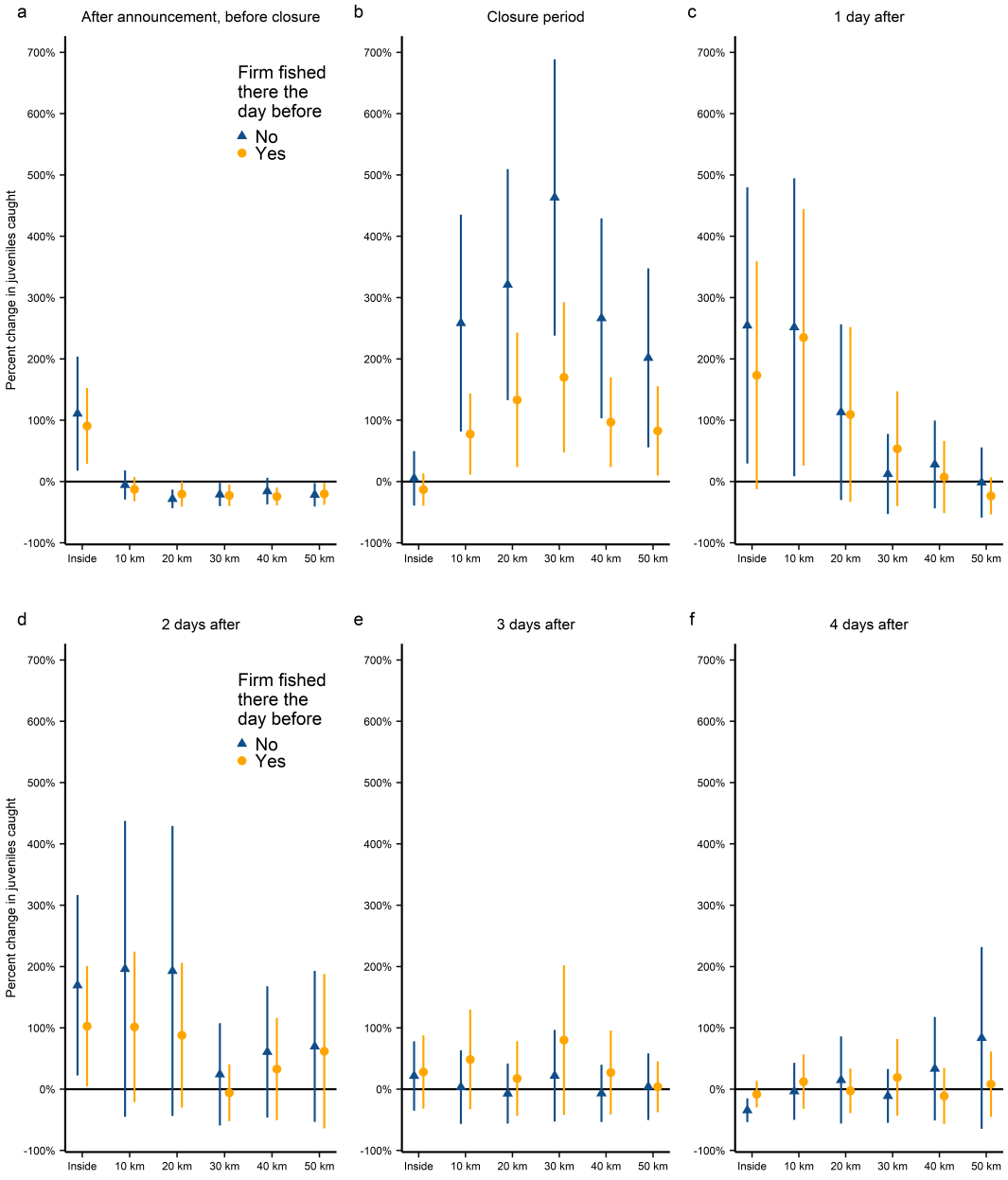

Notes: The six subfigures (a to f) correspond to the six time periods in my treatment window. In each time period, there are six spatial units of interest (x-axis). The points are the treatment effects in percentages and the whiskers are 95% confidence intervals. N = 68,328. Standard errors clustered at level of two-week-of-sample by two-degree grid cell.

While there is a (noisy) decrease in juvenile catch inside closed areas during closure periods, there are large increases in juvenile catch inside closed areas between the announcement and the beginning of closures, just outside closed areas during closures periods, and inside closed areas one and two days after closures end. On net, this policy worsens the target outcome, increasing total juvenile catch by 50%.

The failure of this policy to achieve its objective is not due to a failure of targeting. The regulator is closing the right areas; in the 9 to 12 hours before the beginning of a closure, 47% of individuals caught inside the soon-to-be closed area are juveniles, higher than in any other treatment bin and much higher than the 9% juvenile caught outside the treatment window (Figure A.15). Within the support of the data, longer closures offer no improvement and larger closures perform even worse than smaller closures (Appendix A.2).[34] A conservative estimate implies that the policy reduces exports by $38 million per year (2017 USD).[35] Despite the sophistication of the temporary spatial closures policy, the empirical results in this paper support a new approach to reduce juvenile catch.

The information design literature studies the relationship between a Sender of information and a Receiver who acts based on this information (Kamenica, 2019; Kamenica & Gentzkow, 2011). The Sender's problem is to choose the decision rule that induces the Receiver to act in a way that maximizes the Sender's utility. Here, the regulator (Sender) wants fishermen (Receivers) to catch fewer juveniles, but the signal conveyed by closure announcements directs fishing to the places with the most juveniles. Instead, the regulator could tell fishermen where high percentages of adults are being caught. Because fishermen are paid by the ton, they are not fishing more near closures because they specifically want to catch juveniles. They fish more near closures because they want to reduce their search costs and increase the tons of anchoveta they catch per set. The regulator could use the electronic logbook data to calculate locations with high percentages of adult catch. Fishermen might react to this information in the same way they react to closures, except they would now be reallocating their fishing to places with few juveniles.

I perform a back-of-the-envelope calculation to explore the effect of replacing the current closures policy with an alternative policy that reveals the locations with the highest percentages of adult catch. I identify the 410 potential closures with the highest weighted-

[34]Larger closures could cause larger increases in juvenile catch because congestion costs are lower or if larger closures are a larger positive signal of fishing productivity.

[35]I reproduce the method of Salvatteci and Mendo (2005), who estimate the cost of juvenile catch by comparing status quo landings to a counterfactual where juveniles make up a smaller fraction of individuals landed. I similarly project forward the length distribution of individuals caught during my study period until counterfactual juvenile catch is 33% lower than status quo juvenile catch (equivalently, until status quo juvenile catch is 50% higher than counterfactual juvenile catch). Status quo tons landed are 2.1% lower than in my counterfactual projection because anchoveta growth exceeds natural mortality within the support of the data (i.e., the closures policy causes "growth overfishing"). In the most recent year of data (2017), FOB export revenues were $1.79 billion (PRODUCE, 2018a). Then the closures policy reduces exports by $38 million ($1.79 billion $\times$ -2.1%). This projection is conservative because it does not account for the lower reproductive capacity of juveniles, known as "recruitment overfishing". Recruitment overfishing reduces future spawning, which likely reduces the size of the future stock (Quaas et al., 2013).

average percentage of adult catch.[36] I assume that the 35% increase in tons caught near the 410 closures declared by the regulator instead occur within the treatment window of the 410 potential closures with the highest percentage of adult catch. Juvenile catch changes in three ways in this scenario. First, fishermen catch 47 billion *fewer* juveniles due to the elimination of the closures policy (fewer tons in high percentage juvenile areas). Second, they catch 5 billion *more* juveniles near the 410 high-adult potential closures (more tons in low percentage juvenile areas). Third, they catch 38 billion *fewer* juveniles due to the compensating decrease in tons caught outside the treatment window of the 410 high-adult potential closures in the four of six fishing seasons in which the total allowable catch limit binds (fewer tons in areas with above-average percentage juvenile). On net, juvenile catch is 56% lower in this counterfactual scenario compared to the status quo level of juvenile catch (61 billion juveniles are caught compared to 141 billion). By attracting fishing to the places with the lowest percentage juvenile, the regulator could help fishermen reduce search costs while also reducing the capture of juvenile anchoveta, the most important biological externality in the world's largest fishery.

This calculation illustrates that policy-induced information spillovers need not cause targeted policies to backfire. When carefully designed, targeted policies that convey information about non-targeted units could simultaneously increase economic profits *and* mitigate the externality. Achieving such a win-win outcome requires understanding how the policy's information spillovers relate to agents' economic incentives.

[36] Calculated from the sets that generate each potential closure and weighted by the number of individuals caught by each set.

Chapter 2

Property rights and the protection of global marine resources

2.1 Introduction

Governing[1] global marine resource use is challenging in part because enforcing international agreements is costly (Barrett, 2005). There are many possible institutional structures by which global resource use can be managed, but institutions that lack credible enforcement mechanisms are unlikely to improve ecosystem conservation or economic profits. Assigning property rights to countries incentivizes those countries to protect the resources they own because the more unauthorized use the country prevents, the more resource is available for the country to use. However, countries could fail to deter unauthorized resource use if the costs of enforcement are too high relative to the benefits countries obtain from enforcement.

I estimate whether countries deter unauthorized foreign vessels from fishing in their Exclusive Economic Zones (EEZs), which cover approximately 39% of the ocean's surface and account for more than 95% of global marine fish catch (Pauly & Zeller, 2015). Codified between 1973 and 1982 at the third UN Conference on the Law of the Sea, EEZs are country-level property rights to all resources within a country's EEZ, including fish, minerals, oil, and natural gas (Hannesson, 2013; Wilen, 2000). Countries can prohibit foreign vessels from fishing in their EEZs or they can negotiate access agreements, specifying the allowable target species, quantities, and fishing methods, as well as access fee to be paid by foreign vessels or governments (Belhabib et al., 2015; Cabral et al., 2018). However, the size of EEZs and the remoteness of their boundaries require substantial enforcement capacity and surveillance effort to deter unauthorized foreign fishing. Surveys of fisheries experts and government officials indicate that many countries exhibit limited enforcement capacity and enforcement effort (Melnychuk et al., 2017; Mora et al., 2009).

The maximum width of EEZs with respect to fisheries—200 nautical miles (nm) from a country's coast—is a historical accident (Hollick, 1977) (see Section B.4). Because this

[1]The material from this chapter is a published paper in *Nature Sustainability* (Englander, 2019).

Figure 2.1: Data processing example

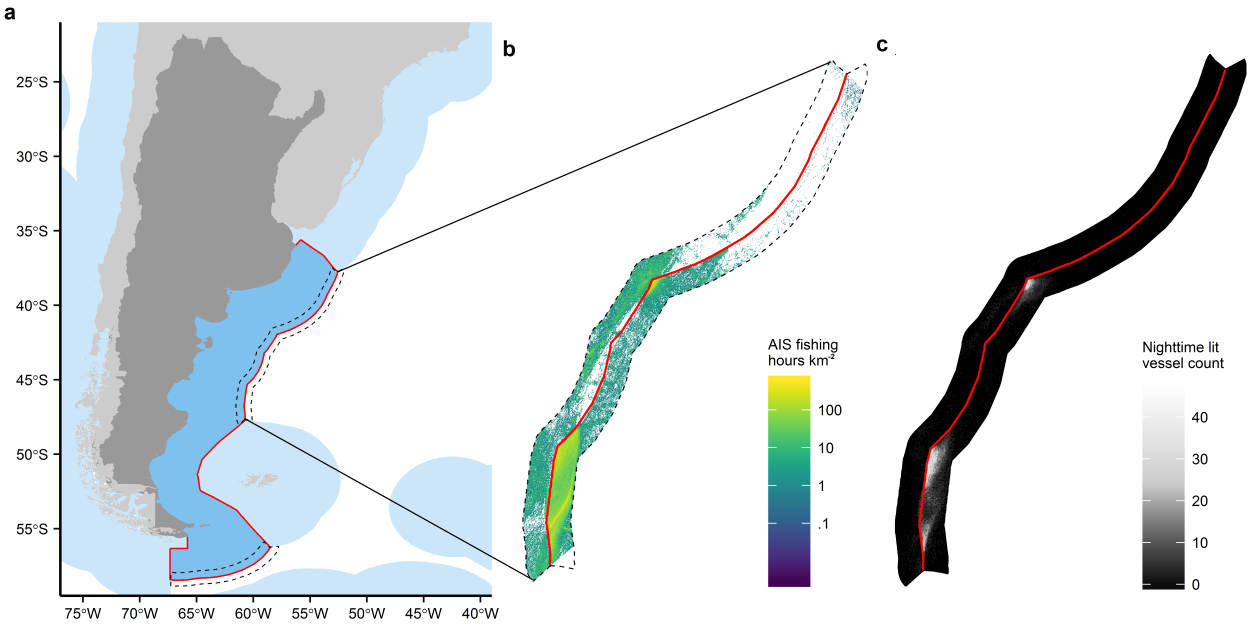

Notes: a, Argentina's EEZ (dark blue) and high seas boundary (red). Other countries' EEZs are light blue. I only analyze fishing within 50 km of an EEZ-high seas boundary (dashed regions). b, Total AIS fishing hours per km2 within 50 km of the northern portion of Argentina's EEZ-high seas boundary between 2012 and 2016. c, Total nighttime lit fishing vessel count in the same region in 2017.

boundary is ecologically arbitrary, fishing vessels close to the boundary face identical fishing opportunities on either side except that on one side, all natural resources belong to a single nation (EEZs), and on the other side they do not (the high seas). For example, there is no difference in ocean depth, sea surface temperature, or net primary productivity just inside EEZs compared to just outside EEZs (Figure B.1). Consequently, the effect of EEZs on fishing effort is the difference in fishing effort just inside EEZs compared to just outside EEZs (see Section B.2). This "regression discontinuity" research design differs from prior research in that other fisheries policies, such as catch shares, marine protected areas, and input restrictions, are often created or modified in response to fish stock levels, making it difficult to estimate the causal effects of these policies on fishing or fish stocks (Costello & Grainger, 2018; Homans & Wilen, 1997; Imbens & Lemieux, 2008; Smith et al., 2010).

Until recently, research has also been limited by fishing effort data that are low-resolution, from heterogeneous sources, or limited in geographic scope (Anticamara et al., 2011; Watson et al., 2013). I use two global, high-resolution fishing effort datasets. First, I use fishing

activity inferred from Automatic Identification System (AIS) vessel movements between 2012 and 2016 (Kroodsma et al., 2018). The second dataset contains the nighttime locations in 2017 of individual fishing vessels that use bright lights to attract catch (Elvidge et al., 2015). While the nighttime locations data mainly includes vessels fishing for squid, the AIS data captures the majority of total fishing effort that occurs near EEZ-high seas boundaries (Kroodsma et al., 2018). I filter both datasets to fishing that occurs within 50 km of an EEZ-high seas boundary (Figure 2.1 and B.2).

2.2 Results

I estimate that total AIS fishing effort and total nighttime fishing effort are 75% lower just inside EEZs compared to just outside EEZs (Figure 2.2a,b and Table B.1). For the AIS dataset, I use EEZ access agreements data to separate fishing into three vessel type categories based on the EEZ nearest to where each vessel is fishing: unauthorized foreign, authorized foreign, and domestic (Lam et al., 2016) (see Section 2.4). I find that unauthorized foreign fishing is 81% lower just inside EEZs compared to just outside EEZs (Figure 2.2c). The EEZ effect sizes in Figs. 2.2a-c are similar because 80% of fishing hours within 50 km of an EEZ-high seas boundary is unauthorized foreign fishing (Table B.2).

I also estimate that fishing by domestic and authorized foreign vessels is 43% and 25% higher just inside EEZs (Figure 2.2d). Unauthorized foreign vessels fishing within 50 km of an EEZ-high seas boundary tend to be larger and more powerful than domestic and authorized foreign vessels fishing in the same area (Table B.3).

I refer to the effect of EEZs on unauthorized foreign fishing as the "deterrence effect". This deterrence effect is not driven by unauthorized foreign fishers turning off their AIS transponders to avoid detection or by potential spillovers in unauthorized foreign fishing effort (see Section B.3, Figures B.3 and B.4, and Table B.4). My results are also robust to estimating deterrence effects separately for fishing vessels from countries with and without public EEZ access agreements (see Section B.3 and Figure B.5). I find that larger vessels have larger deterrence effects (see Section B.3 and Figure B.6), and estimate separate deterrence effects for each type of fishing activity ("gear type") and for the top three fishing countries in each gear type (Figures B.7 and B.8).

The total deterrence effect in Figure 2.2c implies that some countries enforce their EEZs. Otherwise, I would not observe a deterrence effect because fishing opportunities for unauthorized foreign vessels would be identical just inside EEZs compared to just outside EEZs. Given the dearth of comprehensive, standardized data on enforcement capacity and enforcement effort across countries (Melnychuk et al., 2017; Mora et al., 2009), inferring the existence of enforcement from unauthorized foreign fishing behavior is a contribution of this paper. To understand which specific countries enforce their EEZs and deter unauthorized foreign fishing, I estimate an individual deterrence effect for each EEZ-sea region in Figure 2.3a (see Section 2.4). EEZs that occur in multiple oceans or seas, such as the part of the

Figure 2.2: Effect of EEZs on fishing effort

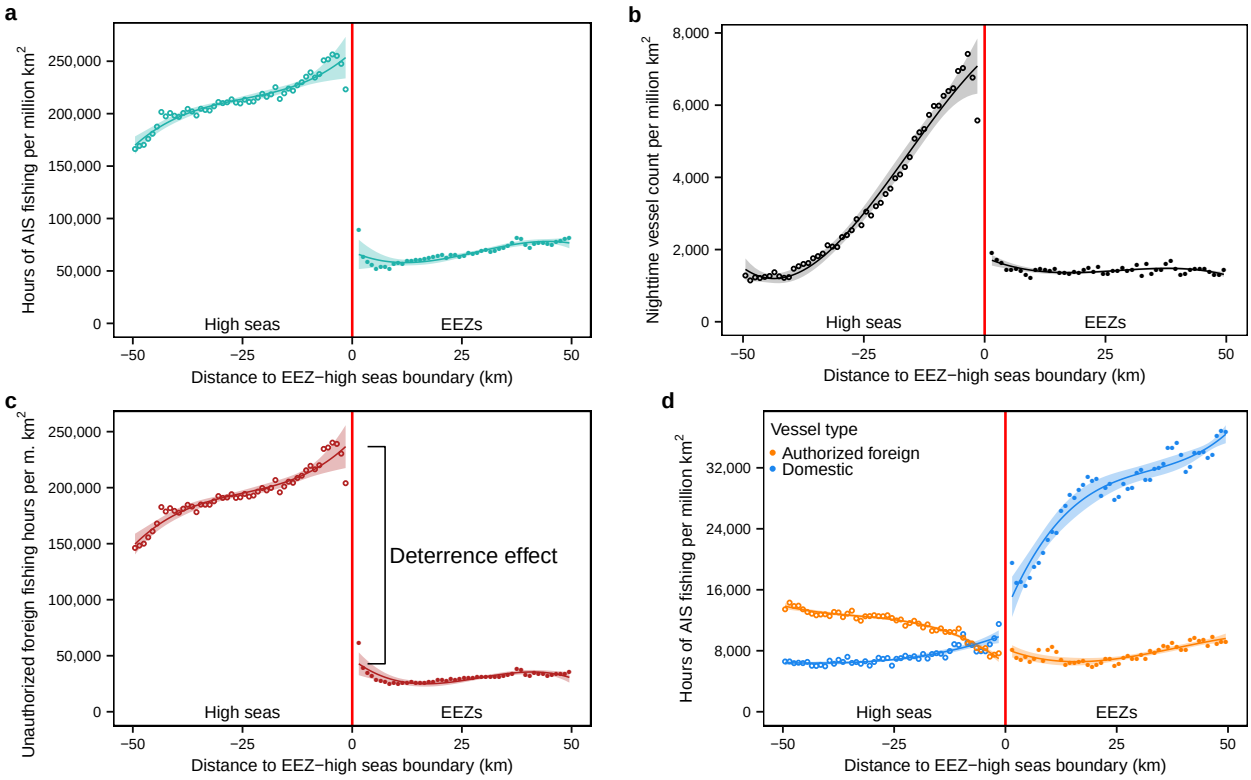

Notes: Total fishing effort per million km^2 within 50 km of any EEZ-high seas boundary in 1 km wide intervals as measured by (a) hours of all AIS fishing, (b) nighttime lit fishing vessel count, (c) hours of AIS unauthorized foreign fishing and (d) hours of AIS authorized foreign and domestic fishing (see Section 2.4). Points are data. Lines are ordinary least squares third-order polynomial fits in distance to the boundary. 95% confidence intervals (shaded) are estimated using standard errors that account for heteroscedasticity and serial correlation (Newey & West, 1987).

United States' EEZ in the Atlantic Ocean and the part in the Pacific Ocean, are analyzed separately to avoid comparing fishing in different ecosystems (VLIZ, 2012).

Figure 2.3: Unauthorized foreign fishing by EEZ-sea region

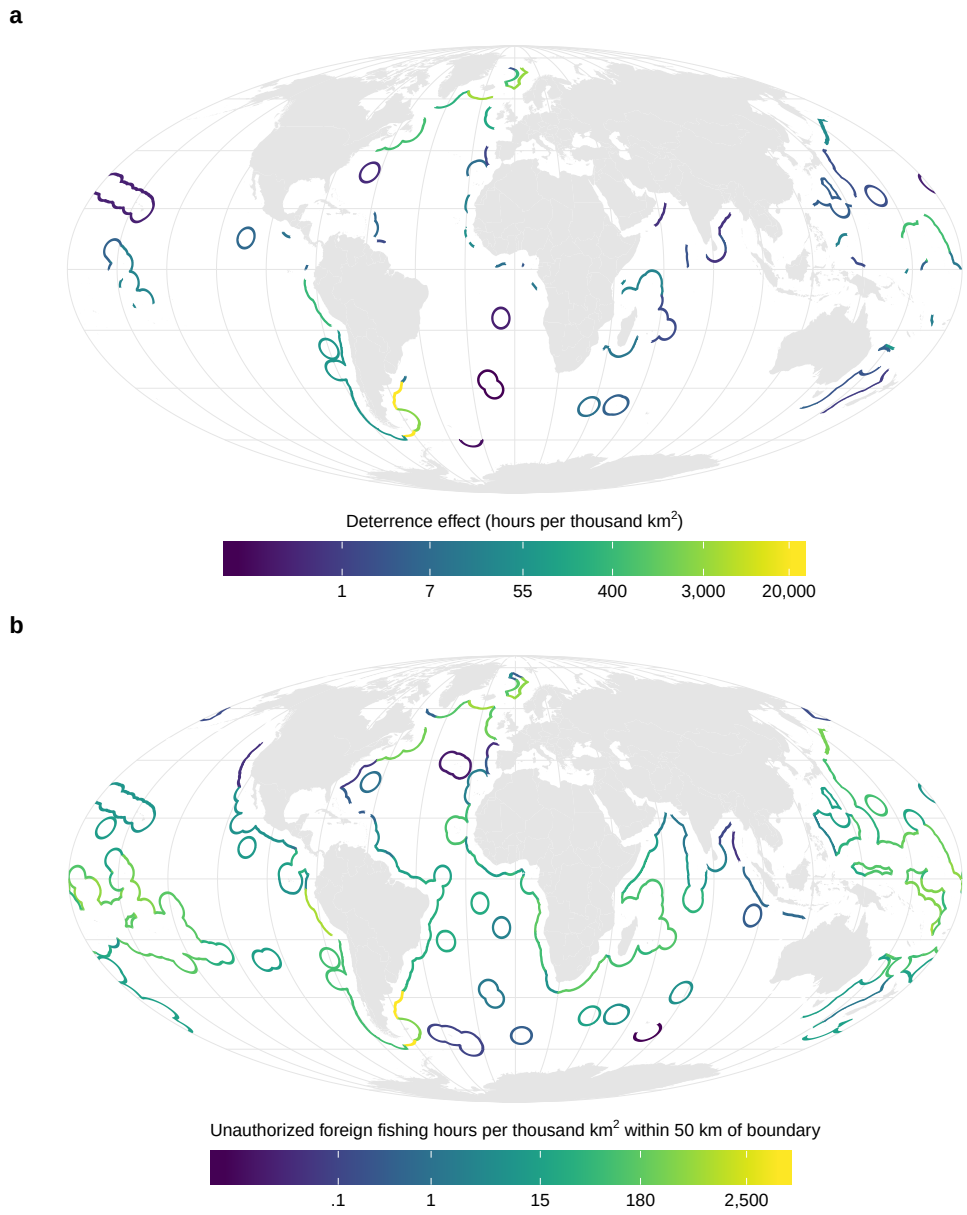

Notes: 50 km buffers around each EEZ-sea region's high seas boundary are filled. a, EEZ-sea region deterrence effects. I estimate an individual deterrence effect for all EEZ-sea regions, but only fill the buffers of EEZ-sea regions that deter unauthorized foreign fishing (see Section 2.4). b, Total hours of unauthorized foreign fishing effort between 2012 and 2016 within 50 km of each EEZ-sea region's high seas boundary, divided by the total surface area in thousands of km^2 within 50 km of each EEZ-sea region's high seas boundary.

I find that 10 EEZ-sea regions account for 97% of the total deterrence effect. These EEZ-sea regions belong to Argentina, Iceland, Norway, the Faroe Islands, the Falkland Islands, Canada, the Marshall Islands, and Peru. Vulnerable species that occur in these EEZ-sea regions, such as Argentine Angelshark, Greenland Shark, and Atlantic Halibut, are being protected by the existence of EEZs (Cuevas et al., 2019; Kyne et al., 2006; Sobel, 1996). However, the remaining EEZ-sea regions either have small deterrence effects (56 EEZ-sea regions) or do not deter unauthorized foreign fishing at all (112 EEZ-sea regions). The latter group of EEZ-sea regions are unfilled in Figure 2.3a. 83 of these 112 EEZ-sea regions have enough unauthorized foreign fishing effort near their high seas boundaries to estimate a deterrence effect (see Section 2.4 and Figure B.9). I find no deterrence effect for these 83 EEZ-sea regions because I estimate that they have slightly higher unauthorized foreign fishing effort just inside their EEZ boundary.

Economic theory predicts that more valuable EEZs could deter more unauthorized foreign fishing because enforcement effort is more profitable for property rights holders of more valuable resources (Arnason, 2013; Demsetz, 1967; Kaffine, 2009; Sutinen & Ande, 1985) (see Section B.5). I use average net primary productivity (NPP) within 50 km of each EEZ-sea region's high seas boundary as a proxy for "fishery value" near the boundary. I chose NPP as my proxy measure for fishery value for three reasons. First, regions with higher NPP can support a more abundant fishery, all else equal (Watson et al., 2014). Second, NPP primarily depends on sunlight, nutrients and temperature, as opposed to fishing effort or fisheries management (Behrenfeld & Falkowski, 1997; Cullen, 2001). NPP can therefore be thought of as an exogenous measure of fishery value near the boundary. Finally, NPP can be measured from satellites at a high spatial resolution (see Section B.1), enabling us to compute average NPP between 2012 and 2016 for each of the EEZ-sea regions using only NPP observations that fall within 50 km of each EEZ-sea region's high seas boundary.

I divide all EEZ-sea regions into groups according to their average NPP and estimate the average deterrence effect for EEZ-sea regions in each group. The EEZ-sea regions that deter unauthorized foreign fishing are those that are most valuable near their high seas boundaries (Figure 2.4). These results are consistent with countries choosing enforcement levels by comparing the benefits of enforcement (e.g., more fish for domestic and authorized foreign fishers to catch) with the costs (e.g., spending on patrol vessels and aircraft).

Future research could examine whether other policies or variables, such as Regional Fisheries Management Organizations or availability of fishing capital, also help explain heterogeneity in deterrence effects. I find no relationship between deterrence effects and fish stock movement patterns (Figure B.10).

Figure 2.4: EEZ-sea regions that are more valuable near their high seas boundaries deter more unauthorized foreign fishing

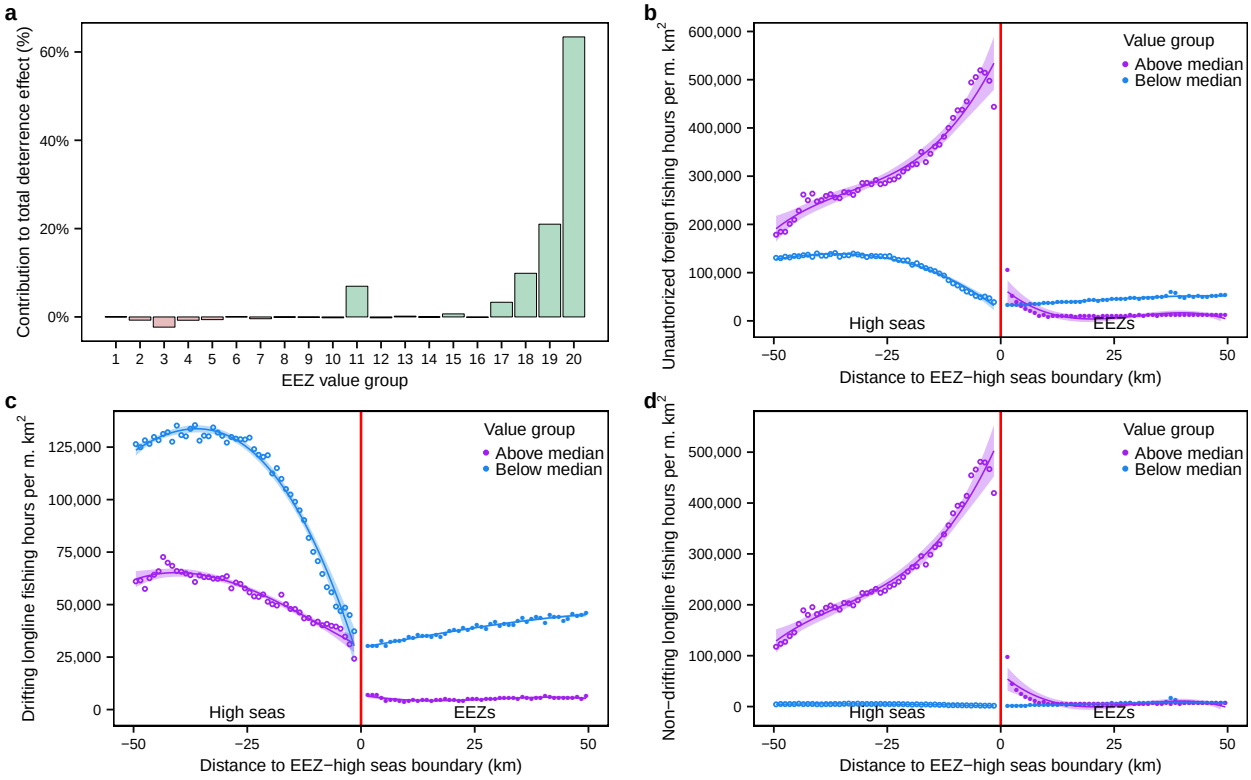

Notes: a, Contribution of each EEZ value group to the total deterrence effect. EEZ-sea regions were divided into 20 groups of equal size based on each EEZ-sea region's average net primary productivity (NPP) within 50 km of its high seas boundary (see Section 2.4). I estimate a deterrence effect for each EEZ value group, and divide each group's effect by the sum of all groups' deterrence effects. EEZ value groups that contribute a positive percentage (green) deter unauthorized foreign fishing. Hours per million km2 of AIS (b) unauthorized foreign fishing for all gear types, (c) unauthorized foreign drifting longline fishing, and (d) unauthorized foreign non-drifting longline fishing in EEZ-sea regions with above median (purple) and below median (blue) average NPP. Points are data. Lines are ordinary least squares third-order polynomial fits in distance to the boundary. 95% confidence intervals (shaded) are estimated using standard errors that account for heteroscedasticity and serial correlation (Newey & West, 1987).

2.3 Discussion

If enforcement levels depend on the benefits and costs enforcement entities yield from enforcement, my results could have implications for the recently convened UN Intergovernmental Conference on Marine Biodiversity of Areas Beyond National Jurisdiction (BBNJ). One of the primary goals of the conference is to create new marine protected areas (MPAs) on the high seas (United National General Assembly, 2018). These MPAs could have even higher enforcement costs than EEZs because of their remoteness and would offer fewer direct benefits to enforcing entities because catch would be restricted. Consequently, they might not incentivize enough enforcement to deter illegal fishing, limiting their ecological and economic benefits. BBNJ negotiators could also consider extending property rights to high seas regions as an alternative or complement to high seas MPAs (Hannesson, 2011).

Previous research has shown that assigning property rights to individuals within a country reduces fishery overexploitation (Arnason, 2013; Costello et al., 2008). In this paper, I am the first to show that assigning property rights across countries leads to the protection of fisheries from unauthorized fishing. My results suggest property rights institutions can enable effective governance of global marine resource use, particularly for resources that are valuable enough to justify enforcement costs. Future research could further analyze this relationship and directly connect deterrence effects to fish stocks and other ecological outcomes. Just as economic incentives matter for individual fishers, the incentives faced by resource managers shape enforcement decisions and conservation outcomes.

2.4 Methods

Data processing

First, I filter EEZ-sea polygons to those that are 200 nm wide and share a boundary with the high seas (Figure B.2). Nations with fewer than 400 nm of ocean separating them typically divide the available ocean area equally. I only use EEZ boundaries that are 200 nm from shore and border the high seas in the analysis.

I create buffer regions along each EEZ-sea polygon's high seas boundary. I create 50 outer buffers for each EEZ-sea polygon and 50 inner buffers. Each buffer is 1 km wider than the previous, and the buffers range from 1 km to 50 km wide. Outer buffers are cropped to the high seas and inner buffers are immediately adjacent to outer buffers. Figure 2.1a shows the union of Argentina's 50 km outer buffer and 50 km inner buffer.

I use grid cell centers to calculate the distance of fishing effort, vessel presence, NPP, ocean depth, and sea surface temperature (SST) observations to an EEZ-high seas boundary. Specifically, I record the buffers each grid cell center intersects, define the distance of the grid cell to the boundary as the minimum width buffer the grid cell intersects, and subtract .5 km. For example, a grid cell center that intersects the 48 km, 49 km, and 50 km inner buffer of an EEZ-sea region would be classified as being 47.5 km inside the EEZ-sea region

(intersecting the 48 km buffer means the grid cell center is between 47 and 48 km from the boundary). I refer to data that have been processed in this way as being in "integer bins". This procedure of grouping grid cells into integer bins is identical to (but computationally faster than) calculating the distance of each grid cell to the nearest EEZ-high seas boundary, rounding up to the nearest integer, and subtracting .5.

Grid cell centers that occur on the high seas are matched to the nearest EEZ-sea region. For example, a fishing observation in the 13-14 km integer bin outside Argentina's EEZ on the high seas and in the 19-20 km integer bin outside the Falkland Islands' EEZ on the high seas would be matched to Argentina's EEZ. Ties are randomly assigned to a single EEZ-sea region.

I use the vessel's flag state, the date of fishing activity, EEZ access agreements data, and the nearest EEZ-sea region to the vessel to separate AIS fishing into three vessel type categories: unauthorized foreign fishing, authorized foreign fishing, and domestic fishing. For example, a Spanish-flagged vessel fishing in the 30-31 km integer bin outside Sierra Leone's EEZ on the high seas on December 4, 2015 would be classified as unauthorized foreign fishing if no access agreement exists between the EU and Sierra Leone for this time period. If there is an access agreement in effect for this time period, this fishing activity would be classified as authorized foreign fishing. Finally, a Sierra Leonean-flagged vessel fishing in the 30-31 km integer bin outside Sierra Leone's EEZ on any day would be classified as domestic fishing. The same classification scheme applies to fishing that occurs inside EEZ-sea regions.

I drop all observations in a given integer bin if some or all grid cells in this integer bin overlap an EEZ-high seas boundary. The number of integer bins dropped depends on the spatial resolution of each dataset. I drop AIS fishing observations that are between 0 and 1 km inside or outside an EEZ-sea region because some grid cells whose centers are inside a 0-1 km inner integer bin or 0-1 km outer integer bin overlap a high seas boundary (at the equator, grid cells in this dataset are approximately 1.1 by 1.1 km). Similarly, I drop nighttime vessel observations within 1 km of an EEZ-high seas boundary because the pixel size of the satellite imagery used to create this data is 742 by 742 m (Elvidge et al., 2015). To create the data used for Figure B.1, I drop NPP data within 5 km of an EEZ-high seas boundary, ocean depth data within 1 km of a boundary, and SST data within 3 km of a boundary.

I divide the raw amount of fishing effort in each integer bin by the surface area of ocean in that integer bin to account for potentially different surface areas in each integer bin. For example, there is slightly less surface area between 1 and 2 km inside an EEZ than there is surface area between 1 and 2 km outside an EEZ. I choose the magnitude of the denominator (e.g. thousand km^2 or million km^2) so that the normalized fishing effort (e.g. hours of fishing per thousand km^2) is the same order of magnitude as the raw amount of fishing effort.

Empirical strategy

I use the 200 nm boundary between EEZs and the high seas as a regression discontinuity (RD) to estimate the effect of EEZs on fishing effort (Imbens & Lemieux, 2008). RD designs

are a commonly used statistical model in social science research (Cattaneo et al., 2019). RD designs can be applied when the researcher has institutional knowledge that treatment assignment partially or completely depends on whether a unit is above a known cutoff value. The discontinuous change in treatment assignment at the cutoff value is used to estimate the effect of treatment by comparing units that are just below the cutoff value to units that are just above the cutoff value. For example, RD designs have been used to estimate the effect of parents' unauthorized immigration status on the health of their children by comparing the children of mothers with birthdates close to the Deferred Action for Childhood Arrivals (DACA) eligibility cutoff (Hainmueller et al., 2017); the effect of harsher punishments on driving under the influence (DUI) by comparing drivers with Blood Alcohol Content levels close to legal thresholds at which DUI penalties become discontinuously more severe (Hansen, 2015); and the effect of Superfund-sponsored cleanups of hazardous waste sites on local housing markets by comparing housing markets with hazardous waste sites whose Hazardous Ranking System score was close to a Superfund-eligibility cutoff (Greenstone & Gallagher, 2008). Section B.2 contains a formal description of the RD design.

Figure 2.2 data processing and estimation details

To create the data used in Figure 2.2, I summed fishing effort over all EEZ-sea regions and over all days to obtain total fishing effort by distance to any EEZ-high seas boundary. Then I divided total fishing effort in each integer bin by the integer bin's total surface area in millions of km^2. For example, the leftmost point in Figure 2.2a is the total hours of AIS fishing effort per million km^2 that occurred between 49 and 50 km outside any EEZ between 2012 and 2016. Similarly, the rightmost point in Figure 2.2b is the total count of nighttime lit fishing vessels per million km^2 that occurred in any EEZs' 49-50 km inner integer bin in 2017.

After summing the data, I estimate the following equation via ordinary least squares regression:

$$Y_i = \alpha + \tau D_i + \sum_{k=1}^{3} \beta_k X_i^k + D_i \sum_{k=1}^{3} \gamma_k X_i^k + u_i \tag{2.1}$$

where Y_i denotes fishing effort in a given integer bin, D_i is an indicator variable that equals 1 for observations inside an EEZ and equals 0 for observations outside an EEZ, Greek letters denote coefficients, k denotes polynomial order, and u_i denotes the error term. The parameter of interest is τ, the treatment effect of EEZs on fishing effort. If τ is estimated to be less than 0, then fishing effort is discontinuously lower just inside EEZs compared to just outside EEZs. I control for third-order polynomials in distance to an EEZ-high seas boundary that are allowed to differ for observations inside an EEZ and for observations outside an EEZ. My results are robust to alternative polynomial orders and to local linear specifications (available upon request). My confidence intervals account for heteroscedasticity and serial correlation (Newey & West, 1987). The optimal lag for these confidence intervals was calculated using

the procedure in Newey and West (1994). Table B.1 contains numeric estimates of the effects of EEZs corresponding to Figures 2.2a-d.

Figure 2.3 data processing and estimation details

There are 178 EEZ-sea regions with more than zero AIS fishing hours within 50 km of their high seas boundary. In Figure 2.3a, I estimate Equation 2.1 separately for each EEZ-sea region using hours of unauthorized foreign fishing per thousand km^2 as the dependent variable. There are 98 observations for each EEZ-sea region (one for each integer bin; recall that AIS integer bins within 1 km of an EEZ-high seas boundary are dropped in the data processing stage). The dependent variable is calculated by summing hours of unauthorized foreign fishing in a given EEZ-sea region's integer bin over days (2012-2016) and dividing by the surface area of that integer bin in thousands of km^2. I plot each EEZ-sea region's estimated deterrence effect ($\hat{\tau}$) in Figure 2.3a. For both Figures 2.3a and 2.3b, the area filled is the union of each EEZ-sea region's 50 km inner buffer and 50 km outer buffer.

In Figure 2.3a, 83 EEZ-sea regions are unfilled because they have no deterrence effect ($\hat{\tau} > 0$). The extent to which unauthorized foreign fishing is slightly higher just inside these EEZs is not informative—the meaningful information content is that they are not deterring unauthorized foreign fishing. These 83 EEZ-sea regions are displayed in Figure B.9. 29 additional EEZ-sea regions are unfilled in Figure 3a because these EEZ-sea regions have fewer than 10 total hours of unauthorized foreign fishing within 50 km of their high seas boundary. 17 of these 29 EEZ-sea regions have zero unauthorized foreign fishing hours within 50 km of their high seas boundaries.

Figure 2.4 data processing and estimation details

I calculate average NPP within 50 km of each EEZ-sea region's high seas boundary as a proxy for "fishery value" near the boundary. For each EEZ-sea region, I record the grid cell centers that fall within 50 km of the high seas boundary. In this case, I do not drop grid cells that overlap the boundary. I calculate average NPP for each EEZ-sea region between 2012 and 2016, weighting grid cell values by their surface area and by the number of days each NPP composite represents (the last composite in each year represents fewer than 8 days). In creating the data for Figure 2.4, grid cell centers that intersect multiple EEZ-sea regions' outer buffers are not assigned to only one EEZ-sea region. They contribute to the average NPP for all EEZ-sea regions they intersect because my goal for Figure 2.4 is to calculate average NPP within 50 km of each EEZ-sea region's high seas boundary.

For Figure 4a, I grouped the 178 EEZ-sea regions with more than zero AIS fishing hours into 20 quantiles according to their average NPP value (8 or 9 EEZ-sea regions in each group). I estimated the following equation via ordinary least squares regression:

$$Y_{ij} = \alpha_j + \tau_j D_{ij} + \sum_{k=1}^{3} \beta_{jk} X_{ij}^k + D_{ij} \sum_{k=1}^{3} \gamma_{jk} X_{ij}^k + u_{ij} \tag{2.2}$$

where the subscript j represents an observation's NPP group and all other terms are as defined in Equation 2.1. The dependent variable is hours of unauthorized foreign fishing per thousand km^2 for a given EEZ-sea region and integer bin (same dependent variable as Figure 2.3a). There are 17,444 observations in this regression (178 EEZ-sea regions $\times$ 98 integer bins). I estimate one deterrence effect for all EEZ-sea regions in a given NPP group (20 estimated deterrence effects), controlling for third-order polynomials in distance to an EEZ-high seas boundary that are different for observations inside an EEZ and for observations outside an EEZ, and different for each NPP group (2 third-order polynomials for each NPP group $\times$ 20 NPP groups). I plot each NPP group's deterrence effect divided by the sum of all NPP groups' deterrence effects. The bars in Figure 2.4a add up to 1.

In Figures 2.4b-d, I categorize the 178 EEZ-sea regions with more than zero AIS fishing hours into those that are above and below median average NPP. Then I sum hours of AIS unauthorized foreign fishing over all EEZs that are above or below median average NPP, and divide by the surface area of each applicable integer bin in millions of km^2. Figure 2.4b is equivalent to Figure 2.2c, except that unauthorized foreign fishing has been divided into these two NPP groups. In Figure 2.4c, I filter the data to unauthorized foreign drifting longline fishing (47% of unauthorized foreign fishing hours within 50 km of an EEZ-high seas boundary; see Table B.2). In Figure 2.4d, I filter the data to all other unauthorized foreign fishing (all gear types other than drifting longline fishing). EEZ-sea regions with below median NPP have discontinuously higher non-drifting longline unauthorized foreign fishing just inside their EEZs (Figure 4d). In all cases, EEZ-sea regions with higher NPP (more valuable near the boundary) have larger deterrence effects.

Data availability

All data used in the analysis are publicly available. In Section B.1, I describe the data used in the analysis in detail and specify how all data can be downloaded or obtained.

Code availability

Replication code is available at https://github.com/englander/replication_eez.

Chapter 3

Armed conflict increases elephant poaching

3.1 Introduction

Between 2002 and 2014, more than 100 armed, intergroup conflicts began near elephant habitat in Africa and Asia. In the same period, many elephant populations have been decimated by poaching (Chase et al., 2016; Thouless et al., 2016; Wittemyer et al., 2014). In this paper, I exploit variation over space and time in conflict onset to estimate the effect of conflict on elephant poaching.

Existing research has built strong suggestive evidence that conflict increases poaching. For example, poaching effort has been shown to increase during conflict when combatants use ivory to fund their operations (Beyers et al., 2011; Hatton et al., 2001). Researchers have also shown that anti-poaching enforcement decreases when park rangers are targeted by combatants or when international organizations withdraw from the conflict zone (Beyers et al., 2011; Dudley et al., 2002; Hanson et al., 2009; Yamagiwa, 2003). Most recently, Daskin and Pringle (Daskin & Pringle, 2018) find an association between years of conflict and declining large wild herbivore populations in African protected areas.

One limitation of existing research is that both conflict and poaching are likely caused by factors that are unobservable or difficult to measure accurately, such as institutional quality (Blattman & Miguel, 2010; Dudley et al., 2002; Gaynor et al., 2016; Hanson et al., 2009). Omitting such variables from analysis biases estimates of the effect of conflict on poaching (Angrist & Pischke, 2008). Given that funding for anti-poaching enforcement is limited, understanding the causal effect of conflict on poaching would enable policymakers and conservation practitioners to better allocate funding among conservation priorities and respond when conflict occurs.

My regression models control for all time-invariant site characteristics, all location-invariant temporal effects, and flexible functions of temperature and precipitation. After controlling for these variables, the estimates are causal as long as the remaining variation in

Figure 3.1: MIKE sites and data processing example

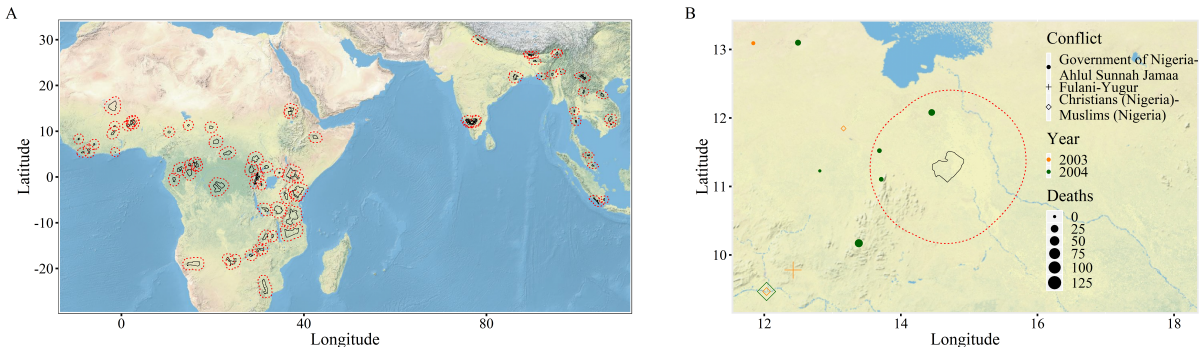

Notes: **A**, MIKE site boundaries (black) and 100 km buffers (red). Some MIKE sites have multiple boundary polygons associated with them. The 100 km buffers were drawn around each boundary polygon, and then unioned by MIKE site. **B**, Conflict onset calculation for Waza National Park, Cameroon, in 2004. The conflict between the Government of Nigeria and Ahlul Sunnah Jamaa began in 2004 because there were fewer than 25 battle deaths associated with this conflict in 2003 and more than 25 battle deaths associated with this conflict in 2004. Conflict onset occurs for Waza National Park in 2004 because at least one of the battles in the Government of Nigeria-Ahlul Sunnah Jamaa conflict in 2004 occurred within 100 km of Waza National Park.

omitted variables is not correlated with both conflict onset and poaching (see Section 3.4). I relax this assumption and test it indirectly using several different methods. Overall, this empirical approach—the best available given the nature of conflict and poaching—seems to yield estimates that are plausibly causal.

The Monitoring the Illegal Killing of Elephants (MIKE) program has operated since 2002 and includes data from 77 sites in 39 countries across Africa and Asia (Figure 3.1A). MIKE's data collection methodology allows for a measure of poaching called the Proportion of Illegally Killed Elephants (PIKE). Each year, each site's PIKE equals the number of observed poached elephant carcasses divided by the total number of observed elephant carcasses. PIKE is a relatively reliable measure of poaching because it is independent of surveyor effort and elephant population stock under an assumption discussed below. Intensive studies of a small number of MIKE sites find that PIKE accurately represents mortality patterns (Jachmann, 2012; Kahindi et al., 2010). Table C.1 provides summary statistics of the MIKE data.

Conflict onset is a commonly used measure of conflict (Bazzi & Blattman, 2014; Blattman & Miguel, 2010; Miguel et al., 2004), and is the preferred measure in this paper for several reasons. As opposed to measures of conflict intensity, such as number of human deaths, conflict onset's implementation in a regression framework requires no assumptions on the structure of its relationship with poaching. Onset events are discrete shocks to the incentives

and resources available to potential poachers and anti-poaching authorities. This characteristic makes onset events arguably more exogenous with respect to poaching than measures of conflict intensity. It also gives conflict onset more statistical power to identify changes in poaching levels. For example, a new conflict beginning will tend to induce greater variation in the behavior of park rangers than would a change in conflict intensity.

A conflict, defined by a unique pair of actors (e.g. Government of Nigeria vs. Ahlul Sunnah Jamaa), is active in a given year if 25 or more battle deaths were associated with it that year (Sundberg & Melander, 2013). I define a conflict to begin this year if last year there were fewer than 25 battle deaths, and this year there were 25 or more battle deaths. My results are robust to using different battle death thresholds to define onset events (Figure C.1).

I connect conflict onset events to MIKE sites by drawing a buffer around each MIKE site, and checking for each site-year whether a battle occurred within the buffer that belongs to a conflict that began that year. Figure 3.1B displays an example of this procedure for one site-year. Compared to all other conflict onset events in Africa and Asia between 2002 and 2014, onset events that occur close to MIKE sites are more likely to involve non-state actors killing civilians (Table C.2). This difference is consistent with rebel groups and terrorists exploiting local populations, in part by poaching their elephants (Christy & Stirton, August 12, 2015).

3.2 Results

Contemporaneous effect

I find that the onset of a new conflict within 100 km of a MIKE site significantly increases contemporaneous PIKE in that MIKE site by .057 to .103 (Table 3.1). Relative to the average PIKE for the entire data (.467), these estimates represent an increase in poaching of 12-22%. This result persists even when additionally controlling for site-specific trends (Column 2), or country-by-year indicator variables (Column 3). These results are robust to using different buffer distances to link onset events to MIKE sites, using different measures of poaching and different estimation procedures, using different measures of conflict, and using MIKE data between 2002 and 2017 without weather control variables (Figure C.2 and Tables C.3 to C.5, respectively). The estimate from the preferred specification in Table 1, Column 1 is more than 2.5 times larger than the estimated upper bound on bias from omitted variables (Altonji et al., 2005), indicating that unobservables correlated with conflict onset and poaching are not driving these results (see Section 3.4).

Temporal dynamics

Conflict onset has both an immediate and a persistent effect on poaching levels, exacerbating its negative impact (Figure 3.2). In the years before conflict onset, poaching levels are

Table 3.1: Conflict onset increases contemporaneous poaching

	Site and year fixed effects	With site trends	With country-by-year fixed effects
Conflict onset	0.103***	0.057**	0.082*
	(0.031)	(0.025)	(0.042)
R-squared	0.567	0.714	0.848

Notes: Coefficients represent the effect of conflict onset on contemporaneous poaching, where poaching is measured by PIKE. All regressions are estimated by ordinary least squares with 631 observations, and include MIKE site fixed effects, year fixed effects, and third-order polynomials in temperature and precipitation as control variables (see Methods). Column 2 adds MIKE site-specific trends to the base specification. Column 3 adds country-by-year fixed effects to the base specification (which subsume the year fixed effects). Clustered standard errors at the country-level are displayed in parentheses and are estimated by bootstrapping with replacement at the country-level (1,000 replications). ***P < 0.01; **P < 0.05; *P < 0.1.

relatively constant, indicating that fighters already present in the area are not increasing poaching to fund an anticipated conflict (no reverse causality). At conflict onset, there is a spike in poaching. Relative to poaching in the year before onset, PIKE increases by .25, a more than 50% increase relative to its mean value. Poaching then slowly declines to baseline levels in the years following the onset event. These sensible temporal dynamics provide further evidence that conflict onset has a causal effect on poaching.

PIKE assumption and reliability of PIKE data

PIKE is independent of population stock and surveyor effort if, conditional on the number of poached and non-poached carcasses available to discover, the probability of finding a poached carcass equals the probability of finding a non-poached carcass (Burn et al., 2011; Hsiang & Sekar, 2016). Violations of this assumption that are uncorrelated with conflict onset induce classical measurement error, which would attenuate my estimates but not cause bias. However, my estimates would be biased if this assumption is systematically violated at conflict onset. For example, if fighters occupy part of a MIKE site and prevent rangers from surveying the area, the probability of detecting poached carcasses may decrease. In this case, my estimates are biased downward and conflict onset actually has an even larger effect on poaching. If instead conflict onset leads to improved intelligence gathering and poached carcass detection increases, I would overestimate the effect of conflict onset on poaching. Reassuringly, even if the probability of detecting a poached carcass becomes up to 35% higher at conflict onset (and is unchanged for all other observations in which conflict onset

Figure 3.2: Temporal dynamics of poaching with respect to conflict onset

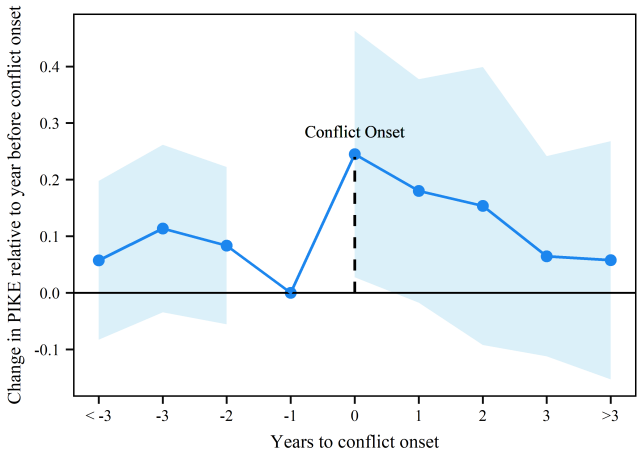

Notes: Each point estimate represents the change in PIKE relative to the year before conflict onset (the omitted category). Regressors used as controls: site fixed effects, year fixed effects, and third-order polynomials in temperature and precipitation. Standard errors are estimated by cluster bootstrapping with replacement at the country-level (1,000 replications). 95% confidence intervals are displayed. N = 631.

does not occur), the effect of conflict onset on PIKE would still be statistically significant at the 95% level after "correcting" for this bias and re-estimating the Table 1, Column 1 regression (Figure C.3).

Conflict onset also does not seem to affect the availability of poaching data (no selective attrition). While poaching data only exists for 631 out of 1,078 possible site-year combinations, the conflict data is comprehensive. The proportion of site-years missing poaching data if conflict onset occurs is 39.4% and is 36.5% if conflict onset does not occur (p-value from a two-sided t-test equals .52). Further, I find that conflict onset does not affect elephant natural mortality, providing indirect evidence that carcasses are classified accurately (Table C.6). To the extent that natural mortality carcass count is an indicator of surveyor effort (conditional on control variables), this null result also suggests that conflict onset does not affect surveyor effort.

3.3 Discussion

As poaching continues to threaten the survival of elephants in the wild, causal estimates of the drivers of poaching can help better allocate limited anti-poaching effort and funds. In this paper, I find that conflict onset causes a substantial increase in poaching. This evidence

supports previous appeals to governments and international conservation organizations to increase support for park rangers during periods of conflict, as rangers and associated law enforcement personnel can help to mitigate the negative effects of conflict on wildlife (Beyers et al., 2011; Dudley et al., 2002; Yamagiwa, 2003).

By using a similar approach as in Figure 3.2, I estimate that ∼30% of poached carcasses in the MIKE data set are attributable to the contemporaneous and persistent effects of conflict (see Section 3.4). By extrapolation, I calculate that conflict is responsible for the illegal killing of about 80,000 elephants in Africa and Asia between 2002 and 2014. For comparison, there are about 600,000 elephants remaining in the wild (Sukumar, 2006; Thouless et al., 2016).

Elephant poaching–and wildlife and habit conservation as a whole–are emotional, salient, and complex problems that could be better addressed with more empirical evidence on the causes of negative outcomes. While I cannot distinguish between the various channels through which conflict affects poaching, this paper is nevertheless the first to present plausibly causal estimates of a driver of site-level poaching dynamics for any species. The wide spatial and temporal range of the data used to obtain these estimates supports their external validity. Future work on identifying channels through which conflict affects poaching will need to balance the use of micro-level data without limiting analysis to a small subset of locations and years.

3.4 Methods

Poaching Data

I use publicly available data on the numbers of carcasses found for each MIKE site and year (Convention on International Trade in Engangered Species, Accessed Feb. 6, 2017). During the course of regular patrols, rangers and associated personnel record each elephant carcass observed and attempt to determine whether the elephant was poached (Burn et al., 2011). Thus for each site-year, two values are recorded: the number of poached carcasses and the total number of carcasses, from which the number of non-poached carcasses (i.e. natural mortality) can be inferred. MIKE sites contain 30-40% of wild elephants (Convention on International Trade in Engangered Species, 2016). In constructing the poaching data I use in the regressions, I dropped three MIKE sites with only one observation. Because I include a separate indicator variable for each site in all regressions ("site fixed effects"), these three sites would not have contributed to my estimates.

Conflict Data

I use the publicly available Uppsala Conflict Data Program (UCDP) Georeferenced Event Dataset (Croicu & Sundberg, Accessed Feb. 6, 2017; Sundberg & Melander, 2013). Each row of this dataset corresponds to an armed battle event and contains the day the battle occurred, GPS coordinates, estimated number of battle deaths, a news source, and the actors

involved. The dataset uses conflict identifiers to group events by unique actor pairs. For example, Lord's Resistance Army vs. Government of Uganda is one conflict, and Lord's Resistance Army vs. civilians is a different conflict. In constructing the conflict data I use in the analysis, I excluded battles where only the country in which the battle took place was known. Battles that occur within MIKE site boundaries are included when connecting onset events to MIKE sites. Conflicts with battles occurring outside MIKE site buffers may still assign onset status to a given MIKE site as long as at least one battle occurs within the MIKE site buffer.

Importance of controlling for temperature and precipitation

As MIKE sites and their surrounding areas are primarily rural, variation in agricultural yields and wages could affect both poaching and the probability of conflict onset. Even if such data was available for all site-years, controlling for agricultural yields, for example, would be a "bad control" because conflict onset likely affects yields (Angrist & Pischke, 2008). Therefore, flexibly controlling for temperature and precipitation, which are not affected by conflict onset and poaching, is the best available approach. It is also important to control for precipitation because low precipitation levels can cause elephant mortality, which reduces PIKE by inflating its denominator (Dudley et al., 2001). As low precipitation levels also increase conflict onset (Miguel et al., 2004), not controlling for precipitation would bias my estimates downward. None of my regression specifications yield statistically significant relationships between poaching and temperature or between poaching and precipitation. Nevertheless, it is important to control for temperature and precipitation because of their theoretical importance as potential determinants of both conflict onset and poaching.

Weather data

I use publicly available data from the University of Delaware to control for third-order polynomials in temperature and precipitation (Matsuura & Willmott, 2015). This data provides cumulative monthly precipitation and mean monthly temperature data at a .5 degree resolution until 2014. I first calculate squared and cubed terms for each grid cell. Then I spatially aggregate grid cells to the site-level by weighting cell values by the proportion of area they make up of a MIKE site and its buffer. Finally, I sum over months in the same year to obtain a third-order polynomial in cumulative annual precipitation for each site-year, and weight monthly mean temperature by the days in a year each month makes up to obtain a third-order polynomial in mean temperature for each site-year.

Regression estimation

In my preferred specification in Table 3.1, Column 1, I estimate the following multivariate panel regression using ordinary least squares:

$$\begin{aligned} PIKE_{sct} =& \beta Onset_{sct} + \gamma_s + \delta_t + \\ & \sum_{k=1}^{3} \alpha_k temp_{sct}^k + \sum_{k=1}^{3} \theta_k precip_{sct}^k + \epsilon_{sct} \end{aligned} \tag{3.1}$$

where s indexes site, c indexes country, t indexes year, γ_s are site fixed effects (separate indicator variable for each site), δ_t are year fixed effects (separate indicator variable for each year), and k indicates the term of the third-order polynomial in temperature and precipitation. The distribution of residuals from estimating this equation is approximately normal (Figure C.4). The coefficient on conflict onset (β) is causally identified if $Onset_{sct}$ is uncorrelated in expectation with ϵ_{sct} (time-varying, within-site unobservable determinants of $PIKE_{sct}$).

Unobservable changes over time at particular sites that affect both poaching and conflict onset, such as a deterioration in local institutions, could violate this assumption. The Table 1, Column 2 regression adds site-specific trends ($\gamma_s t$) to the controls in Equation 1. The estimated effect in this specification is slightly smaller than in the preferred specification, but its statistical significance implies that these types of unobservable changes are not driving my results.

Time-varying, country-level shocks are another threat to the above assumption. For example, changes in political or economic conditions, such as a coup or export price shock, or changes in national anti-poaching policy, could simultaneously affect poaching and the probability of conflict onset. The Table 1, Column 3 regression controls for all such confounders by replacing the year fixed effects in Equation 1 with country-by-year fixed effects (δ_{ct}). This specification yields a similar estimate as Equation 1, indicating that my results are not due to time-varying, country-level confounders.

MIKE sites in the same country may have serially correlated errors. I therefore estimate standard errors in all ordinary least squares regressions by cluster bootstrapping with replacement at the country-level (1,000 replications). Clustering at the country-level allows the errors of sites in the same country to be arbitrarily correlated across all time periods, but assumes the errors of sites in different countries are uncorrelated. I bootstrap instead of using the standard clustering formula because the small number of countries in my data (39) may make standard errors calculated by the formula too small (Cameron et al., 2008).

Upper bound on omitted variables bias

In case the assumption necessary for Equation 3.1 to estimate a causal effect is violated, it is important to assess the extent to which my estimates are confounded by omitted variables. Altonji et al. (Altonji et al., 2005) provide a proof and method for estimating an upper

bound on omitted variables bias given the following assumption: the relationship between conflict onset and observable determinants of PIKE (control variables) is at least as strong as the relationship between conflict onset and unobservable determinants of PIKE. This assumption is reasonable because of the strong predictive power of my control variables. The site fixed effects are especially relevant because some sites are more prone to conflict than others, for reasons that vary little over the study period. For example, 61% of sites have no conflict onset events in years with poaching data, and Virunga National Park has an onset event every year (results are robust to dropping these sites and re-estimating Equation 3.1).

I estimate the upper bound on omitted variables bias to be .041. My coefficient estimate is .103 (Table 3.1, Column 1), or 2.5 times greater than this upper bound. Therefore, my finding that conflict onset increases poaching is not driven by omitted variables bias.

Estimating temporal dynamics

An event study maps temporal dynamics of the dependent variable relative to the date of treatment (Jacobson et al., 1993). Figure 3.2 presents results from estimating the following regression by ordinary least squares:

$$PIKE_{sct} = \sum_{y=-4}^{4\backslash\{-1\}} \beta_y Onset_{y,sct} + \gamma_s + \delta_t + \sum_{k=1}^{3} \alpha_k temp_{sct}^k + \sum_{k=1}^{3} \theta_k precip_{sct}^k + \epsilon_{sct} \tag{3.2}$$

where subscript y indexes time relative to the year of conflict onset. All other variables and subscripts are as defined for Equation 3.1. For $y < 0$ ($y > 0$), $Onset_{y,sct} = 1$ if conflict onset occurs in y years (occurred y years ago), and equals 0 otherwise. $Onset_{0,sct} = 1$ for site-years with onset events and equals 0 otherwise.

For each observation, I calculate the number of years until the next conflict onset, and the number of years since the most recent conflict onset (within the same MIKE site). This calculation is not affected by missing poaching data because the conflict data is comprehensive. I include indicator variables (the $Onset_{y,sct}$ terms) for observations that occur three years before conflict onset, two years before onset, year of onset, and one, two, and three years after onset. I group observations that occur four or more years before the next conflict onset into an additional indicator variable, and do the same for observations that occur four or more years after the most recent conflict onset. Sites that never have a conflict begin are not included in any of these indicator variables by definition. The year before conflict onset is the omitted category (including it would cause collinearity with site fixed effects).

Extrapolation

I first estimate a modified version of Equation 3.2. Because I want to calculate the number of poached elephants attributable to conflict onset, I use poached carcass count as the dependent variable, add ln(natural mortality count + 1) as an additional control variable, and estimate Equation 3.2 using a negative binomial regression with a log link function. I chose a negative binomial model instead of a Poisson model because of overdispersion in poached carcass counts (Table C.1). Figure C.5 plots the $Onset_{y,sct}$ coefficients and standard errors from this regression. I use this model to predict the number of poached carcasses in the data, and to predict the number of poached carcasses if conflict onset did not occur (set $Onset_{y,sct} = 0$ if $y \geq 0$, then predict). The difference in these two predictions is 2,092 (equal to 30% of total poached carcasses in the MIKE data between 2002 and 2014). The interpretation of this difference is that there would have been 2,092 fewer poached carcasses in the MIKE data if no conflict onset events occurred.

I rely on estimates of the number of African elephants poached between 2010 and 2012 in order to extrapolate from the MIKE data to the total number of elephants poached in Africa and Asia between 2002 and 2014 (Wittemyer et al., 2014). Wittemyer et al. (Wittemyer et al., 2014) estimate that 100,891 African elephants were poached between 2010 and 2012 (average of empirical and model-based method in Table 1 of that paper). These estimates are the best available because there are no peer-reviewed, global estimates of the number of elephants poached each year.

There were 2,743 poached carcasses discovered in MIKE's African sites between 2010 and 2012. Compared to (Wittemyer et al., 2014), a poached carcass discovered at an African MIKE site in this period represents 36.8 poached carcasses ($= \frac{100,891}{2,743}$). Given the strong assumption that this ratio is constant between 2002 and 2014 and holds for Asia as well, conflict onset is responsible for the illegal killing of 76,963 elephants between 2002 and 2014 ($= 2,092 \times 36.8$). This rough extrapolation is meant to emphasize the important contribution of conflict to overall poaching levels.

Data availability

All data required to reproduce this analysis is publicly available and detailed in Section 3.4.

Code availability

All data processing and analysis was completed in R. All R code will be published on GitHub upon publication of this chapter.

Bibliography

Abadie, A., Athey, S., Imbens, G. W., & Wooldridge, J. (2017). *When Should You Adjust Standard Errors for Clustering?* (Working Paper No. 24003). National Bureau of Economic Research.

Abadie, A., Diamond, A., & Hainmueller, J. (2010). Synthetic Control Methods for Comparative Case Studies: Estimating the Effect of California's Tobacco Control Program. *Journal of the American Statistical Association*, *105*(490), 493–505.

Abadie, A., Diamond, A., & Hainmueller, J. (2011). Synth: An R Package for Synthetic Control Methods in Comparative Case Studies. *Journal of Statistical Software*, *42*(13), 1–17.

Abadie, A., & Gardeazabal, J. (2003). The Economic Costs of Conflict: A Case Study of the Basque Country. *American Economic Review*, *93*(1), 113–132.

Acemoglu, D., Makhdoumi, A., Malekian, A., & Ozdaglar, A. (2020). *Testing, Voluntary Social Distancing and the Spread of an Infection* (Working Paper No. 27483). National Bureau of Economic Research.

Agnarsson, S., Matthiasson, T., & Giry, F. (2016). Consolidation and distribution of quota holdings in the Icelandic fisheries. *Marine Policy*, *72*, 263–270.

Altonji, J. G., Elder, T. E., & Taber, C. R. (2005). Selection on Observed and Unobserved Variables: Assessing the Effectiveness of Catholic Schools. *J Polit Econ*, *113*(1), 151–184.

Amante, C. (2009). ETOPO1 1 arc-minute global relief model: Procedures, data sources and analysis [type: dataset]. https://doi.org/10.7289/V5C8276M

Angrist, J. D., & Pischke, J. (2008). *Mostly harmless econometrics: An empiricist's companion*. Princeton University Press.

Anticamara, J., Watson, R., Gelchu, A., & Pauly, D. (2011). Global fishing effort (1950–2010): Trends, gaps, and implications. *Fisheries Research*, *107*(1), 131–136. https://doi.org/10.1016/j.fishres.2010.10.016

Arnason, R. (2013). Individual Transferable Quotas in Fisheries. In J. F. Shogren (Ed.), *Encyclopedia of Energy, Natural Resource, and Environmental Economics* (pp. 183–191). Elsevier.

Asriyan, V., Fuchs, W., & Green, B. (2017). Information Spillovers in Asset Markets with Correlated Values. *American Economic Review*, *107*(7), 2007–40.

Assunção, J., McMillan, R., Murphy, J., & Souza-Rodrigues, E. (2019). *Optimal Environmental Targeting in the Amazon Rainforest* (Working Paper No. 25636). National Bureau of Economic Research.

Barreca, A. I., Guldi, M., Lindo, J. M., & Waddell, G. R. (2011). Saving babies? revisiting the effect of very low birth weight classification. *The Quarterly Journal of Economics*, *126*(4), 2117–2123. https://doi.org/10.1093/qje/qjr042

Barrett, S. (2005). *Environment and statecraft*. Oxford University Press. https://doi.org/10.1093/0199286094.001.0001

Bazzi, S., & Blattman, C. (2014). Economic Shocks and Conflict: Evidence from Commodity Prices. *Am Econ J Macroecon*, *6*(4), 1–38.

Behrenfeld, M. J., & Falkowski, P. G. (1997). Photosynthetic rates derived from satellite-based chlorophyll concentration. *Limnology and Oceanography*, *42*(1), 1–20. https://doi.org/10.4319/lo.1997.42.1.0001

Belhabib, D., Sumaila, U. R., Lam, V. W. Y., Zeller, D., Billon, P. L., Kane, E. A., & Pauly, D. (2015). Euros vs. yuan: Comparing european and chinese fishing access in west africa. *PLOS ONE*, *10*(3), e0118351. https://doi.org/10.1371/journal.pone.0118351

Bellemare, M. F., & Wichman, C. J. (2020). Elasticities and the Inverse Hyperbolic Sine Transformation. *Oxford Bulletin of Economics and Statistics*, *82*(1), 50–61.

Beyers, R. L., Hart, J. A., Sinclair, A. R. E., Grossmann, F., Klinkenberg, B., & Dino, S. (2011). Resource Wars and Conflict Ivory: The Impact of Civil Conflict on Elephants in the Democratic Republic of Congo - The Case of the Okapi Reserve. *PLoS ONE*, *6*(11), e27129. https://doi.org/10.1371/journal.pone.0027129

Blattman, C., Green, D., Ortega, D., & Tobón, S. (2019). *Place-Based Interventions at Scale: The Direct and Spillover Effects of Policing and City Services on Crime* (Working Paper No. 23941). National Bureau of Economic Research.

Blattman, C., & Miguel, E. (2010). Civil War. *J Econ Lit*, *48*(1), 3–57. https://doi.org/10.1257/jel.48.1.3

Boettiger, C., Lang, D. T., & Wainwright, P. C. (2012). Rfishbase: Exploring, manipulating and visualizing FishBase data from r. *Journal of Fish Biology*, *81*(6), 2030–2039. https://doi.org/10.1111/j.1095-8649.2012.03464.x

Burn, R. W., Underwood, F. M., & Blanc, J. (2011). Global Trends and Factors Associated with the Illegal Killing of Elephants: A Hierarchical Bayesian Analysis of Carcass Encounter Data. *PLoS ONE*, *6*(9), e24165. https://doi.org/10.1371/journal.pone.0024165

Cabral, R. B., Mayorga, J., Clemence, M., Lynham, J., Koeshendrajana, S., Muawanah, U., Nugroho, D., Anna, Z., Mira, Ghofar, A., Zulbainarni, N., Gaines, S. D., & Costello, C. (2018). Rapid and lasting gains from solving illegal fishing. *Nature Ecology & Evolution*, *2*(4), 650–658.

Cameron, A. C., Gelbach, J. B., & Miller, D. L. (2008). Bootstrap-based improvements for inference with clustered errors. *Rev Econ Stat*, *90*(3), 414–427.

Castillo, R., Dalla Rosa, L., García Diaz, W., Madureira, L., Gutierrez, M., Vásquez, L., & Koppelmann, R. (2019). Anchovy distribution off Peru in relation to abiotic pa-

rameters: A 32-year time series from 1985 to 2017. *Fisheries Oceanography*, *28*(4), 389–401.

Cattaneo, M. D., Idrobo, N., & Titiunik, R. (2019). *A practical introduction to regression discontinuity designs: Foundations*. Cambridge University Press.

Chamberlain, S., & Reis, R. S. (2017). seaaroundus: Sea Around Us API Wrapper. R package version 1.2.0.

Chase, M. J., Schlossberg, S., Griffin, C. R., Bouché, P. J., Djene, S. W., Elkan, P. W., Ferreira, S., Grossman, F., Kohi, E. M., Landen, K., et al. (2016). Continent-wide survey reveals massive decline in African savannah elephants. *PeerJ*, *4*, e2354.

Christy, B., & Stirton, B. (August 12, 2015). How Killing Elephants Finances Terror in Africa [Available at https://www.nationalgeographic.com/tracking-ivory/article.html]. *National Geographic*.

Convention on International Trade in Engangered Species. (2016). *Report on Monitoring the Illegal Killing of Elephants (MIKE)* [Available at https://cites.org/sites/default/files/eng/cop/17/WorkingDocs/E-CoP17-57-05.pdf].

Convention on International Trade in Engangered Species. (Accessed Feb. 6, 2017). *Numbers of carcasses found for each reporting site and year* [Available at https://cites.org/eng/prog/mike/data_and_reports].

Costello, C., Gaines, S. D., & Lynham, J. (2008). Can Catch Shares Prevent Fisheries Collapse? *Science*, *321*(5896), 1678–1681.

Costello, C., & Grainger, C. A. (2018). Property rights, regulatory capture, and exploitation of natural resources. *Journal of the Association of Environmental and Resource Economists*, *5*(2), 441–479. https://doi.org/10.1086/695612

Costello, C., Ovando, D., Clavelle, T., Strauss, C. K., Hilborn, R., Melnychuk, M. C., Branch, T. A., Gaines, S. D., Szuwalski, C. S., Cabral, R. B., et al. (2016). Global fishery prospects under contrasting management regimes. *Proceedings of the National Academy of Sciences*, *113*(18), 5125–5129.

Croicu, M., & Sundberg, R. (Accessed Feb. 6, 2017). UCDP GED Codebook version 5.0 [Available at http://ucdp.uu.se/downloads/ged/ged50-rdata.zip].

Cuevas, J., Awruch, C., Barreto, R., Charvet, P., Chiaramonte, G., Dolphine, P., Faria, V., Paesch, L., & Rincon, G. (2019). *Squatina argentina* (e.T39329A116841596) [type: dataset]. International Union for Conservation of Nature. https://doi.org/10.2305/IUCN.UK.2019-1.RLTS.T39329A116841596.en

Cullen, J. J. (2001). Primary production methods. In J. H. Steele (Ed.), *Encyclopedia of ocean sciences (first edition)* (pp. 2277–2284). Academic Press. https://doi.org/10.1016/B978-012374473-9.00203-4

Daskin, J. H., & Pringle, R. M. (2018). Warfare and wildlife declines in Africa's protected areas. *Nature*.

Demsetz, H. (1967). Toward a theory of property rights. *The American Economic Review*, *57*(2), 347–359. http://www.jstor.org/stable/1821637

Dudley, J. P., Criag, G. C., Gibson, D. S. C., Haynes, G., & Klimowicz, J. (2001). Drought mortality of bush elephants in Hwange National Park, Zimbabwe. *Afr J Ecol*, *39*(2), 187–194.

Dudley, J. P., Ginsberg, J. R., Plumptre, A. J., Hart, J. A., & Campos, L. C. (2002). Effects of War and Civil Strife on Wildlife and Wildlife Habitats. *Conserv Biol*, *16*(2), 319–329. https://doi.org/10.1046/j.1523-1739.2002.00306.x

Duflo, E., Greenstone, M., Pande, R., & Ryan, N. (2013). Truth-telling by third-party auditors and the response of polluting firms: Experimental evidence from India. *The Quarterly Journal of Economics*, *128*(4), 1499–1545.

Dunn, D. C., Maxwell, S. M., Boustany, A. M., & Halpin, P. N. (2016). Dynamic ocean management increases the efficiency and efficacy of fisheries management. *Proceedings of the National Academy of Sciences*, *113*(3), 668–673.

Elvidge, C. D., Zhizhin, M., Baugh, K., & Hsu, F.-C. (2015). Automatic Boat Identification System for VIIRS Low Light Imaging Data. *Remote Sensing*, *7*(3), 3020–3036.

Englander, G. (2019). Property rights and the protection of global marine resources. *Nature Sustainability*, *2*(10), 981–987.

Erdem, T., Imai, S., & Keane, M. P. (2003). Brand and Quantity Choice Dynamics Under Price Uncertainty. *Quantitative Marketing and Economics*, *1*(1), 5–64.

ESR. (2009). OSCAR third degree resolution ocean surface currents. ver. 1. PO.DAAC, CA, USA [type: dataset]. https://doi.org/10.5067/OSCAR-03D01

FAO. (2018). The State of World Fisheries and Aquaculture 2018 - Meeting the sustainable development goals [Food and Agricultural Organization of the United Nations (FAO)].

Ferraro, P. J., Sanchirico, J. N., & Smith, M. D. (2018). Causal inference in coupled human and natural systems. *Proceedings of the National Academy of Sciences*, 201805563. https://doi.org/10.1073/pnas.1805563115

Fréon, P., Sueiro, J. C., Iriarte, F., Evar, O. F. M., Landa, Y., Mittaine, J.-F., & Bouchon, M. (2014). Harvesting for food versus feed: A review of Peruvian fisheries in a global context. *Reviews in Fish Biology and Fisheries*, *24*(1), 381–398.

Gaynor, K. M., Fiorella, K. J., Gregory, G. H., Kurz, D. J., Seto, K. L., Withey, L. S., & Brashares, J. S. (2016). War and wildlife: Linking armed conflict to conservation. *Front Ecol Environ*, *14*(10), 533–542. https://doi.org/10.1002/fee.1433

Getu, A., Misganaw, K., & Bazezew, M. (2015). Post-harvesting and Major Related Problems of Fish Production. *Fisheries and Aquaculture Journal*, *6*(4).

Gibson, M., & Carnovale, M. (2015). The effects of road pricing on driver behavior and air pollution. *Journal of Urban Economics*, *89*, 62–73.

Gordon, H. S. (1954). The Economic Theory of a Common-Property Resource: The Fishery. *Journal of Political Economy*, *62*(2), 124–142.

Gray, W. B., & Shimshack, J. P. (2011). The Effectiveness of Environmental Monitoring and Enforcement: A Review of the Empirical Evidence. *Review of Environmental Economics and Policy*, *5*(1), 3–24.

Greenstone, M., & Gallagher, J. (2008). Does hazardous waste matter? evidence from the housing market and the superfund program. *The Quarterly Journal of Economics*, *123*(3), 951–1003. https://doi.org/10.1162/qjec.2008.123.3.951

Greenstone, M., & Jack, B. K. (2015). Envirodevonomics: A Research Agenda for an Emerging Field. *Journal of Economic Literature*, *53*(1), 5–42.

Hainmueller, J., Lawrence, D., Martén, L., Black, B., Figueroa, L., Hotard, M., Jiménez, T. R., Mendoza, F., Rodriguez, M. I., Swartz, J. J., & Laitin, D. D. (2017). Protecting unauthorized immigrant mothers improves their children's mental health. *Science*, *357*(6355), 1041–1044. https://doi.org/10.1126/science.aan5893

Hannesson, R. (2013). Exclusive Economic Zone. *Encyclopedia of Energy, Natural Resource, and Environmental Economics* (pp. 150–153). Elsevier.

Hannesson, R. (2011). Rights based fishing on the high seas: Is it possible? *Marine Policy*, *35*(5), 667–674. https://doi.org/10.1016/j.marpol.2011.02.007

Hansen, B. (2015). Punishment and deterrence: Evidence from drunk driving. *American Economic Review*, *105*(4), 1581–1617. https://doi.org/10.1257/aer.20130189

Hansman, C., Hjort, J., León-Ciliotta, G., & Teachout, M. (2020). Vertical Integration, Supplier Behavior, and Quality Upgrading among Exporters. *Journal of Political Economy*, *128*(9), 3570–3625.

Hanson, T., Brooks, T. M., Da Fonseca, G. a. B., Hoffmann, M., Lamoreux, J. F., Machlis, G., Mittermeier, C. G., Mittermeier, R. A., & Pilgrim, J. D. (2009). Warfare in Biodiversity Hotspots. *Conserv Biol*, *23*(3), 578–587. https://doi.org/10.1111/j.1523-1739.2009.01166.x

Hatton, J., Couto, M., & Oglethorpe, J. (2001). Biodiversity and war: A case study of Mozambique.

Hazen, E. L., Scales, K. L., Maxwell, S. M., Briscoe, D. K., Welch, H., Bograd, S. J., Bailey, H., Benson, S. R., Eguchi, T., Dewar, H., et al. (2018). A dynamic ocean management tool to reduce bycatch and support sustainable fisheries. *Science Advances*, *4*(5), eaar3001.

Holland, P. W. (1986). Statistics and Causal Inference. *Journal of the American Statistical Association*, *81*(396), 945–960.

Hollick, A. L. (1977). The Origins of 200-Mile Offshore Zones. *The American Journal of International Law*, *71*(3), 494–500.

Homans, F. R., & Wilen, J. E. (1997). A Model of Regulated Open Access Resource Use. *Journal of Environmental Economics and Management*, *32*(1), 1–21.

Homans, F. R., & Wilen, J. E. (2005). Markets and rent dissipation in regulated open access fisheries. *Journal of Environmental Economics and Management*, *49*(2), 381–404.

Hsiang, S., & Sekar, N. (2016). Does Legalization Reduce Black Market Activity? Evidence from a Global Ivory Experiment and Elephant Poaching Data.

Huang, L., & Smith, M. D. (2014). The Dynamic Efficiency Costs of Common-Pool Resource Exploitation. *American Economic Review*, *104*(12), 4071–4103.

IMARPE. (2018). *Situación del Stock Norte-Centro de la anchoveta peruana (Engraulis ringens) al 01 de Abril de 2018 y perspectivas de explotación para la primera temporada de pesca de 2018*. Instituto del Mar del Perú (IMARPE).

IMARPE. (2019). *Elaboración de la Tabla de Decisión para la determinación del Límite Máximo de Captura Total Permisible por temporada de pesca en la pesquería del Stock Norte-Centro de la anchoveta peruana* (IMP-DGIRP/AFDPERP Edición 4 Revisión 1). Instituto del Mar del Perú (IMARPE).

Imbens, G. W., & Lemieux, T. (2008). Regression discontinuity designs: A guide to practice. *Journal of Econometrics*, *142*(2), 615–635. https://doi.org/10.1016/j.jeconom.2007.05.001

Instituto Humboldt, & SNP. (2017). Segundo conversatorio sobre el diseño de las redes de cerco de anchoveta y el diseño de una red experimental para su uso en Operaciones Eureka [Instituto Humboldt de Investigación Marina y Acuícola (Instituto Humboldt) and Sociedad Nacional de Pesquería (SNP)].

Instituto Humboldt, SNP, & CeDePesca. (2018). Propuesta de modificaciones al régimen sancionador pesquero en relación con las limitaciones de selectividad y el incentivo de prácticas que apoyen la sostenibilidad de la pesquería del recurso anchoveta desde la perspectiva de la pesca industrial [Instituto Humboldt de Investigación Marina y Acuícola (Instituto Humboldt), Sociedad Nacional de Pesquería (SNP), Centro Desarrollo y Pesca Sustentable (CeDePesca)].

Isaksen, E. T., & Richter, A. (2019). Tragedy, Property Rights, and the Commons: Investigating the Causal Relationship from Institutions to Ecosystem Collapse. *Journal of the Association of Environmental and Resource Economists*, *6*(4), 741–781.

Jachmann, H. (2012). Pilot study to validate PIKE-based inferences at site level. *Pachyderm*, *52*, 72–87.

Jacobson, L. S., LaLonde, R. J., & Sullivan, D. G. (1993). Earnings Losses of Displaced Workers. *Am Econ Rev*, *83*(4), 685–709.

Joo, R., Salcedo, O., Gutierrez, M., Fablet, R., & Bertrand, S. (2015). Defining fishing spatial strategies from VMS data: Insights from the world's largest monospecific fishery. *Fisheries Research*, *164*, 223–230.

Kaffine, D. T. (2009). Quality and the commons: The surf gangs of california. *The Journal of Law & Economics*, *52*(4), 727–743. https://doi.org/10.1086/605293

Kahindi, O., Wittemyer, G., King, J., Ihwagi, F., Omondi, P., & Douglas-Hamilton, I. (2010). Employing participatory surveys to monitor the illegal killing of elephants across diverse land uses in Laikipia-Samburu, Kenya. *Afr J Ecol*, *48*(4), 972–983.

Kamenica, E. (2019). Bayesian Persuasion and Information Design. *Annual Review of Economics*, *11*, 249–272.

Kamenica, E., & Gentzkow, M. (2011). Bayesian Persuasion. *American Economic Review*, *101*(6), 2590–2615.

Keane, M. P., & Neal, T. (2020). *Consumer Panic in the COVID-19 Pandemic* (No. 2020-06). UNSW Economics Working Paper.

Kroetz, K., Sanchirico, J. N., Contreras, E. G., Novoa, D. C., Collado, N., & Swiedler, E. W. (2016). *Examination of the Peruvian anchovy Individual Vessel Quota (IVQ) System* (Working Paper No. 749). Inter-American Development Bank.

Kroetz, K., Sanchirico, J. N., Contreras, E. G., Novoa, D. C., Collado, N., & Swiedler, E. W. (2019). Examination of the Peruvian Anchovy Individual Vessel Quota (IVQ) System. *Marine Policy*, *101*, 15–24.

Kroodsma, D. A., Mayorga, J., Hochberg, T., Miller, N. A., Boerder, K., Ferretti, F., Wilson, A., Bergman, B., White, T. D., Block, B. A., et al. (2018). Tracking the global footprint of fisheries. *Science*, *359*(6378), 904–908.

Kyne, P. M., Sherrill-Mix, S. A., & Burgess, G. H. (2006). *Somniosus microcephalus*. International Union for Conservation of Nature.

Ladino, J. F., Saavedra, S., & Wiesner, D. (2019). *One Step Ahead of the Law: The Net Effect of Anticipation and Implementation of Colombia's Illegal Crops Substitution Program* (Documentos de Trabajo No. 017581). Universidad del Rosario.

Lam, V., Tavakolie, A., Zeller, D., & Pauly, D. (2016). The sea around us catch database and its spatial expression. In D. Pauly & D. Zeller (Eds.), *Global atlas of marine fisheries: A critical appraisal of catches and ecosystem impacts* (pp. 59–67). Island Press.

Lewison, R., Hobday, A. J., Maxwell, S., Hazen, E., Hartog, J. R., Dunn, D. C., Briscoe, D., Fossette, S., O'Keefe, C. E., Barnes, M., et al. (2015). Dynamic Ocean Management: Identifying the Critical Ingredients of Dynamic Approaches to Ocean Resource Management. *BioScience*, *65*(5), 486–498.

List, J. A., Margolis, M., & Osgood, D. E. (2006). *Is the Endangered Species Act Endangering Species?* (Working Paper No. 12777). National Bureau of Economic Research.

Matsuura, K., & Willmott, C. J. (2015). Terrestrial Air Temperature: 1900–2014 Gridded Monthly Time Series. Version 4.01. [Available at http://climate.geog.udel.edu/~climate/html_pages/Global2014/README.GlobalTsT2014.html. Accessed January 8, 2017].

Maxwell, S. M., Hazen, E. L., Lewison, R. L., Dunn, D. C., Bailey, H., Bograd, S. J., Briscoe, D. K., Fossette, S., Hobday, A. J., Bennett, M., et al. (2015). Dynamic ocean management: Defining and conceptualizing real-time management of the ocean. *Marine Policy*, *58*, 42–50.

Melnychuk, M. C., Peterson, E., Elliott, M., & Hilborn, R. (2017). Fisheries management impacts on target species status. *Proceedings of the National Academy of Sciences*, *114*(1), 178–183. https://doi.org/10.1073/pnas.1609915114

Miguel, E., Satyanath, S., & Sergenti, E. (2004). Economic Shocks and Civil Conflict: An Instrumental Variables Approach. *J Polit Econ*, *112*(4), 725–753.

Mora, C., Myers, R. A., Coll, M., Libralato, S., Pitcher, T. J., Sumaila, R. U., Zeller, D., Watson, R., Gaston, K. J., & Worm, B. (2009). Management effectiveness of the world's marine fisheries. *PLOS Biology*, *7*(6), e1000131. https://doi.org/10.1371/journal.pbio.1000131

Natividad, G. (2016). Quotas, productivity, and prices: The case of anchovy fishing. *Journal of Economics & Management Strategy*, *25*(1), 220–257.

Newey, W. K., & West, K. D. (1987). A simple, positive semi-definite, heteroskedasticity and autocorrelation consistent covariance matrix. *Econometrica*, *55*(3), 703–708. https://doi.org/10.2307/1913610

Newey, W. K., & West, K. D. (1994). Automatic lag selection in covariance matrix estimation. *The Review of Economic Studies*, *61*(4), 631–653. https://doi.org/10.2307/2297912

OBPG. (2015). MODIS aqua level 3 SST thermal IR 8 day 4km daytime v2014.0 [type: dataset]. https://doi.org/10.5067/MODSA-8D4D4

Oliva, P. (2015). Environmental Regulations and Corruption: Automobile Emissions in Mexico City. *Journal of Political Economy*, *123*(3), 686–724.

Paredes, C. E. (2014). *La anchoveta: Pesca y descarte de juveniles. Análisis de la regulación pesquera y propuestas para su perfeccionamiento* (Cuadernos de Investigación Edición N° 20). Universidad de San Martín de Porres.

Pauly, D., & Zeller, D. (2015). Sea around us concepts, design and data. seaaroundus.org

Peraltilla, S., & Bertrand, S. (2014). *IN SITU* MEASUREMENTS OF THE SPEED OF PERUVIAN ANCHOVY SCHOOLS. *Fisheries Research*, *149*, 92–94.

Pfaff, A., & Robalino, J. (2017). Spillovers from conservation programs. *Annual Review of Resource Economics*, *9*, 299–315.

Pikitch, E., Boersma, P. D., Boyd, I., Conover, D., Cury, P., Essington, T., Heppell, S., Houde, E., Mangel, M., Pauly, D., et al. (2012). *Little fish, big impact: Managing a crucial link in ocean food webs*. Lenfest Ocean Program.

PRODUCE. (2012). Decreto Supremo N° 008-2012: Decreto Supremo que establece medidas para la conservacion del recurso hidrobiologico [Ministerio de la Producción (PRODUCE)].

PRODUCE. (2015). Resolución Directoral N° 035-2015-PRODUCE/DGSF [Ministerio de la Producción (PRODUCE)].

PRODUCE. (2016a). Decreto Supremo N° 024-2016: Decreto Supremo que establece medidas para fortalecer el control y vigilancia de la actividad extractiva para la conservación y aprovechamiento sostenible del recurso anchoveta [Ministerio de la Producción (PRODUCE)].

PRODUCE. (2016b). Resolución Directoral N° 014-2016-PRODUCE/DGSF [Ministerio de la Producción (PRODUCE)].

PRODUCE. (2017a). I temporada de pesca – 2017 Zona Norte-Centro: Resumen Ejecutivo de Seguimiento y Control [Ministerio de la Producción (PRODUCE)].

PRODUCE. (2017b). Resolución Directoral N° 687-2017-PRODUCE/DS-PA [Ministerio de la Producción (PRODUCE)].

PRODUCE. (2018a). Anuario Estadístico Pesquero y Acuícola 2017 [Ministerio de la Producción (PRODUCE)].

PRODUCE. (2018b). I temporada de pesca – 2018 Zona Norte-Centro: Resumen Ejecutivo de Seguimiento y Control [Ministerio de la Producción (PRODUCE)].

PRODUCE. (2018c). II temporada de pesca – 2017 Zona Norte-Centro: Resumen Ejecutivo de Seguimiento y Control [Ministerio de la Producción (PRODUCE)].

PRODUCE. (2018d). Resolución Directoral N° 127-2018-PRODUCE/DGSFS-PA [Ministerio de la Producción (PRODUCE)].

PRODUCE. (2020a). Comunicado N° 010-2020-PRODUCE/DGSFS-PA-SP Suspensión Preventiva de Actividades de Extractivas del Recurso Caballa [Ministerio de la Producción (PRODUCE)].

PRODUCE. (2020b). Resolución Ministerial N° 015-2020-PRODUCE [Ministerio de la Producción (PRODUCE)].

PRODUCE. (2020c). Suspensiones preventivas de zonas DGSFS - PA – SP [Ministerio de la Producción (PRODUCE)]. https://www.produce.gob.pe/index.php/dgsfs-pa/suspensiones-preventivas-de-pesca

Quaas, M. F., Requate, T., Ruckes, K., Skonhoft, A., Vestergaard, N., & Voss, R. (2013). Incentives for optimal management of age-structured fish populations. *Resource and Energy Economics*, *35*(2), 113–134.

R Core Team. (2019). *R: A language and environment for statistical computing*. R Foundation for Statistical Computing. Vienna, Austria. https://www.R-project.org/

Reimer, M., & Wilen, J. (2013). Regulated Open Access and Regulated Restricted Access Fisheries. *Encyclopedia of Energy, Natural Resource, and Environmental Economics* (pp. 215–223). Elsevier.

Rubin, D. B. (1974). Estimating causal effects of treatments in randomized and nonrandomized studies. *Journal of Educational Psychology*, *66*(5), 688–701. https://doi.org/http://dx.doi.org/10.1037/h0037350

Sala, E., Mayorga, J., Costello, C., Kroodsma, D., Palomares, M. L., Pauly, D., Sumaila, U. R., & Zeller, D. (2018). The economics of fishing the high seas. *Science Advances*, *4*(6), eaat2504.

Salvatteci, R., & Mendo, J. (2005). Estimación de las pérdidas bio-económicas causadas por la captura de juveniles de anchoveta (*Engraulis ringens*, j.) en la Costa Peruana (Estimation of bio-economic losses caused by the capture of juvenile anchovy (*Engraulis ringens*, j.) in the Peruvian Coast). *Ecología Aplicada*, *4*(1-2), 113–120.

Scott, A. (1955). The Fishery: The Objectives of Sole Ownership. *Journal of Political Economy*, *63*(2), 116–124.

Smith, M. D., Lynham, J., Sanchirico, J. N., & Wilson, J. A. (2010). Political economy of marine reserves: Understanding the role of opportunity costs. *Proceedings of the National Academy of Sciences*, *107*(43), 18300–18305. https://doi.org/10.1073/pnas.0907365107

Smith, M. D. (2012). The New Fisheries Economics: Incentives Across Many Margins. *Annual Review of Resource Economics*, *4*(1), 379–402.

Smith, T. D. (1994). *Scaling Fisheries: The Science of Measuring the Effects of Fishing, 1855-1955*. Cambridge University Press.

Smith, V. L. (1969). On Models of Commercial Fishing. *Journal of Political Economy*, *77*(2), 181–198.

Sobel, J. (1996). *Hippoglossus hippoglossus* (e.T10097A3162182).

Sukumar, R. (2006). A brief review of the status, distribution and biology of wild Asian elephants. *Int Zoo Yearb*, *40*, 1–8.

Sundberg, R., & Melander, E. (2013). Introducing the UCDP Georeferenced Event Dataset. *J Peace Res*, *50*(4), 523–532.

SUPNEP. (2017). Convenio Colectivo por Rama de Actividad, SUPNEP - AANEP, 12 de marzo 2017 al 11 marzo del 2022 [Sindicato Univo de Pescadores de Nuevas Embarcaciones del Peru (SUPNEP)]. http://www.supnep.pe/assets/convenio_colectivo_supnep_aanep_2017_2022.pdf

Sutinen, J. G., & Ande, P. (1985). The economics of fisheries law enforcement. *Land Economics*, *61*(4), 387–397.

Thouless, C. R., Dublin, H. T., Blanc, J. J., Skinner, D. P., Daniel, T. E., Taylor, R., Maisels, F., Frederick, H. L., & Bouché, P. (2016). African Elephant Status Report 2016: An update from the African Elephant Database.

Tveteras, S., Paredes, C. E., & Peña-Torres, J. (2011). Vessel Quotas in Peru: Stopping the Race for Anchovies. *Marine Resource Economics*, *26*(3), 225–232.

United National General Assembly. (2018). Concluding Session to Draft Marine Biodiversity Treaty. https://www.un.org/press/en/2018/sea2086.doc.htm

VLIZ. (2012). Intersect of IHO Sea Areas and Exclusive Economic Zones (version 2) [Accessed January 14, 2018]. http://www.marineregions.org/

Wallace, R. K., & Fletcher, K. M. (1997). Understanding fisheries management: A Manual for understanding the Federal Fisheries Management Process, Including Analysis of the 1996 Sustainable Fisheries Act.

Watson, R., Zeller, D., & Pauly, D. (2014). Primary productivity demands of global fishing fleets. *Fish and Fisheries*, *15*(2), 231–241. https://doi.org/10.1111/faf.12013

Watson, R. A., Cheung, W. W. L., Anticamara, J. A., Sumaila, R. U., Zeller, D., & Pauly, D. (2013). Global marine yield halved as fishing intensity redoubles. *Fish and Fisheries*, *14*(4), 493–503. https://doi.org/10.1111/j.1467-2979.2012.00483.x

Wilen, J. E. (2000). Renewable Resource Economists and Policy: What Differences Have We Made? *Journal of Environmental Economics and Management*, *39*(3), 306–327.

Wittemyer, G., Northrup, J. M., Blanc, J., Douglas-Hamilton, I., Omondi, P., & Burnham, K. P. (2014). Illegal killing for ivory drives global decline in African elephants. *Proc Natl Acad Sci USA*, *111*(36), 13117–13121.

Yamagiwa, J. (2003). Bushmeat Poaching and the Conservation Crisis in Kahuzi-Biega National Park, Democratic Republic of the Congo. *J Sustain Forest*, *16*(3-4), 111–130.

Appendix A

Information and spillovers from targeting policy in Peru's anchoveta fishery

A.1 Robustness checks

Balance tests: Pre-period juvenile catch levels and trends and observable measures of fishing productivity

In this section, I test whether treatment and control potential closures are balanced in their level of pre-period juvenile catch, trend in pre-period juvenile catch, and observable measures of fishing productivity.

First, I calculate juvenile catch and treatment fraction for inside potential closures on the day before sets would generate an actual closure.[1] I calculate treatment fraction for this inside, day-before bin in the same way as for the other bins (overlap with inside, day-before bin of actual closures declared by the regulator). I add these rows to my main dataset and estimate versions of Equation 3.1 in Table A.1. I estimate treatment effects for all treatment bins (now 37 instead of 36), but only report the coefficient on the inside, day-before treatment bin.

[1]This time period is 48 to 72 hours before the beginning of the closure period, rather than 24 to 48 hours before the beginning of the closure period, because in some instances sets influence the probability of actual closures up to 48 hours before the beginning of the closure period. Therefore, there might be a mechanical correlation between juvenile catch 24 to 48 hours before the beginning of the closure period due to reverse causality. In the cases when a cluster of sets 24 to 48 hours before the closure period affect the probability of an actual closure, the treatment fraction for the potential closure generated by that cluster of sets could be up to one-third smaller than the true treatment fraction (because the potential closure could end one day before the actual closure, and the closure period for potential closures is three days). This occasional measurement error in treatment fraction does not affect my results, which exhibit the same pattern when I replace treatment fraction in Equation 3.1 with an indicator that equals 1 if the treatment fraction for a potential closure-bin is greater than 0 (Figure A.5).

Table A.1: Test for difference in pre-period juvenile catch

Dependent variable: asinh(juvenile catch)					
	(1)	(2)	(3)	(4)	(5)
Treatment fraction	0.235	-0.056	-0.033	-0.074	-0.061
	(0.143)	(0.175)	(0.152)	(0.152)	(0.176)
Fixed effects		X			X
Length distribution			X	X	X
Other controls				X	X

Notes: All regressions have 35,113 observations. Dependent variable is the inverse hyperbolic sine of millions of juveniles caught. All regressions estimate treatment effects for all 37 treatment bins, but only the coefficent on treatment fraction for the inside, day-before bin is displayed in this table. Standard errors clustered at level of two-week-of-sample by two-degree grid cell.

Without control variables or fixed effects, there is a marginally significant correlation between treatment and juvenile catch in the inside, day-before treatment bin (Column 1). Potential closures that will eventually be closed (treatment fraction = 1) have 26% higher juvenile catch than potential closures that will not be declared actual closures by the regulator (treatment fraction = 0). In Columns 2 to 5 of Table A.1, I test whether the control variables and fixed effects in Equation 3.1 eliminate this difference in pre-period juvenile catch, which would support the identifying assumption that treatment and control potential closures are comparable conditional on control variables and fixed effects.

I include day-of-sample and two-week-of-sample by two-degree grid cell fixed effects in Column 2, length distribution controls in Column 3 (excluding fixed effects and the six other control variables in Equation 3.1), all potential closure-level controls from Equation 3.1 in Column 4 (excluding fixed effects), and the full set of potential closure-level controls and fixed effects from Equation 3.1 in Column 5. In all four specifications, these control variables and fixed effects are sufficient to balance treatment and control potential closures on pre-period juvenile catch. They reduce the treatment coefficient by an order of magnitude without meaningfully increasing the standard error, emphasizing their importance for the validity of the identifying assumption.

To examine trends in pre-period juvenile catch, I also calculate juvenile catch and treatment fraction for inside potential closures up to six days before the period in which sets would generate an actual closure. I add these rows to my main dataset, so that there are now 42 treatment bins of interest (the original 36 plus the six new pre-period bins). I es-

timate treatment effects for all treatment bins (now 42 instead of 36), but only display the treatment coefficients for the inside potential closure treatment bins in Figure A.1.

Without control variables or fixed effects, pre-period juvenile catch is consistently higher in the potential closures that will eventually be closed, though the trend is not different from zero (Figure A.1a). But when I include the full set of control variables and fixed effects in Equation 3.1, the difference in pre-period juvenile catch levels is eliminated and the trend remains indistinguishable from zero (Figure A.1b). The treatment coefficients after closures would be announced mirror my main result: an increase in juvenile catch after closure announcements but before the beginning of closure periods, a noisy decrease in juvenile catch during closure periods, increases in juvenile catch one and two days after closures end, and a dissipation of effects three and four days after closures end. The absence of a trend in pre-period juvenile catch lends further credence to the primary identification strategy I use in this paper.

To test whether potential closures are balanced on observables, I focus on three of the control variables in Equation 3.1 that are likely correlated with fishing productivity: distance to the coast, tons per set, and tons per area (km^2).[2] If treated potential closures are more desirable to fish near, juvenile catch inside the treatment window will be mechanically higher for treated potential closures than for control potential closures, all else equal, because there will be more fishing near treated potential closures. Indeed, in Table A.2 I find positive, significant correlations between juvenile catch inside potential closure-treatment bins and each of these three variables (Columns 1 to 3). When I regress juvenile catch on all three variables together in Column 4, all three coefficients remain positive, though tons per area is no longer significantly correlated with juvenile catch. I record these fitted values and also use them to test for balance in Table A.3.

In Table A.3, I test whether potential closures are balanced on each variable and on the fitted values, conditional on the length distribution caught by the sets that generate the potential closure and the fixed effects in Equation 3.1. I find a significant correlation between treatment fraction and tons per area, but not between treatment fraction and distance to the coast, tons per set, or the fitted values. The non-correlations between treatment fraction and tons per set and between treatment fraction and distance to the coast are more relevant than the correlation between treatment fraction and tons per area because tons per area is not a significant predictor of juvenile catch when juvenile catch is regressed on all three variables (Column 4 of Table A.2). The lack of a correlation between treatment fraction and the fitted values is also reassuring because the fitted values are based on all three variables. These results should therefore be interpreted as evidence that treatment and control potential closures would offer similar fishing opportunities to vessels if not for treatment.

[2]In addition to being a proxy for fishing costs, distance to the coast is a proxy for fishing productivity because anchoveta are more abundant closer to the coast (Castillo et al., 2019).

Figure A.1: Test for pre-trend in juvenile catch inside potential closures

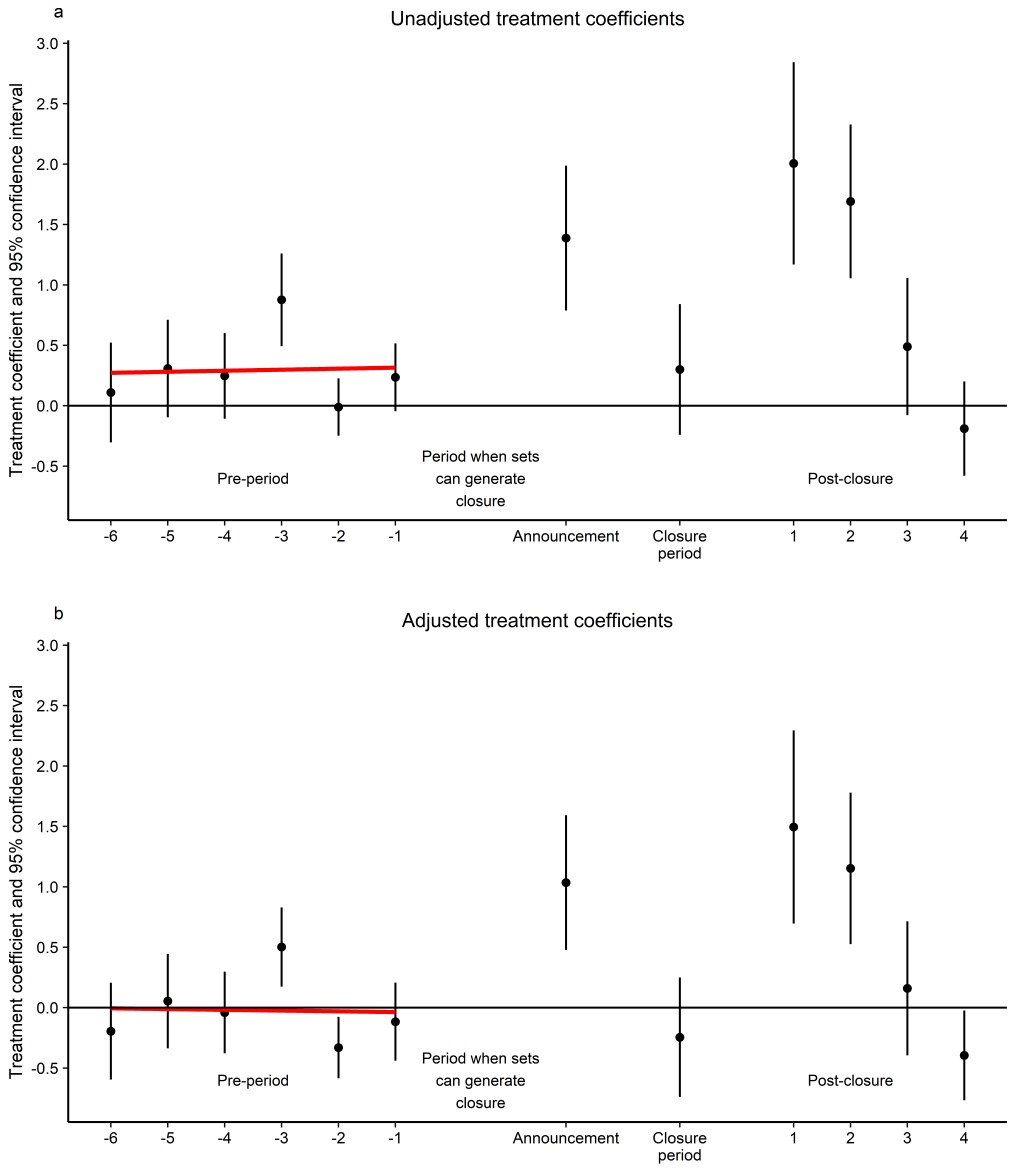

Notes: N=39,858 for both regressions. The dependent variable is the inverse hyperbolic sine of millions of juveniles caught. Both regressions estimate treatment effects for all 42 treatment bins, but only the treatment fraction coefficients for inside potential closures treatment bins are displayed in this figure. In the second regression (b), I include the control variables and fixed effects in Equation 3.1. The red line is the linear trend in pre-period treatment coefficients. Points are coefficients and whiskers are 95% confidence intervals. Standard errors clustered at level of two-week-of-sample by two-degree grid cell.

Table A.2: Correlation between juvenile catch and measures of fishing productivity

	Dependent variable: asinh(juvenile catch)			
	(1)	(2)	(3)	(4)
DistToCoast	0.0052			0.0028
	(0.0017)			(0.0015)
TonsPerSet		0.0073		0.0068
		(0.0007)		(0.0009)
TonsPerArea			0.0142	0.0023
			(0.0039)	(0.0034)
Intercept	0.6394	0.3985	0.7029	0.3284
	(0.0663)	(0.0535)	(0.0515)	(0.0570)

All regressions have 34,164 observations. Dependent variable is inverse hyperbolic sine of millions of juveniles caught in a potential closure-treatment bin. Standard errors clustered at level of two-week-of-sample by two-degree grid cell.

Table A.3: Test for balance on measures of fishing productivity

	DistToCoast	TonsPerSet	TonsPerArea	FittedVals
	(1)	(2)	(3)	(4)
Treatment	-1.091	3.578	3.377	0.029
fraction	(1.824)	(4.368)	(1.190)	(0.033)

All regressions have 34,164 observations and control for two-week-of-sample by two-degree-grid-cell fixed effects, day-of-sample fixed effects, and potential closure-level length distribution. Standard errors clustered at level of two-week-of-sample by two-degree grid cell.

Treatment coefficients from Estimating Equation 3.1 and variants of Equation 3.1

Figure A.2 displays the treatment coefficients from estimating Equation 3.1. My results exhibit the same pattern if I drop zero values and use a logarithmic transformation on the dependent variable instead of an inverse hyperbolic sine transformation (Figure A.3). They

also hold if I replace the dependent variable in Equation 3.1 with a binary indicator for positive juvenile catch (Figure A.4) or if I replace treatment fraction with a binary indicator for positive treatment fraction (Figure A.5).

My results are also robust to replacing the outcome variable with the inverse hyperbolic sine of tons of juveniles caught (Figure A.6). Juvenile catch in tons is the number of individuals in each length interval times the weight of an individual in each length interval, summed over length intervals less than 12 cm.[3] When I convert these treatment coefficients into changes in levels and account for the reallocation in tons (of juveniles and adults) caught due to the total allowable catch limit, I estimate that the temporary spatial closures policy increases juvenile catch by 332 thousand tons of juveniles, or 44% (delta method standard errors are 70 thousand tons and 9.3%). For comparison, the regulator calculates that the temporary spatial closures policy "protected" 1,049,411 tons of juvenile anchoveta in the first and second season of 2017 and the first season of 2018 (PRODUCE, 2017a, 2018b, 2018c). The regulator does not describe how they calculate this number, nor do they define the meaning of "protected" in this context.

Finally, my results are robust to assuming potential closures last for four or five days (instead of three days) and to making my potential closures 40% larger (so that they are the same average size as actual closures). I display the treatment coefficients for these three alternative specifications in Figures A.7 to A.9. When I convert the treatment coefficients from each of the three specifications into changes in levels and account for the reallocation in tons caught due to the total allowable catch limit, I find that the closures policy increases total juvenile catch by 49%, 66% and 52%, respectively (delta method standard errors are 4.7%, 4.5%, and 5.8%, respectively).

If closures shift juvenile catch forward in time during a fishing season, then my treatment effects would be upward biased because some of the increase in juvenile catch due to closures would have occurred later in the season, even if the closures policy did not exist. This "harvesting" concern also occurs in studies on human mortality (e.g., some of the people killed by heat waves would have died soon anyway). I re-estimate Equation 3.1 with one change: I interact treatment fraction with an indicator for whether potential closure i occurs in the first or second half of a fishing season (defined relative to the start of potential closure i's closure period). I find no evidence of heterogeneity along this dimension and display the treatment coefficients from this regression in Figure A.10. When I convert the treatment coefficients into changes in levels and account for the reallocation in tons caught due to the total allowable catch limit, I find that 56% of the increase in juvenile catch due to the closures policy occurs in the first half of fishing seasons. For reference, 59% of tons are landed during the first half of fishing seasons. This result indicates that closures do not cause significant "harvesting" of juveniles that would have been caught even in the absence of closures (i.e., in the second-half of fishing seasons).

[3]For a given set, tons of juveniles caught equals $\sum_{\ell=[3,3.5)}^{[11.5,12)} w_\ell N_\ell$, where w_ℓ is the weight of an individual in length interval ℓ and N_ℓ is the number of individuals in length interval ℓ that the set caught.

Figure A.2: Treatment coefficients from estimating Equation 3.1

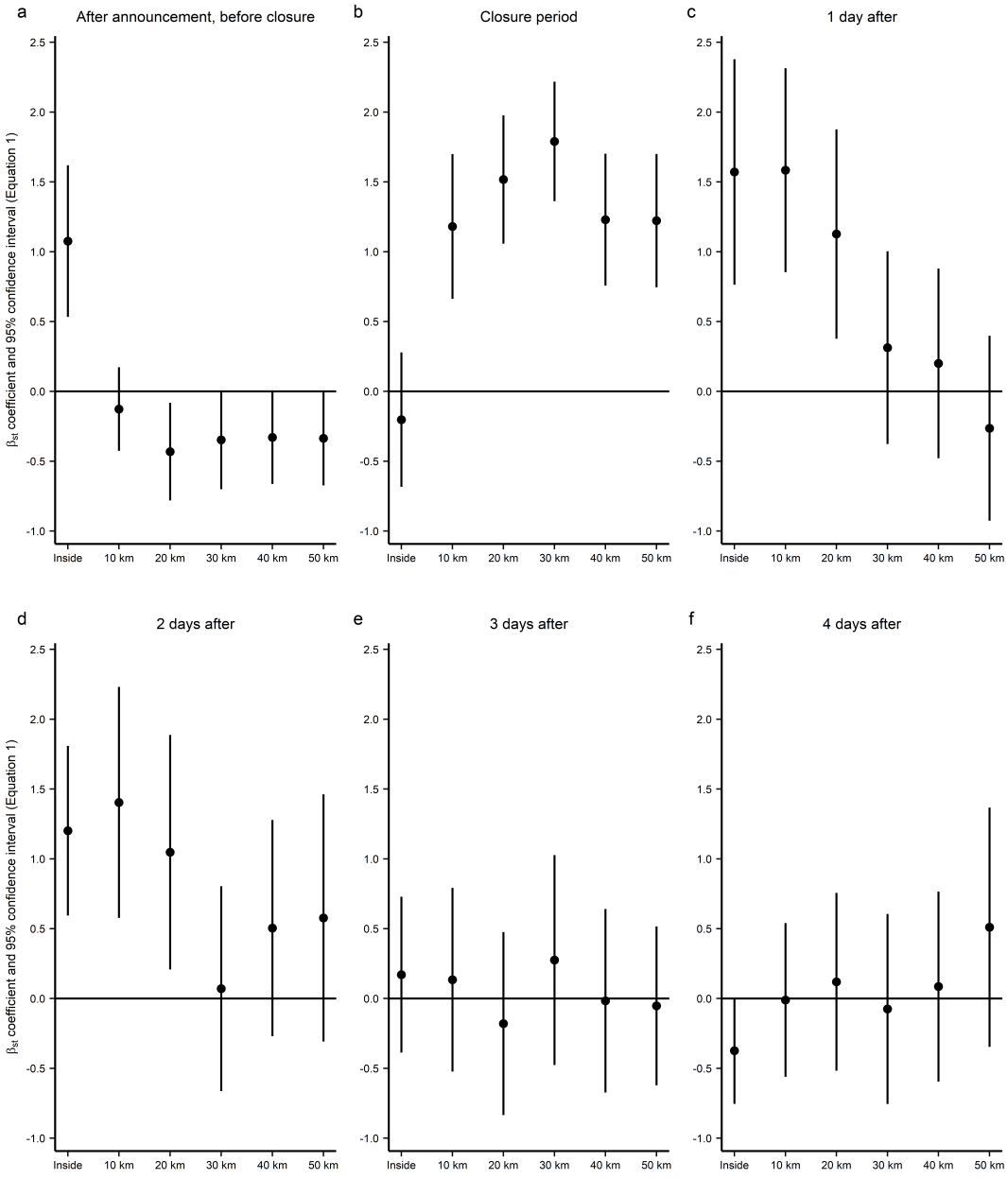

Notes: N = 34,164. Points are coefficients and whiskers are 95% confidence intervals. Standard errors clustered at level of two-week-of-sample by two-degree grid cell.

Figure A.3: Treatment coefficients from dropping observations with zero juvenile catch and re-estimating Equation 3.1 with a logarithmic transformation instead of an inverse hyperbolic sine transformation

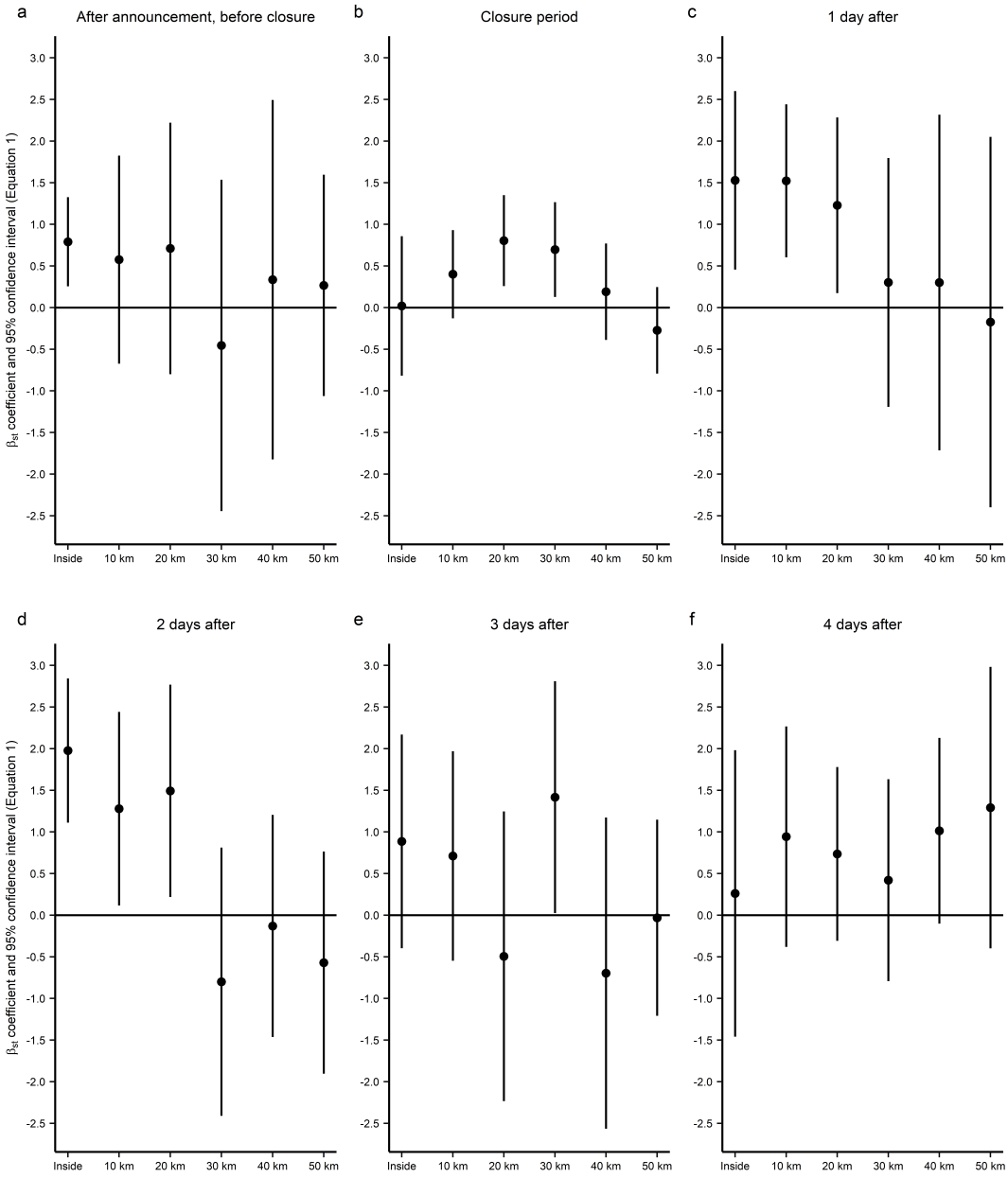

Notes: N = 12,220. Points are coefficients and whiskers are 95% confidence intervals. Standard errors clustered at level of two-week-of-sample by two-degree grid cell.

Figure A.4: Treatment coefficients from re-estimating Equation 3.1 with a binary indicator for positive juvenile catch as the dependent variable

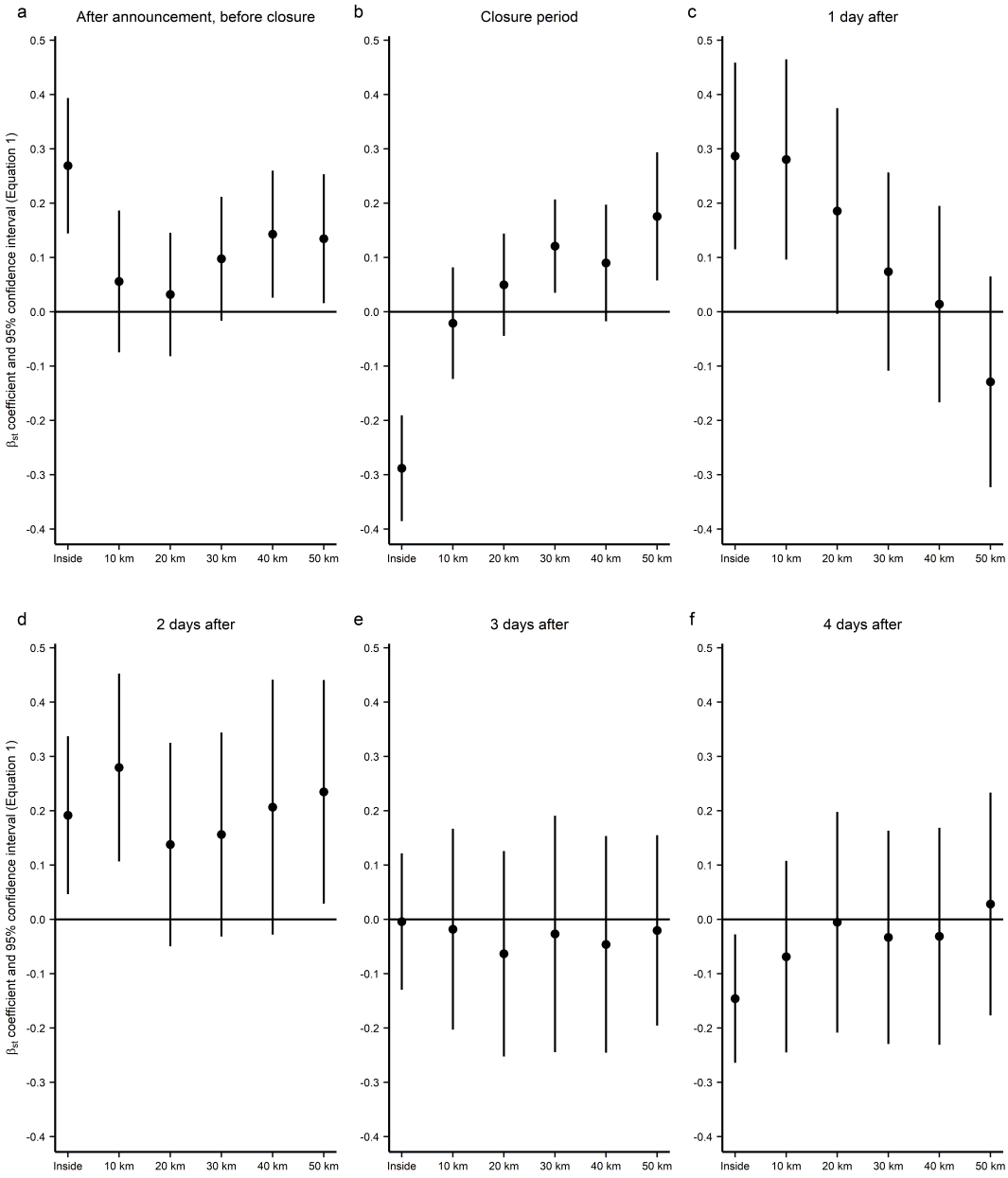

Notes: N = 34,164. Points are coefficients and whiskers are 95% confidence intervals. Standard errors clustered at level of two-week-of-sample by two-degree grid cell.

Figure A.5: Treatment coefficients from re-estimating Equation 3.1 with a binary indicator for positive treatment fraction, rather than defining treatment fraction as a continuous variable

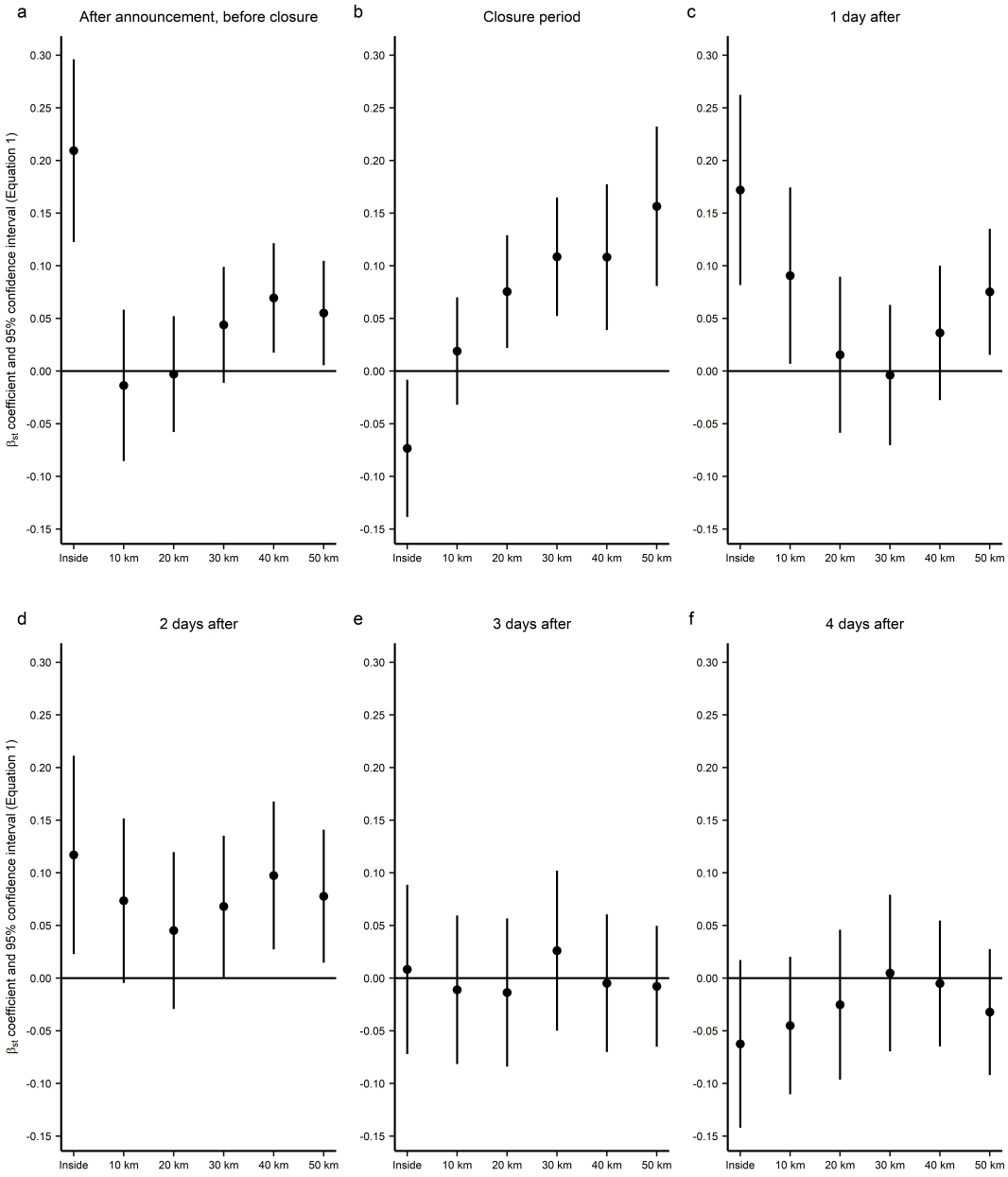

Notes: N = 34,164. Points are coefficients and whiskers are 95% confidence intervals. Standard errors clustered at level of two-week-of-sample by two-degree grid cell.

Figure A.6: Treatment coefficients from re-estimating Equation 3.1 with tons of juveniles caught as the dependent variable

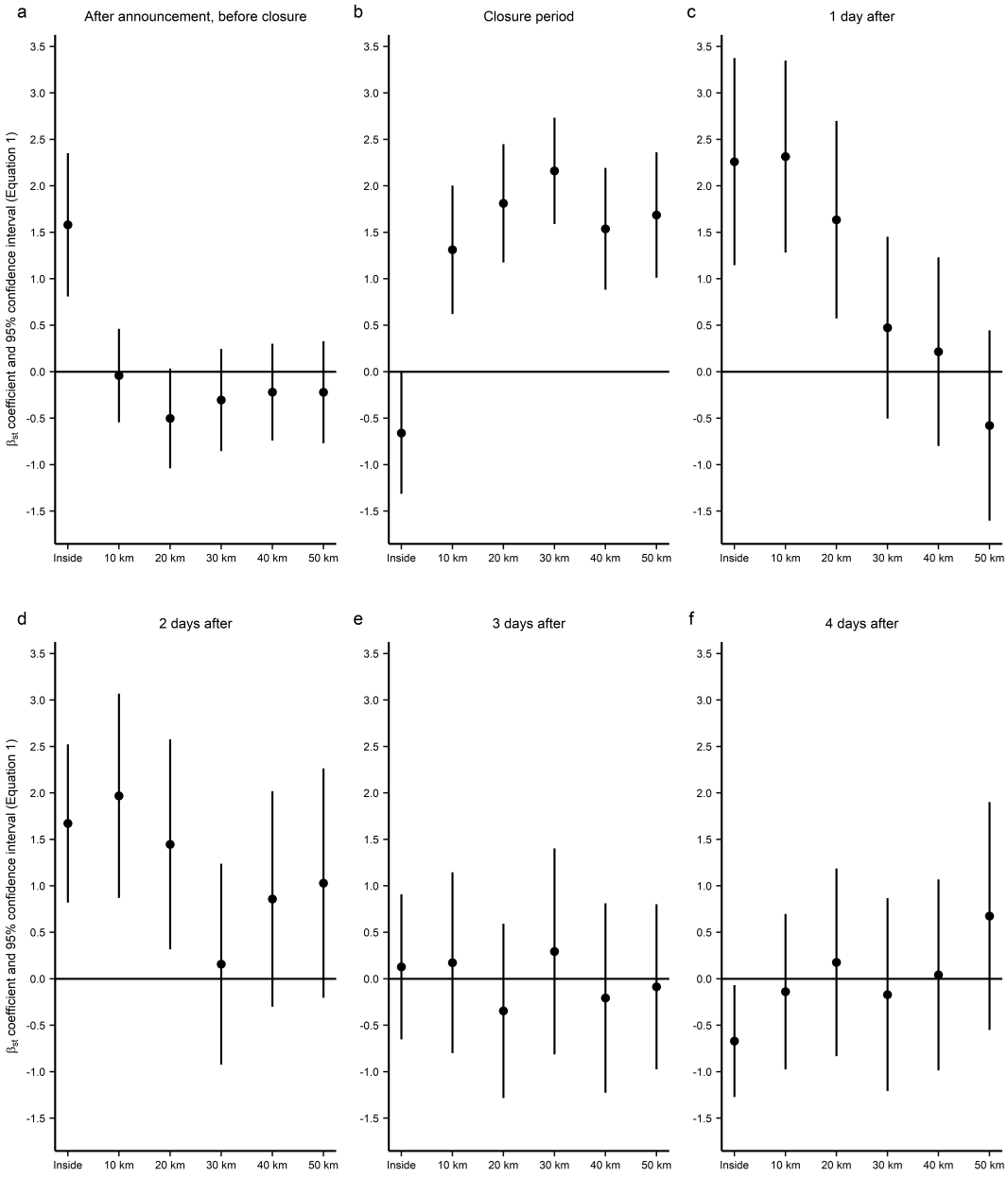

Notes: The dependent variable is the inverse hyperbolic sine of tons of juveniles caught in each potential closure-treatment bin. N = 34,164. Points are coefficients and whiskers are 95% confidence intervals. Standard errors clustered at level of two-week-of-sample by two-degree grid cell.

Figure A.7: Treatment coefficients from re-estimating Equation 3.1 with potential closures that last four days

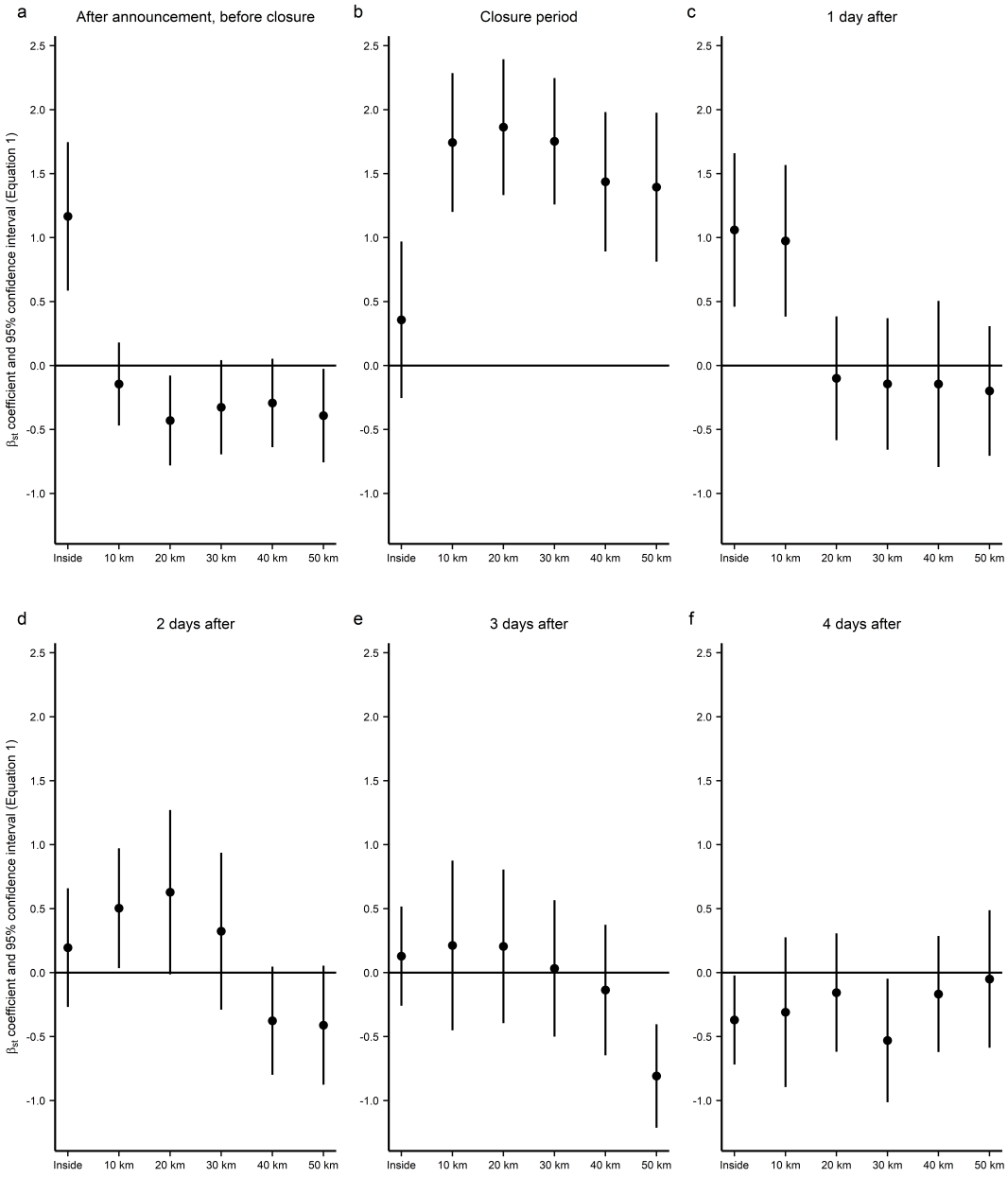

Notes: N = 31,608. Points are coefficients and whiskers are 95% confidence intervals. Standard errors clustered at level of two-week-of-sample by two-degree grid cell.

Figure A.8: Treatment coefficients from re-estimating Equation 3.1 with potential closures that last five days

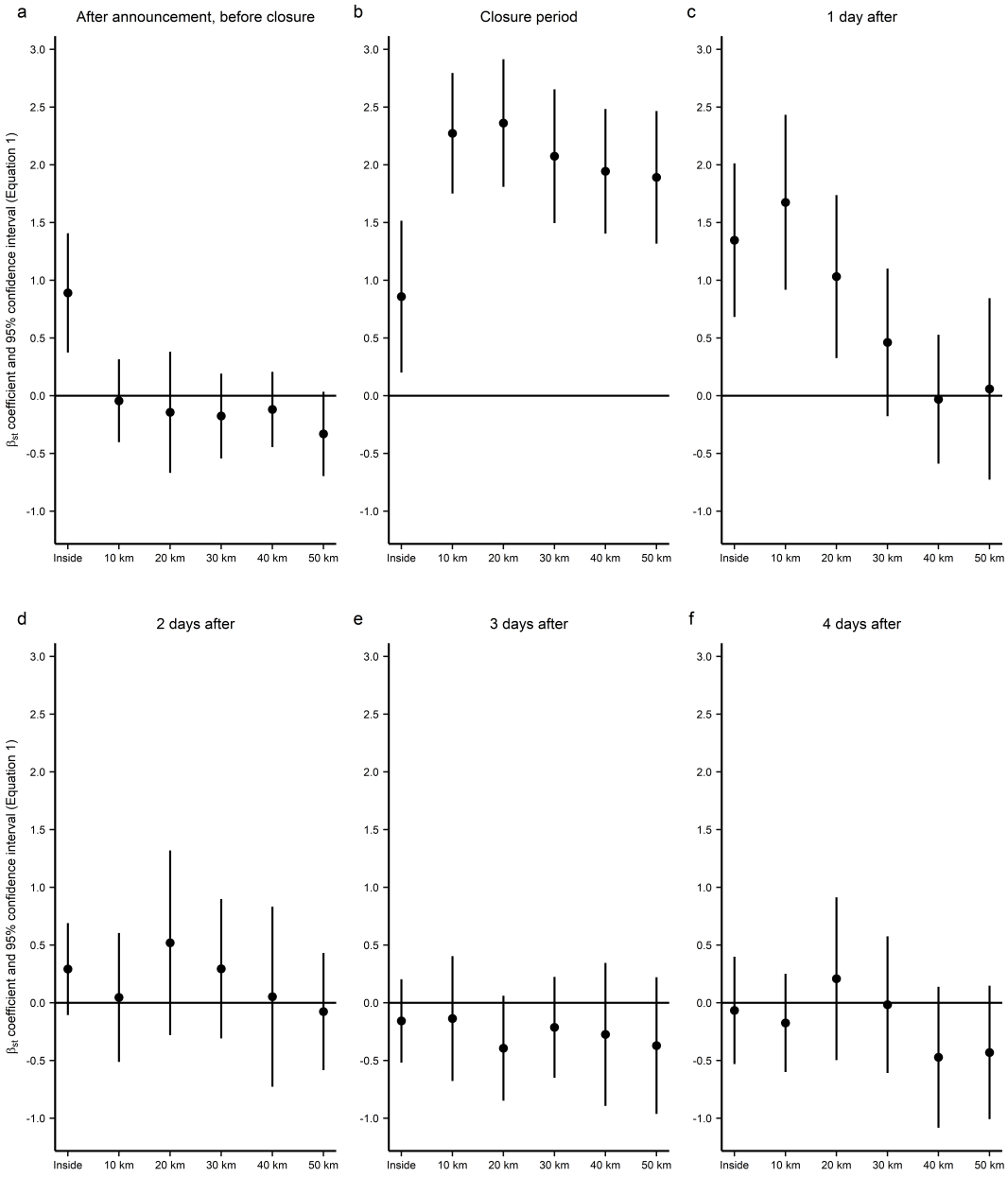

Notes: N = 29,664. Points are coefficients and whiskers are 95% confidence intervals. Standard errors clustered at level of two-week-of-sample by two-degree grid cell.

Figure A.9: Treatment coefficients from re-estimating Equation 3.1 with potential closures 40% larger

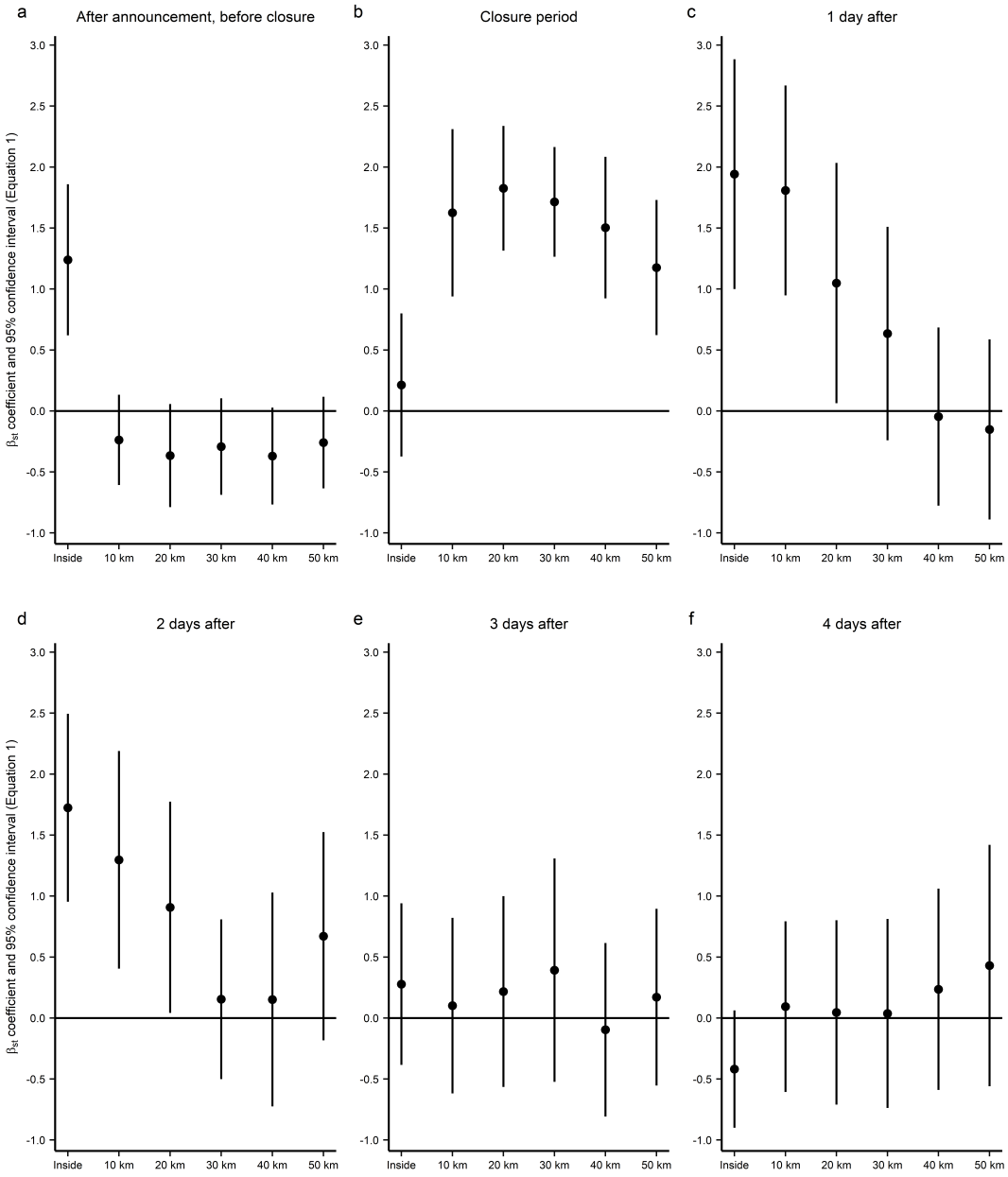

Notes: N = 34,164. Points are coefficients and whiskers are 95% confidence intervals. Standard errors clustered at level of two-week-of-sample by two-degree grid cell.

Figure A.10: Treatment coefficients from re-estimating Equation 3.1 with time-of-season interactions

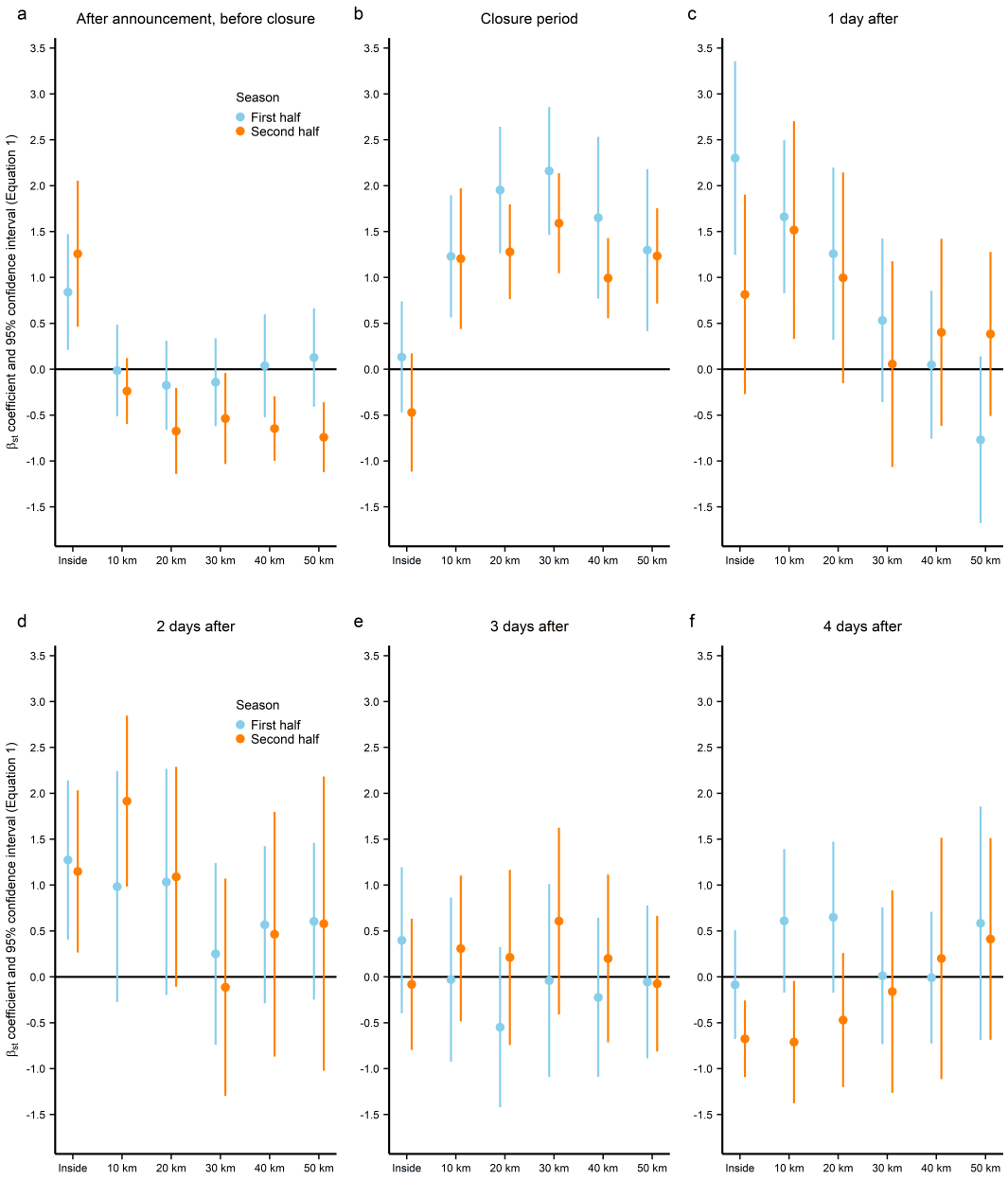

Notes: N = 34,164. I re-estimate Equation 3.1 with one change: I interact treatment fraction with an indicator for whether potential closure i occurs in the first- or second-half of a fishing season (defined relative to the start of potential closure i's closure period). Points are coefficients and whiskers are 95% confidence intervals. Standard errors clustered at level of two-week-of-sample by two-degree grid cell.

Re-estimating the effect of the policy on juvenile catch with gridded, balanced panel data

As an alternative estimation approach, I create a regular grid of .05° cells covering the North-Central zone and calculate the millions of juveniles caught in each cell each three-hour period during a fishing season. I rasterize the data at this resolution to match the resolution of treatment assignment as closely as possible without exceeding my server's memory capacity. This procedure yields 95,416,620 observations, or 21,346 grid cells × 4,470 three-hour time periods. I regress juvenile catch in a grid cell-time period on indicators for whether the centroid of the grid cell-time period is inside each of the 36 treatment bins in the treatment window of actual closures, .05° grid cell fixed effects, three-hour time period fixed effects, and two-week-of-sample by two-degree grid cell fixed effects:

$$JuvenileCatch_{jk} = \beta_{st}\mathbb{1}\{jk \in st\} + \alpha_j + \delta_k + \sigma_{wg} + \epsilon_{jk} \tag{A.1}$$

where j = .05° cell, k = three-hour time period, s = spatial unit, t = (treatment bin) time period, w = two-week-of-sample, and g = two-degree grid cell. For a given cell-period jk and treatment bin st, $\mathbb{1}\{jk \in st\}$ equals 1 if the centroid of jk is inside treatment bin st of an actual closure and equals 0 otherwise. I cluster standard errors at the level of two-week-of-sample by two-degree grid cell. The dependent variable is the inverse hyperbolic sine of millions of juveniles caught, as in Equation 3.1.

I plot the coefficients of interest, β_{st}, in Figure A.11. The coefficient magnitudes are smaller than in Figure A.2, possibly due to the large number of zeros in the rasterized data (99.96% of observations have 0 juvenile catch). However, the treatment effects are precisely estimated and the pattern of treatment effects is the same as in my preferred specification (Figure A.2). My finding that closures cause temporal and spatial spillovers and increase total juvenile catch is robust to this alternative estimation strategy.

Figure A.11: Treatment coefficients from estimating Equation A.1

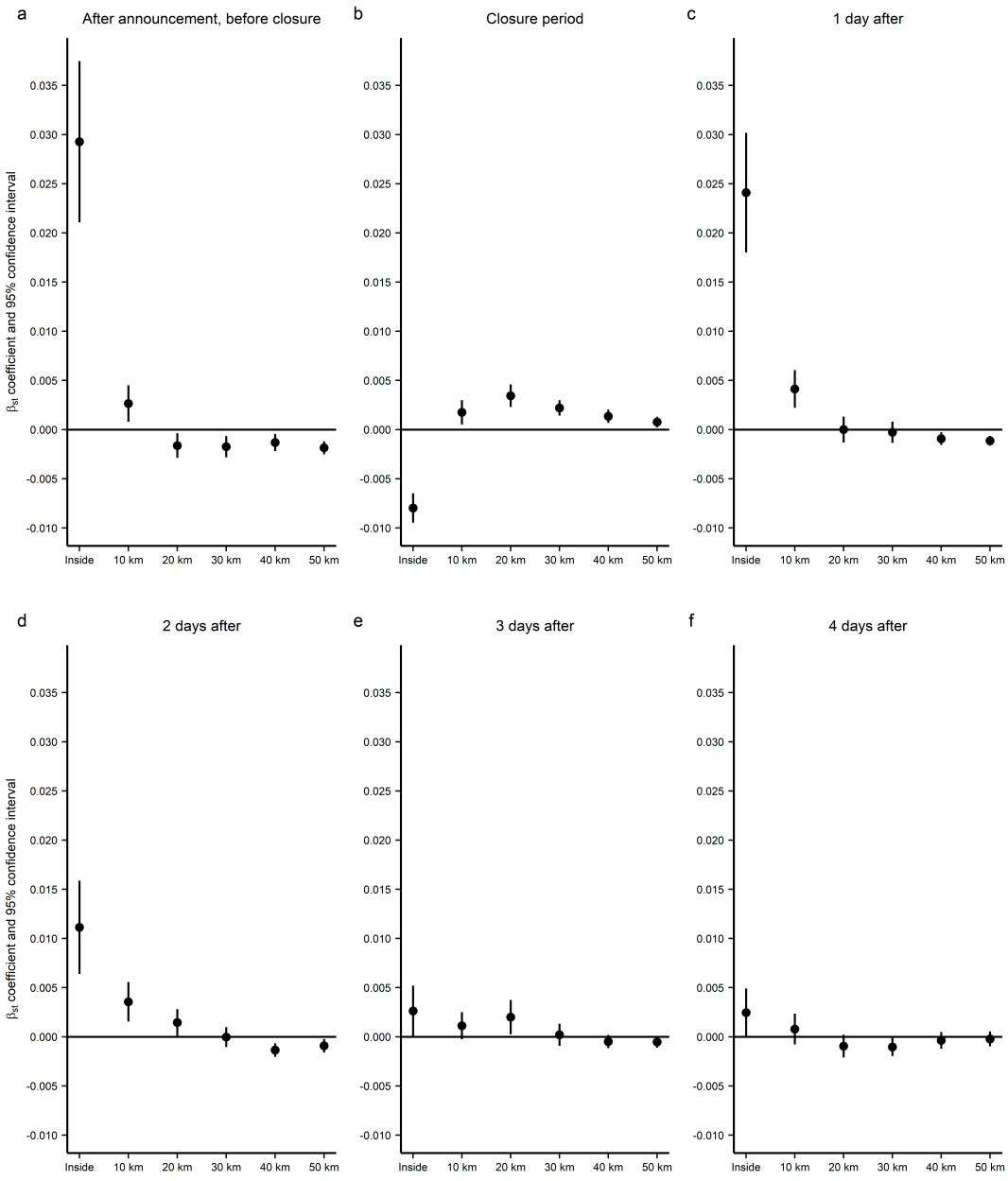

Notes: N = 95,416,620. Points are coefficients and whiskers are 95% confidence intervals. Standard errors clustered at level of two-week-of-sample by two-degree grid cell.

Re-estimating the effect of the policy on juvenile catch with actual closures as treated units and potential closures as control units

In my preferred specification, I estimate the effect of the temporary spatial closures policy across potential closures, where actual closures declared by the regulator are only used to calculate the treatment fraction for each potential closure-treatment bin. An alternative estimation approach is to use actual closures declared by the regulator as the treated units and potential closures whose treatment fraction equals 0 as the control units. I estimate the effect of the closures policy with this alternative approach here.

In my preferred specification in Equation 3.1, I control for characteristics of the sets that generate potential closures, such as the length distribution of anchoveta caught by the sets that generate potential closures. For each actual closure declared by the regulator, I now also construct these same control variables from the sets that occur inside the closure in the 9 to 24 hours before the closure begins.[4] 8 of the 410 actual closures declared by the regulator do not have sets inside them with non-missing length distribution values (see Footnote 7). I drop these 8 actual closures from this analysis because I cannot construct length distribution control variables for them. I create the same spatial and temporal leads and lags as for potential closures, yielding 14,472 observations (36 treatment bins $\times$ 402 = 14,472). I construct the same fixed effects as in Equation 3.1 and calculate juvenile catch inside each actual closure-treatment bin by summing juvenile catch over sets that occur inside the same actual closure-treatment bin.

The control units are potential closure-treatment bin observations whose treatment fraction equals 0. I re-estimate Equation 3.1 with 39,334 observations: 14,472 treated observations and 24,862 control observations. Figure A.12 displays the treatment coefficients. The treatment coefficients display the same pattern as in my preferred specification except that there is a small decrease in juvenile catch four days after closures end. When I convert the treatment coefficients into changes in the number of juveniles caught because of the policy, accounting for the reallocation in tons caught due to the total allowable catch limit, I estimate that the policy increases total juvenile catch by 34 billion juveniles, or 32% (delta method standard errors are 2.9 billion and 2.7%, respectively). My finding that closures cause temporal and spatial spillovers and increase total juvenile catch is robust to this alternative estimation strategy.

I also re-estimate the effect of the policy using synthetic controls (Abadie et al., 2010; Abadie & Gardeazabal, 2003). For each actual closure declared by the regulator, I construct a synthetic control group from the potential closures whose treatment fraction equals 0. I include as predictors all of the control variables in Equation 3.1 (excluding fixed effects) as well as pre-period juvenile catch up to 8 days before the beginning of closure periods. I use the Synth package in R, which returns an error for 115 out of 410 actual closures (Abadie et

[4]For the 9% of closures during my study period that begin at 6 AM instead of midnight, I construct control variables from the sets that occur inside the closure in the 12 to 27 hours before the closure begins, because closures that begin at 6 AM must be announced by 6 PM the previous day.

al., 2011).[5] However, I am able to obtain a synthetic control group for each of the remaining 295 actual closures.

Figure A.13 displays the synthetic control results. The y-axis is the average juvenile catch for treated observations (actual closures) minus the average juvenile catch for control observations (weighted average of potential closures). As in my preferred specification, juvenile catch is the inverse hyperbolic sine of millions of juveniles caught. I do not provide confidence intervals in Figure A.13 because the synthetic control procedure of computing weights on potential closures for each actual closure is computationally intensive (the single run I performed took several hundred CPU hours). When I convert the difference in average juvenile catch in each treatment bin into changes in the number of juveniles caught because of the policy, accounting for the reallocation in tons caught due to the total allowable catch limit, I estimate that the policy increases total juvenile catch by 40 billion juveniles, or 40%. This result is similar to my preferred estimate of the effect of the temporary spatial closures policy—an increase in juvenile catch of 47 billion juveniles, or 50%—even though it was obtained with a different identification strategy.

[5] 8 of these error instances are due to the absence of length distribution control variables described above.

Figure A.12: Treatment coefficients from re-estimating Equation 3.1 with actual closures as treated units and potential closures as control units

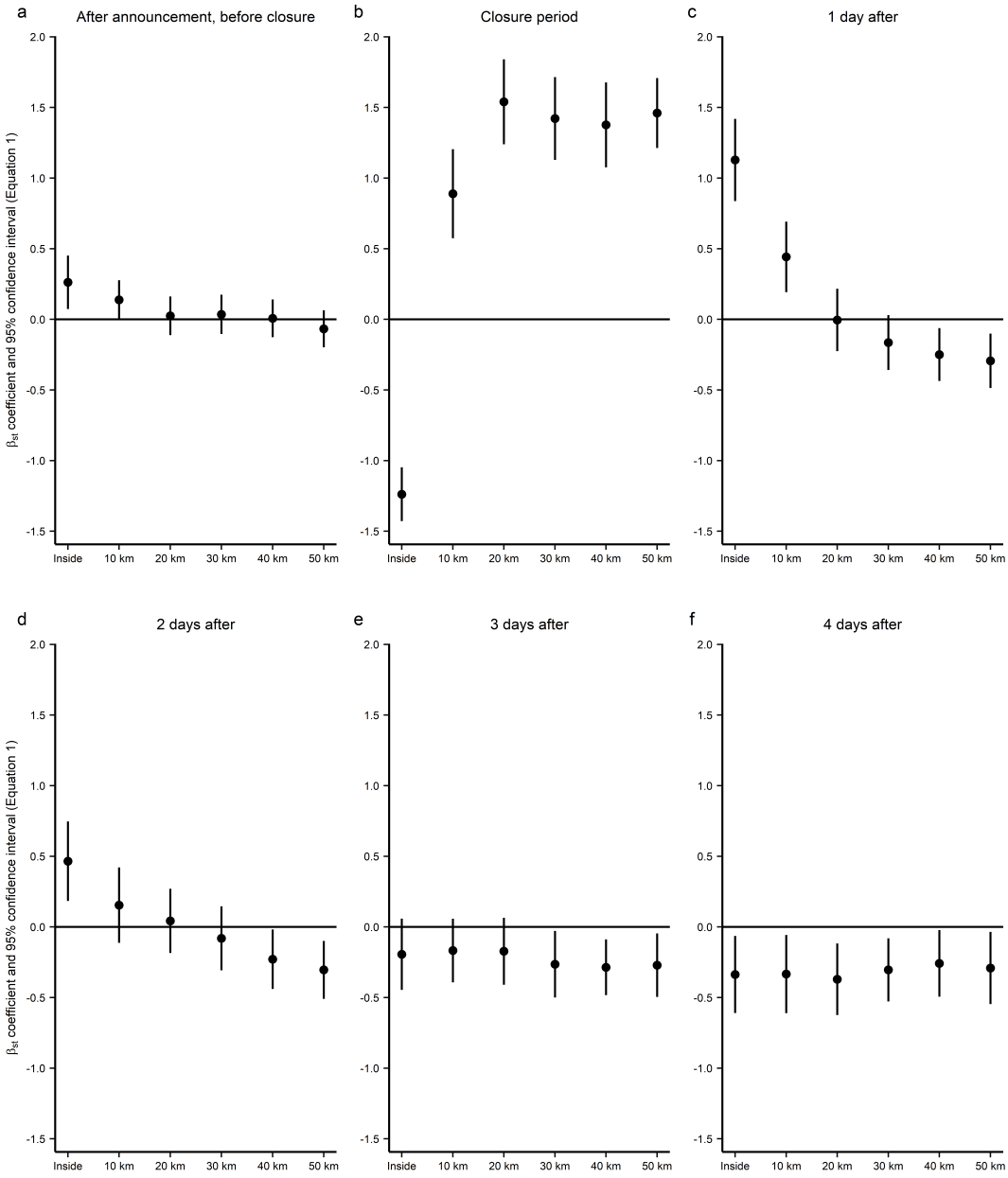

Notes: Actual closure-treatment bins are the treated units. Potential closure-treatment bins whose treatment fraction equals 0 are the control units. N = 39,422. Points are coefficients and whiskers are 95% confidence intervals. Standard errors clustered at level of two-week-of-sample by two-degree grid cell.

Figure A.13: Synthetic control estimates of the effect of closures

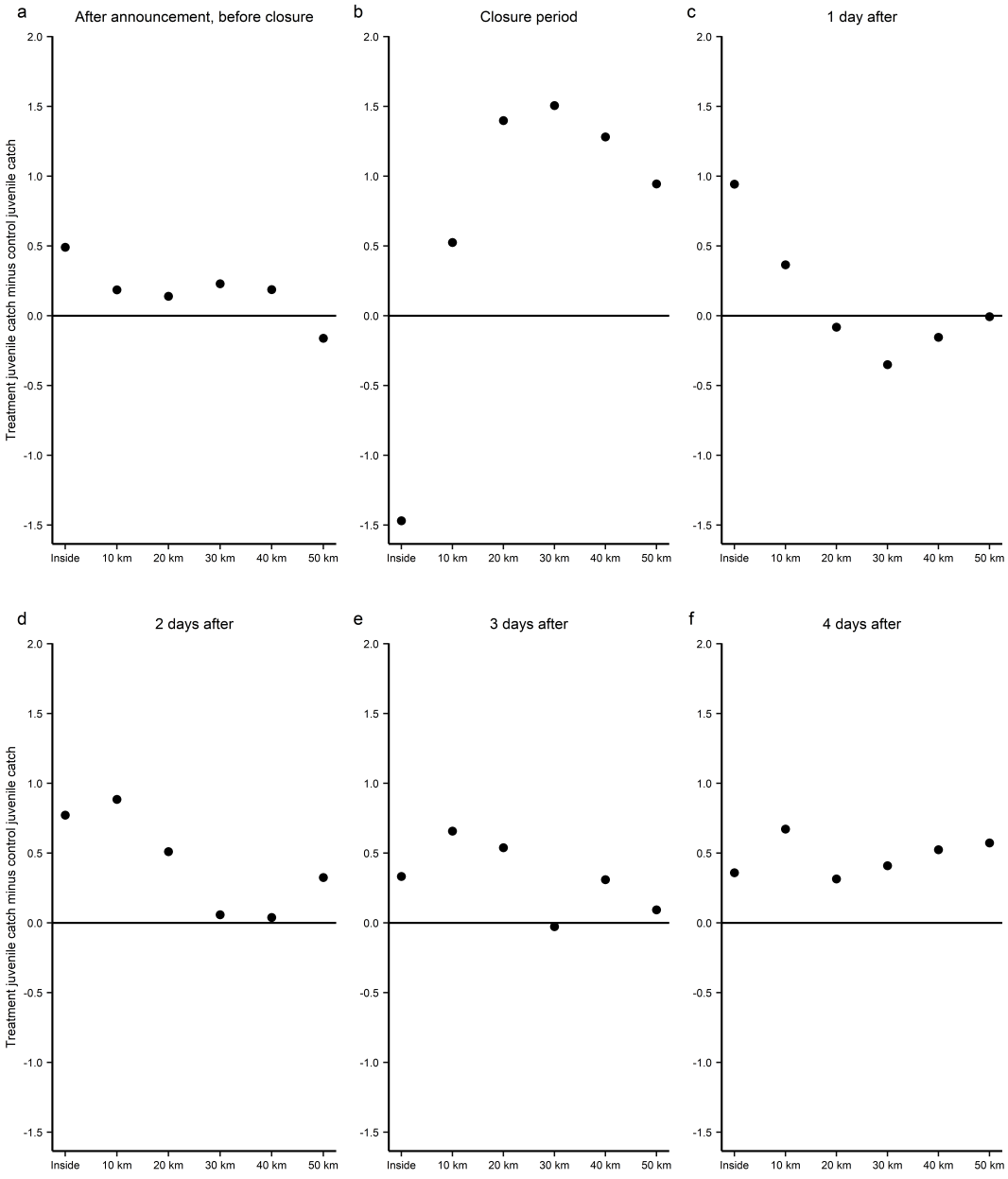

Notes: Points are average juvenile catch for treated observations (actual closures) minus the average juvenile catch for control observations (weighted average of potential closures) in a given treatment bin, where juvenile catch is the inverse hyperbolic sine of millions of juveniles caught.

A.2 Additional results

Heterogeneity by size of closure and length of closure period

Perhaps the temporary spatial closures policy does not reduce juvenile catch because the closures are not large enough or do not last long enough. The average size of a closure declared by the regulator is 1,328 km^2, or 36 by 36 km for a square closure. A school of anchoveta can swim 20 to 30 km in a day (Peraltilla & Bertrand, 2014). If juvenile anchoveta swim outside the closed area during the closure period, then closures might not be large enough to prevent them from being caught. With respect to the length of the closure period, the closures policy is intended to reduce juvenile catch by encouraging fishermen to find new places to fish (Section 1.2). The regulator can declare closures that last three to five days, which might not be enough time for this process to occur.

I test for treatment effect heterogeneity by size of closure and by the length of the closure period. I estimate the following regression:

$$\begin{aligned} JuvenileCatch_{ist} =& \alpha_{sth} + \beta_{sth} TreatFraction_{isth} + \sum_{\ell=[3,3.5)}^{[18.5,19)} \xi_\ell Prop_{i\ell} + \\ & \gamma_1 Sets_i + \gamma_2 Tons_i + \gamma_3 Area_i + \gamma_4 DistToCoast_i + \\ & \gamma_5 TonsPerSet_i + \gamma_6 TonsPerArea_i + \sigma_{wg} + \delta_d + \epsilon_{isth} \end{aligned} \tag{A.2}$$

where h indicates heterogeneity category and all other variables and subscripts are as defined for Equation 3.1.

The outcome variable, control variables, and the number of observations are the same as in Equation 3.1. The only difference is there are now twice as many treatment coefficients (72, instead of 36). In the test for heterogeneity by size of closure, h denotes treatment fraction overlap with actual closures that are either above-median size or below-median size. For example, to estimate Equation 3.1 I estimated treatment fraction overlap between potential closure-treatment bin ist and actual closure-treatment bin ist. Now I calculate treatment fraction overlap between potential closure-treatment bin ist and actual closure-treatment bin ist for actual closures that are above-median size, and also calculate treatment fraction overlap between potential closure-treatment bin ist and actual closure-treatment bin ist for actual closures that are below-median size.

In the test for heterogeneity by length of closure, h indicates treatment fraction overlap with actual closures that last either three days or five days. I do not estimate treatment effect heterogeneity for actual closures that last 4 days because only 15% of actual closures are 4 days long. I compute treatment fraction overlap with 3- and 5-day actual closures separately, creating 72 treatment bins of interest. I do not include bins that are four days after the closure period in my regression because the treatment effect estimates for these bins for five-day closures are very large and noisy. As Figure 1.8 shows, these bins are not important for understanding the effect of the policy, and including them in this test for

heterogeneity by length of closure distorts the total percentage change I calculate for 5-day closures.

I convert the treatment coefficients from these two regressions into total percentage changes in juvenile catch because of the policy in the same manner as in Section 1.6. Larger closures seem to perform even worse than smaller closures. Above-median-size closures increase juvenile catch by 58%, while below-median-size closures increase juvenile catch by 34% (p-value on this difference is .048). Larger closures could cause larger increases in juvenile catch because congestion costs are lower or if larger closures are a larger positive signal of fishing productivity. There does not appear to be treatment effect heterogeneity by length of closure. 3-day closures increase juvenile catch by 48%, while 5-day closures increase juvenile catch by 50% (p-value on this difference is .95). Within the support of the data, it does not seem that making closures larger or longer improves the performance of the policy.

Heterogeneity by firm size and vessel size

Certain types of vessels may respond to closures more than others. I test for treatment effect heterogeneity along two related dimensions: firm size, measured by the number of vessels a firm owns that are authorized to fish in the North-Central zone, and vessel size, measured by vessel length in meters. These dimensions are related because large firms tend to own large vessels (see Table A.4). I test for treatment effect heterogeneity by re-estimating Equation 1.3 from Section 1.8, with subscript h now denoting firm size category in the first regression and vessel size category in the second regression. I convert the treatment coefficients from these two regressions into total percentage changes in juvenile catch because of the policy in the same manner as in Section 1.6.

First, I find that vessels belonging to large firms have larger treatment effects than vessels belonging to smaller firms. The increase in total juvenile catch because of the closures policy is 60% for the vessels that belong to the seven largest firms, which each own at least 19 vessels. The increase in total juvenile catch is 44% for vessels that belong to medium-sized firms, who own between 2 and 10 vessels, and is 11% for vessels that belong to firms that own only one vessel. Large-firm vessels account for 77% of the closures policy treatment effect, which is greater than their share of total juvenile catch in the fishery (70%).

Second, I find that above-median-length vessels have larger treatment effects than below-median-length vessels. The increase in juvenile catch because of the closures policy is 59% for above-median vessels, compared to 24% for below-median vessels. Above-median vessels account for 90% of the closures policy treatment effect, which is greater than their share of total juvenile catch in the fishery (83%).

It is difficult to determine whether above-median-length vessels respond more to closures because they are large, so have more flexibility in the length of their fishing trips, or because they belong to larger firms. 96% of large-firm vessels are above-median length, but among medium firms it is possible to examine heterogeneity by vessel length because 75% are below-median length and 25% are above-median length. I re-estimate equation 1.3 using only juvenile catch among medium firms to calculate the outcome variable. In contrast to

Table A.4: Vessel characteristics in the six fishing seasons of 2017, 2018, and 2019

	All vessels (1)	Large-firm vessels (2)	Medium-firm vessels (3)	Singleton vessels (4)
A. Average tons landed per season				
Minimum	3.11	105.45	14.64	3.11
Mean	2607.41	6311.44	1842.81	903.56
Median	1324.49	6004.34	1303.62	722.86
Max	22261.65	22261.65	10852.99	9389.83
B. Average number of active vessels per season				
Minimum	708	178	263	256
Mean	730.17	182	276.67	271.5
Median	731	182	278.5	269
Maximum	750	185	283	288
C. Vessel length (m)				
Minimum	11.23	15.85	11.3	11.23
Mean	26.05	41.64	24.06	17.62
Median	20.9	40.48	21.72	17.05
Max	77	77	53.75	42.57

Large-firm vessels are vessels that belong to one of the seven largest firms, which each own at least 19 vessels. Medium-firm vessels belong to firms that own 2 to 10 vessels. Singleton vessels belong to a firm that owns only one vessel. Data is for the North-Central zone only. Landings data is used to calculate the number of active vessels each season. Landings and vessel length data are from PRODUCE.

the result using all vessels, I find the that increase in juvenile catch because of the closures policy is smaller for above-median-length vessels (25%) than for below-median-length vessels (47%). This difference is statistically significant and could indicate that firm size is the more relevant dimension of heterogeneity. Larger firms may be more able to aggregate information from closures and dispatch vessels accordingly.

A.3 Data Appendix

The main outcome variable of interest in this paper is juvenile catch: the number of individual anchoveta that are caught that are less than 12 cm. There are two challenges in calculating juvenile catch in an unbiased and accurate manner.

First, fishermen may underreport percentage juvenile in the electronic logbook data in order to avoid triggering a closure in the area they are fishing. If I only used raw electronic logbook data to calculate juvenile catch and underreporting is correlated with closures declared by the regulator, my treatment effect estimates would be biased.

Second, even if percentage juvenile reported by fishermen in the electronic logbook data is unbiased, percentage juvenile and tons caught are not sufficient for calculating juvenile catch because the number of individuals caught depends on the length distribution of those individuals. For example, consider two sets that both catch 40 tons of anchoveta that are 20% juvenile. In the first set, 20% of individuals are between 11.5 and 12 cm and 80% of individuals are between 12 and 12.5 cm (actual length distributions are much more diffuse; see Figure A.14). In the second set, 20% of individuals are between 10 and 10.5 cm and 80% of individuals are between 14 and 14.5 cm. The weight of an anchoveta in grams equals $.0036 length^{3.238}$ (IMARPE, 2019). Therefore, 683,137 juvenile anchoveta are caught by the first set and 469,685 are caught by the second set, even though both sets caught the same tons and percentage juvenile.[6]

Recall from Section 1.4 that fishermen report percentage juvenile to the regulator in the electronic logbook data, but not the length distribution from which percentage juvenile is calculated (percentage juvenile is the percentage of measured individuals that are less than 12 cm). I obtained a supplementary electronic logbook dataset for a group of vessels that report length distribution data to their owners. These vessels represent 56% of landings and their data was provided by Sociedad Nacional de Pesquería (SNP), a consortium of fishing companies, in January 2020.

To calculate juvenile catch for each set, I first use the length distribution values from sets in the SNP electronic logbook data to impute length distributions for non-SNP sets, based on the location, time, and percentage juvenile caught by non-SNP sets. After obtaining length distributions for all sets in the electronic logbook data, I match sets to landings events. I then use the percentage juvenile measured by third-party inspectors at landing to update length distributions in the electronic logbook data and calculate juvenile catch for each set.

Specifically, I first identify sets in the full electronic logbook data (reported to the regulator) that are also in the SNP data based on unique vessel identifiers and the time each set occurred. I calculate the number of individual anchoveta (both juveniles and adults) caught by these sets based on their length distribution and tons caught. When percentage juvenile for a set in the SNP data does not match its counterpart in the full electronic logbook data (i.e., the vessel reported a different percentage juvenile to its owner than to the regulator), I shift the length distribution up or down in half-cm increments until the absolute difference between the implied percentage juvenile (percentage of individuals that are less than 12 cm, as implied by the updated length distribution) and the percentage juvenile reported to the regulator is minimized (i.e., a one unit shift of the length distribution in either direction would result in a larger absolute difference between implied and reported percentage juvenile).

[6]My results are robust to measuring juvenile catch in terms of tons of juveniles caught (Figure A.6).

I then impute length distributions for non-SNP sets as follows. For each two-week-of-sample by two-degree grid cell, I calculate the individuals-weighted average proportion of individuals in each half-cm length interval. Given the percentage juvenile value for each non-SNP set, I adjust the length distribution for that set's two-week-of-sample by two-degree grid cell to match the set's percentage juvenile value. For sets with percentage juvenile above (below) the individuals-weighted average percentage juvenile for their two-week-of-sample by two-degree grid cell, I inflate (deflate) the proportion of individuals below 12 cm and deflate (inflate) the proportion of individuals above 12 cm so that the imputed length distribution for each set implies a percentage juvenile equal to the percentage juvenile reported for that set.[7] I use the resulting length distribution and tons caught to calculate the number of individuals caught by non-SNP sets.

For example, suppose the reported percentage juvenile for a non-SNP set is 20%, the individuals-weighted average percentage juvenile among SNP sets in the two-week-of-sample by two-degree grid cell is 10%, and the average length distribution for the two-week-of-sample by two-degree grid cell is as follows: 2% of individuals are between 11 and 11.5 cm, 8% of individuals are between 11.5 and 12 cm, 60% of individuals are between 12 and 12.5 cm, and 30% of individuals are between 12.5 and 13 cm. Then the imputed length distribution for the set is: 4% of individuals are between 11 and 11.5 cm, 16% of individuals are between 11.5 and 12 cm, 53.33% of individuals are between 12 and 12.5 cm, and 26.67% of individuals are between 12.5 and 13 cm. This length distribution implies that the average weight of individuals caught by this set is 12.1 grams. If the set caught 50 tons of anchoveta, then it caught 4,132,685 individual anchoveta, of which 826,537 are juvenile.[8]

Next, I match sets to landing events in order to correct the length distribution, percentage juvenile, and number of individuals caught by each set. Unlike fishermen in the electronic logbook data, the closures policy does not give third-party inspectors an incentive to misreport percentage juvenile because the regulator does not use landings data to determine closures during my study period.

Fishermen report when each fishing trip begins and ends in the electronic logbook data. For each landing event by a vessel, I record the vessel's most recent preceding electronic logbook fishing trip and the sets that occurred on the trip. I matched 93.1% of sets to landing events. When the individuals-weighted average percentage juvenile across sets on a trip does not equal the percentage juvenile measured by third-party inspectors at landing, I multiply each set-level percentage juvenile value by the ratio of landing-level percentage juvenile to average set-level percentage juvenile. For the 6.9% of sets I was unable to match to landing events, I multiply percentage juvenile by the ratio of average landing-level percentage juvenile to average set-level percentage juvenile, where averages are calculated among matched sets in

[7] 96.5% of non-SNP sets occur in a two-week-of-sample by two-degree grid cell that also contains SNP sets. For the remaining 3.5% of non-SNP sets, I use the average length distribution at the two-week-of-sample level in the above procedure. 58 non-SNP sets (.04%) occur during a two week period without any SNP sets. I record the length distribution values, number of individuals caught, and number of juveniles caught as missing for these 58 sets.

[8] Recall from Section 1.4 that fishermen do not underreport tons caught.

the same two-week-of-sample by two-degree grid cell and weighted by number of individuals caught.

For example, suppose there are two sets on a trip, the first set caught 1 million individuals of which 10% are reported juvenile, the second set caught 4 million individuals of which 5% are reported juvenile, and 12% juvenile is measured at landing, when the fishing trip ends. The "corrected" percentage juvenile values are 20% and 10% for the first and second set and the weighted average percentage juvenile across sets is now 12%. I make additional adjustments when this procedure results in set-level percentage juvenile values that are undefined or greater than 100%. After this procedure, percentage juvenile averaged across sets in a trip equals landing-level percentage juvenile.

Finally, I shift the length distribution of each set up or down in half-cm increments until the absolute difference between the implied percentage juvenile (updated percentage of individuals that are less than 12 cm) and the corrected percentage juvenile is minimized. I use the resulting length distribution to calculate the corrected number of individuals caught by each set. The number of juveniles caught by each set is the corrected number of individuals times the corrected percentage juvenile. The procedure described in this section preserves the resolution of the electronic logbook data while ensuring that my main outcome of interest—juvenile catch at a given location and time—is not systematically manipulated.

Figure A.14: Corrected length distribution of anchoveta caught in the North-Central zone, 2017 to 2019 fishing seasons

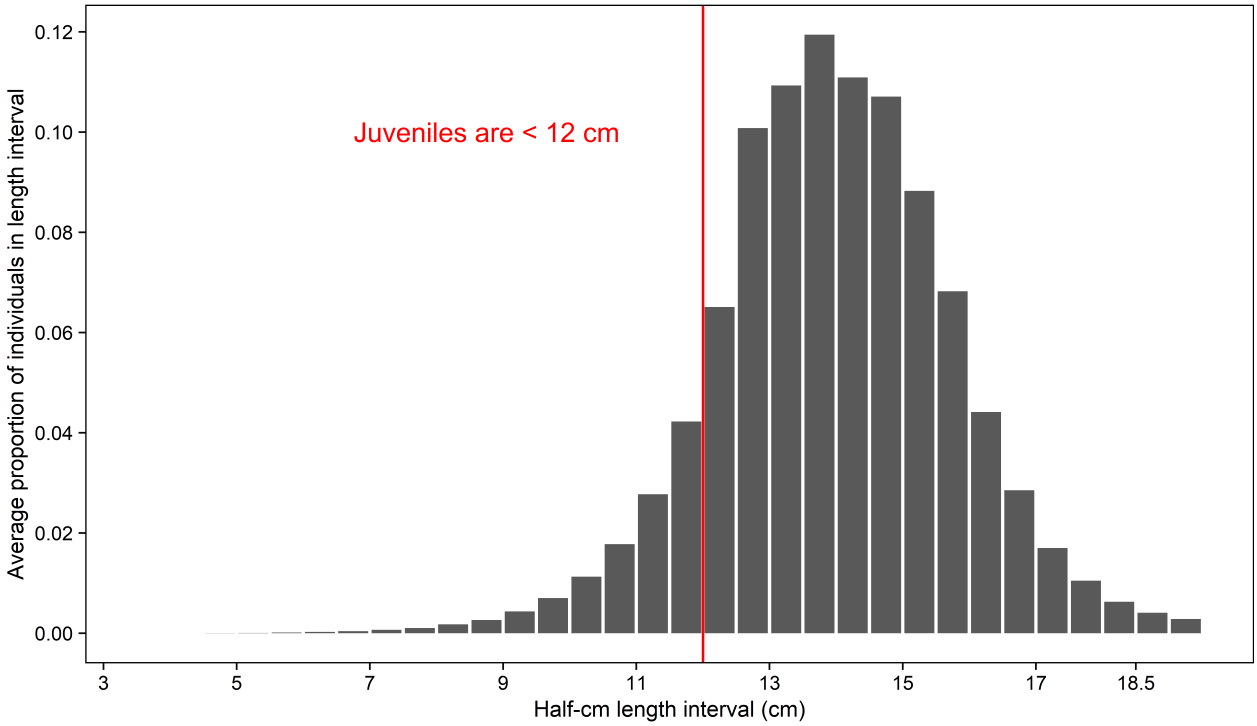

Notes: The y-axis indicates the average proportion of anchoveta caught in each half-cm length interval, weighted by the number of individuals caught by each set. I calculated these values from the corrected electronic logbook data. There are 246,914 sets (observations) in the corrected electronic logbook data. 18.3% of individuals caught during my study period are juvenile.

Figure A.15: Individuals-weighted average percentage juvenile in each treatment bin, for actual closures declared by the regulator

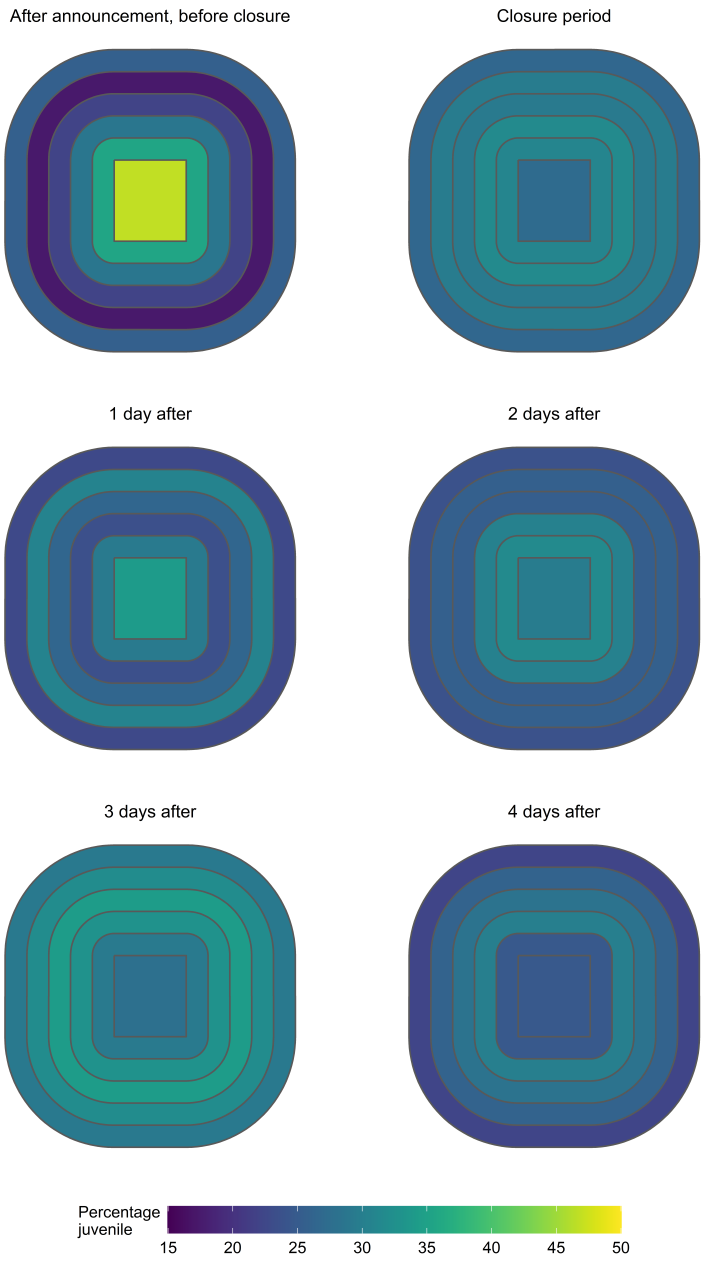

Notes: Percentage juvenile values are from the corrected electronic logbook data. Average percentage juvenile outside the treatment window is 9%.

A.4 Proofs of Propositions 1 to 3

I prove Proposition 2 first because the proof of Proposition 1 relies on the proof of Proposition 2a.

Proof of Proposition 2a. To prove the equality of expected profit in locations g and k, suppose the contradiction that $\exists j$ s.t. $\mathrm{E}[\pi_{j,g}(\mu_g, I_{-j,g})|\tilde{\mu_g}, \tilde{\mu_k}, C=0] \neq \mathrm{E}[\pi_{j,k}(\mu_k, I_{-j,k})|\tilde{\mu_g}, \tilde{\mu_k}, C=0]$. Suppose without loss of generality that $\mathrm{E}[\pi_{j,g}(\mu_g, I_{-j,g})|\tilde{\mu_g}, \tilde{\mu_k}, C=0] > \mathrm{E}[\pi_{j,k}(\mu_k, I_{-j,k})|\tilde{\mu_g}, \tilde{\mu_k}, C=0]$. If $j \in I_k$, then vessel j could increase expected profit by choosing g instead. If $j \in I_g$, $\exists r \in I_k$ s.t. vessel r could increase their expected profit by choosing g instead (because vessels are identical). To satisfy the definition of a Bayes-Nash equilibrium, expected profit from fishing in location g must equal expected profit from fishing in location k. The same argument proves the claim for when $C=1$ as well.

Uniqueness. Suppose there exists Bayes-Nash equilibria $(\hat{I}^*_g, \hat{I}^*_k)$ and $(\hat{I}^*_h, \hat{I}^*_k)$ such that $(\hat{I}^*_g, \hat{I}^*_k) \neq (I^*_g, I^*_k)$ and $(\hat{I}^*_h, \hat{I}^*_k) \neq (I^*_h, I^*_k)$. Without loss of generality, suppose $\hat{I}^*_g > I^*_g$. Then $\hat{I}^*_k < I^*_k$ since I is fixed. Since profit is decreasing in the number of vessels who fish in the same location ($\frac{\partial \pi_{i,\ell}(\mu_\ell, I_{-i,\ell})}{\partial I_{-i,\ell}} < 0$), expected profit from fishing in location g is lower in the $(\hat{I}^*_g, \hat{I}^*_k)$ equilibrium than in the (I^*_g, I^*_k) equilibrium ($\mathrm{E}[\pi_{i,g}(\mu_g, \hat{I^*}_{-i,g})|\tilde{\mu_g}, \tilde{\mu_k}, C=0] < \mathrm{E}[\pi_{i,g}(\mu_g, I^*_{-i,g})|\tilde{\mu_g}, \tilde{\mu_k}, C=0] \ \ \forall i$). Similarly, expected profit from fishing in location k is higher in the $(\hat{I}^*_g, \hat{I}^*_k)$ equilibrium than in the (I^*_g, I^*_k) equilibrium ($\mathrm{E}[\pi_{i,k}(\mu_k, \hat{I^*}_{-i,k})|\tilde{\mu_g}, \tilde{\mu_k}, C=0] > \mathrm{E}[\pi_{i,k}(\mu_k, I^*_{-i,k})|\tilde{\mu_g}, \tilde{\mu_k}, C=0] \ \ \forall i$). By the proof of Proposition 2a, $\mathrm{E}[\pi_{i,g}(\mu_g, I^*_{-i,g})|\tilde{\mu_g}, \tilde{\mu_k}, C=0] = \mathrm{E}[\pi_{i,k}(\mu_k, I^*_{-i,k})|\tilde{\mu_g}, \tilde{\mu_k}, C=0] \ \ \forall i$. Then $(\hat{I}^*_g, \hat{I}^*_k)$ cannot be a Bayes-Nash equilibrium because $\mathrm{E}[\pi_{i,g}(\mu_g, \hat{I^*}_{-i,g})|\tilde{\mu_g}, \tilde{\mu_k}, C=0] < \mathrm{E}[\pi_{i,k}(\mu_k, \hat{I^*}_{-i,k})|\tilde{\mu_g}, \tilde{\mu_k}, C=0] \ \ \forall i$. $(\hat{I}^*_h, \hat{I}^*_k)$ cannot be a Bayes-Nash equilibrium by the same argument. Therefore the Bayes-Nash equilibria (I^*_g, I^*_k) and (I^*_h, I^*_k) are unique.

Proof of Proposition 2b. Note that $\frac{\partial I_\ell}{\partial \mu_\ell} = 0$; fishing location decisions I_ℓ depend on $\tilde{\mu_\ell}$, but not true productivity μ_ℓ because μ_ℓ is unobserved. Then $\pi_{i,g}(\mu_g, I_{-i,g}) > \ \pi_{i,k}(\mu_k, I_{-i,k}) \ \forall i$ because vessels are identical and $\frac{\partial \pi_{i,\ell}(\mu_\ell, I_{-i,\ell})}{\partial \mu_\ell} > 0$. If the closure announcement contains valuable information in that it informs vessels that the true productivity of location g is higher than location k, then vessels that happen to fish in location g when $C=0$ have higher profits because there is no closure announcement that vessels can use to change their fishing location decisions.

Proof of Proposition 1. I will first prove $\frac{\partial I_\ell}{\partial \tilde{\mu_\ell}} > 0$ in the case where congestion costs are the same across locations, then use this fact to complete the proof. Because marginal congestion costs are in fact higher in location h than in locations g and k, the positive signal from the closure announcement must be sufficiently large in order for there to be an increase in the number of vessels fishing in h when $C=1$ relative to the number of vessels fishing in g when $C=0$ ($\tilde{\mu_h} >> \tilde{\mu_k}$ in order for $I^*_h > I^*_g$). If this condition is met, total juvenile catch will be higher with the closure than without it as long as percentage juvenile is sufficiently high in location h relative to locations g and k.

To prove $\frac{\partial I_\ell}{\partial \tilde{\mu_\ell}} > 0$ when congestion costs are the same across locations, I suppress some of the arguments of expected profit for notational compactness. For example, let $\mathrm{E}[i,g]$ denote $\mathrm{E}[\pi_{i,g}(\mu_g, I_{-i,g})|\tilde{\mu_g}, \tilde{\mu_k}, C=0]$. Suppose the contradiction, that the number of vessels who choose location ℓ is not increasing in $\tilde{\mu_\ell}$ ($\frac{\partial I_\ell}{\partial \tilde{\mu_\ell}} \leq 0$). Since profit is decreasing in the number of vessels who fish in the same location ($\frac{\partial \pi_{i,\ell}(\mu_\ell, I_{-i,\ell})}{\partial I_{-i,\ell}} < 0$), expected profit from fishing in location h is higher than in g ($\mathrm{E}[i,h^*] > \mathrm{E}[i,g^*] \ \ \forall i$), because marginal congestion costs are the same in h and g and the number of vessels who choose h is not higher by assumption ($I_h^* \leq I_g^*$). Because the total number of vessels is fixed, the number of vessels who choose location k when $C=1$ is greater than or equal to the number of vessels who choose location k when $C=0$ ($I^*_{k|C=1} \geq I^*_{k|C=0}$). Since vessels have the same beliefs about k's productivity in both states of the world, expected profit from fishing in location k when $C=0$ is at least as great as expected profit from fishing in k when $C=1$ ($\mathrm{E}[i,k^*|C=0] \geq \mathrm{E}[i,k^*|C=1] \ \ \forall i$). Since (I_g^*, I_k^*) is a Bayes-Nash equilibrium, $\mathrm{E}[i,g^*] = \mathrm{E}[i,k^*|C=0]$ by the proof of Proposition 2a. Then $\mathrm{E}[i,h^*] > \mathrm{E}[i,k^*|C=1] \ \ \forall i$ because $\mathrm{E}[i,h^*] > \mathrm{E}[i,g^*] = \mathrm{E}[i,k^*|C=0] \geq \ \mathrm{E}[i,k^*|C=1]$. Then (I_h^*, I_k^*) cannot be a Bayes-Nash equilibrium by the proof of Proposition 2a. Contradiction. Therefore, $\frac{\partial I_\ell}{\partial \tilde{\mu_\ell}} > 0$ when congestion costs are the same across locations.

However, marginal congestion costs are in fact higher in location h (because h covers less area than g and k). Though vessels believe mean productivity is higher in h than in g and k, the higher marginal congestion cost in h counteracts the effect of higher mean productivity on the number of vessels who choose h. For this reason, it is not necessarily the case that the closures policy increases fishing near closures ($I_h^* > I_g^*$).

To see how higher marginal congestion costs in h reduce the number of vessels who choose h, consider the case when $\tilde{\mu_h} = \tilde{\mu_g}$ and suppose the contradiction that $I_h^* \geq I_g^*$. Expected profits are lower in h than in g because marginal congestion costs are higher in h ($\mathrm{E}[i,h^*] < \mathrm{E}[i,g^*] \ \ \forall i$). Since $\tilde{\mu_k}$ is the same in both states of the world and $I^*_{k|C=0} \geq I^*_{k|C=1}$ (because $I_g^* \leq I_h^*$), expected profit in k when $C=0$ is less than or equal to expected profit in k when $C=1$ ($\mathrm{E}[i,k^*|C=0] \leq \mathrm{E}\ [i,k^*|C=1] \ \ \forall i$). Since (I_g^*, I_k^*) is a Bayes-Nash equilibrium, $\mathrm{E}[i,g^*] = \mathrm{E}[i,k^*|C=0]$ by the proof of Proposition 2a. Then $\mathrm{E}[i,h^*] < \mathrm{E}[i,k|C=1] \ \ \forall i$ because $\mathrm{E}[i,h^*] < \mathrm{E}[i,g^*] = \mathrm{E}[i,k|C=0] \leq \mathrm{E}[i,k|C=1]$. Then (I_h^*, I_k^*) cannot be a Bayes-Nash equilibrium by the proof of Proposition 2a. Contradiction. Therefore, the higher marginal congestion costs in h reduce the number of vessels who fish in location h when $\tilde{\mu_h} = \tilde{\mu_g}$ ($I_h^* < I_g^*$).

Together, the fact that vessels believe mean productivity in h is higher but know that marginal congestion costs are also higher in h means that the effect of the closures policy on fishing location choice is ambiguous. The closure announcement must be a sufficiently large positive signal relative to congestion costs in order to increase the number of vessels who choose to fish near closures (location h). In this case, there is a second condition necessary for the closures policy to increase total juvenile catch: productivity and percentage juvenile must be sufficiently high in location h relative to locations g and k.

The treatment effect τ of the closures policy on total juvenile catch is

$$\begin{aligned}\tau &= TotJuv^*(C=1) - TotJuv^*(C=0) \\ &= \gamma(I_h^*\mu_h\rho_h + I_{k|C=1}^*\mu_k\rho_k - (I_g^*\mu_g\rho_g + I_{k|C=0}^*\mu_k\rho_k)) \\ &= \gamma(I_h^*\mu_h\rho_h - I_g^*\mu_g\rho_g + \mu_k\rho_k(I_{k|C=1}^* - I_{k|C=0}^*))\end{aligned} \tag{A.3}$$

If $I_h^* > I_g^*$, the third term in the expression, $\mu_k\rho_k(I_{k|C=1}^* - I_{k|C=0}^*)$, is negative because $I_{k|C=1}^* < I_{k|C=0}^*$. In order for the closures policy to increase total juvenile catch ($\tau > 0$), the number of vessels fishing, productivity, and percentage juvenile in location h must be sufficiently high relative to location g when there is no closure ($I_h^*\mu_h\rho_h >> I_g^*\mu_g\rho_g$), as well as sufficiently high relative to productivity and percentage juvenile in location k.

Parametric example of Propositions 1 and 2a. Figure 1.3 displays the Bayes-Nash equilibria when $\mathrm{E}[\pi_{i,\ell}(\mu_\ell, I_{-i,\ell})|\tilde{\vec{\mu}}, C] = \tilde{\mu}_\ell - \alpha_\ell I_{-i,\ell}$, where α_ℓ is the cost to vessel i from one additional vessel fishing in location ℓ. The equilibrium when $C = 0$ results from setting $\tilde{\mu}_g - \alpha_g I_{-i,g} = \tilde{\mu}_k - \alpha_k I_{-i,k}$ and the equilibrium when $C = 1$ is similarly defined. Recall that marginal congestion costs are only different for h; $\alpha_g = \alpha_k$ and let α represent this value. The equilibrium when $C = 0$, (I_g^*, I_k^*), is $(\frac{\tilde{\mu_g}-\tilde{\mu_k}}{2\alpha} + \frac{1}{2}I,\ \frac{\tilde{\mu_k}-\tilde{\mu_g}}{2\alpha} + \frac{1}{2}I)$. The equilibrium when $C = 1$, (I_h^*, I_k^*), is $(\frac{\tilde{\mu_h}-\tilde{\mu_k}}{\alpha_h+\alpha} + \frac{\alpha}{\alpha_h+\alpha}I,\ \frac{\tilde{\mu_k}-\tilde{\mu_h}}{\alpha_h+\alpha} + \frac{\alpha_h}{\alpha_h+\alpha}I)$. Substituting these values into Equation A.3 gives the change in total juvenile catch due to the policy.

Proof of Proposition 3. Since $\tilde{\mu_{g,a}} > \tilde{\mu_{g,-a}}$ and congestion costs are the same in locations g and k, the proof of Proposition 1 implies that type $-a$ vessels will only choose g after all type a vessels have chosen g ($\frac{I_{g,-a}^*}{I_{-a}} > 0$ only when $\frac{I_{g,a}^*}{I_a} = 1$). Since the Bayes-Nash equilibria are interior by assumption, $\frac{I_{g,-a}^*}{I_{-a}} < 1$ (if $\frac{I_{g,-a}^*}{I_{-a}} = 1$, then $I_k^* = 0$). Then a greater percentage of type a vessels choose g than type $-a$ vessels: $\frac{I_{g,a}^*}{I_a} > \frac{I_{g,-a}^*}{I_{-a}}$. Conversely, a lower percentage of type a vessels choose k than type $-a$ vessels: $\frac{I_{k,a}^*}{I_a} < \frac{I_{k,-a}^*}{I_{-a}}$.

Since type a and type $-a$ vessels are identical when $C = 1$ ($\tilde{\mu_{h,a}} = \tilde{\mu_{h,-a}}$), the same percentage of each type choose locations h and k ($\frac{I_{h,a}^*}{I_a} = \frac{I_{h,-a}^*}{I_{-a}}$ and $\frac{I_{k,a}^*}{I_a} = \frac{I_{k,-a}^*}{I_{-a}}$). Since both types of vessels catch the same number of juveniles when they fish in the same location, $\frac{TotJuv(C=1)_{-a}^*}{I_{-a}} = \frac{TotJuv(C=1)_a^*}{I_a}$. Then the percentage difference in treatment effects between

the two types of vessels can be written as

$$\begin{aligned}
\frac{\tau_{-a}}{I_{-a}} - \frac{\tau_a}{I_a} &= \frac{TotJuv(C=1)^*_{-a} - TotJuv(C=0)^*_{-a}}{I_{-a}} - \frac{TotJuv(C=1)^*_a - TotJuv(C=0)^*_a}{I_a} \\
&= \frac{TotJuv(C=0)^*_a}{I_a} - \frac{TotJuv(C=0)^*_{-a}}{I_{-a}} \\
&= \gamma\left(\frac{I^*_{g,a}\mu_g\rho_g + I^*_{k,a}\mu_k\rho_k}{I_a} - \frac{I^*_{g,-a}\mu_g\rho_g + I^*_{k,-a}\mu_k\rho_k}{I_{-a}}\right) \\
&= \gamma\left(\mu_g\rho_g\left(\frac{I^*_{g,a}}{I_a} - \frac{I^*_{g,-a}}{I_{-a}}\right) + \mu_k\rho_k\left(\frac{I^*_{k,a}}{I_a} - \frac{I^*_{k,-a}}{I_{-a}}\right)\right) \\
&= \gamma\left(\mu_g\rho_g\left(\frac{I^*_{g,a}}{I_a} - \frac{I^*_{g,-a}}{I_{-a}}\right) + \mu_k\rho_k\left(\frac{I_a - I^*_{g,a}}{I_a} - \frac{I_{-a} - I^*_{g,-a}}{I_{-a}}\right)\right) \\
&= \gamma\left((\mu_g\rho_g - \mu_k\rho_k)\left(\frac{I^*_{g,a}}{I_a} - \frac{I^*_{g,-a}}{I_{-a}}\right)\right) \\
&> 0
\end{aligned}$$

because $\mu_g\rho_g > \mu_k\rho_k$ and $\frac{I^*_{g,a}}{I_a} > \frac{I^*_{g,-a}}{I_{-a}}$.

Appendix B

Property rights and the protection of global marine resources

B.1 Data description and availability

The primary AIS dataset in my analysis contains global, daily hours of fishing by gear type and flag state from 2012 to 2016 at a .01 degree resolution (Kroodsma et al., 2018). Gear type is the type of fishing activity (e.g. drifting longline fishing). Flag state is the country in which a vessel is registered. Vessels in this data have transponders that send identifying information and their location, speed and course to satellites and terrestrial receivers every 2 to 30 seconds. Convolutional neural networks were applied to this vessel movement data to identify fishing vessels and fishing activity. The creators of this dataset estimate that it captures 50-70% of total fishing effort that occurs more than 100 nautical miles (nm) from shore1. This dataset is publicly available at https://globalfishingwatch.force.com/gfw/s/data-download under the heading "Daily Fishing Effort and Vessel Presence at 100th Degree Resolution by Flag State and GearType, 2012-2016."

I used individual fishing vessel characteristics and hours of fishing by individual vessels to construct Figure B.6 and Table B.3. These two datasets are publicly available at the same url as above under the headings "Fishing Vessels Included in Fishing Effort Data" and "Daily Fishing Effort at 10th Degree Resolution by MMSI, 2012-2016", respectively.

Finally, Global Fishing Watch (GFW) provided us with the data used to construct Figure B.3. This data contains the last location and date of all instances in which a vessel with a class A AIS transponder stopped transmitting for more than 24 hours. This data can be obtained from GFW upon request.

Daily nighttime locations of individual lit fishing vessels are publicly available at https://data.ngdc.noaa.gov/instruments/remote-sensing/passive/spectrometers-radiometers/imaging/viirs/vbd/v23/global-saa/daily/. This data was created by applying spike detection algorithms to daily nighttime satellite imagery (Elvidge et al., 2015). Vessels in this dataset use bright lights to attract catch. I used data for each day in 2017, as this is the first year

in which global data is consistently available.

EEZ access agreements data were provided by the Sea Around Us (Lam et al., 2016). This data contains the start and end year of access agreements between countries in which one country pays another country to fish in that country's EEZ. Access agreements can also be multilateral. This data can be requested from the Sea Around Us, or by visiting http://www.seaaroundus.org/data/#/eez, choosing an EEZ, and clicking "Internal Fishing Access Agreements". This data only includes access agreements that began on or before 2014. I added European Union (EU) access agreements that began after 2014 to this data (the EU is the paying entity). EU access agreements are available at https://ec.europa.eu/fisheries/cfp/international/agreements_en.

EEZ-sea shapefiles are publicly available at http://marineregions.org/download_file.php?name=Intersect_IHO_EEZ_v2_2012.zip (VLIZ, 2012). Global, gridded net primary productivity (NPP) data are publicly available at http://www.science.oregonstate.edu/ocean.productivity/standard.product.php5 (Behrenfeld & Falkowski, 1997). I downloaded 8-day NPP composites from 2012 to 2016 at a .083 degree resolution. Global, gridded ocean depth data at a .0167 degree resolution are publicly available at https://www.ngdc.noaa.gov/mgg/global/relief/ETOPO1/data/bedrock/grid_registered/georeferenced_tiff/ETOPO1_Bed_g_geotiff.zip (Amante, 2009). Global, gridded sea surface temperature (SST) data are available at https://podaac.jpl.nasa.gov/dataset/MODIS_AQUA_L3_SST_THERMAL_8DAY_4KM_DAYTIME_V2014.0?ids=Measurement:Platform:Sensor:TemporalResolution&values=Ocean%20Temperature:AQUA:MODIS:Weekly. I downloaded 8-day SST composites from 2012 to 2016 at a .041 degree resolution (OBPG, 2015). I downloaded annual, taxon-level catch data for each EEZ-sea region in my analysis from 2012 to 2014 (the most recent year available) from the Sea Around Us using the seaaroundus R package (Chamberlain & Reis, 2017; Pauly & Zeller, 2015). I obtained life history data for taxa caught in the EEZ-sea regions in my analysis from FishBase and SeaLifeBase using the rfishbase R package (Boettiger et al., 2012). Finally, global, gridded ocean surface currents data are available at ftp://podaac-ftp.jpl.nasa.gov/allData/oscar/preview/L4/oscar_third_deg. I downloaded annual files for 2012 to 2016 that contain surface current velocity at the 5-day, .33 degree resolution (ESR, 2009).

B.2 Empirical strategy

I use the 200 nautical mile (nm) boundary between EEZs and the high seas as a regression discontinuity to estimate the causal effect of EEZs on fishing effort. In a regression discontinuity, treatment assignment for observation i, D_i, is partially or completely determined by whether a predictor variable, X_i, is above or below a certain cutoff value, c (Imbens & Lemieux, 2008). Let $Y_i(1)$ denote the potential outcome if i is assigned to treatment and $Y_i(0)$ denote the potential outcome if i is assigned to the control group (Rubin, 1974). The assumption in a regression discontinuity design is that $Y_i(1)$ and $Y_i(0)$ are continuous in X_i; they depend on X_i but do not change discontinuously as X_i changes. In other words, if

not for the change in treatment assignment at the cutoff value, the outcome variable would change smoothly across the cutoff value. Given this assumption, any discontinuous change in Y_i as X_i crosses the cutoff value is the causal effect of the treatment.

In this paper, after controlling for distance (X_i) to an EEZ-high seas boundary (c), the discontinuous change in fishing effort (Y_i) at the boundary is the causal effect of EEZs (D_i) on fishing effort. I have normalized EEZ-high seas boundaries to be distance 0 ($c = 0$). Observations inside EEZs have positive distance values ($X_i > 0$) and observations on the high seas have negative distance values ($X_i < 0$). If $X_i > 0$, observations are treated and $D_i = 1$. If $X_i < 0$, $D_i = 0$.

I estimate equations of the following general form via ordinary least squares regression:

$$Y_i = \alpha + \tau D_i + \sum_{k=1}^{3} \beta_k X_i^k + D_i \sum_{k=1}^{3} \gamma_k X_i^k + u_i \tag{B.1}$$

where Y_i denotes an outcome variable (usually fishing effort), Greek letters denote coefficients, k denotes polynomial order, and u_i denotes the error term. The parameter of interest is τ, the treatment effect of EEZs on the outcome variable. If $\hat{\tau} < 0$, there is a discontinuous decrease in the outcome variable at the boundary (e.g., fishing effort is lower just inside EEZs compared to just outside EEZs). I typically set $K = 3$, which controls for third-order polynomials in distance to the boundary that are allowed to differ for observations inside an EEZ and for observations outside an EEZ.

I provide estimation details for specific figures and tables in Section 2.4, in Section B.3, and in figure and table captions. Replication code for all figures and tables is available at https://github.com/englander/replication_eez (except for Tables B.2 and B.3, which are summary statistics tables). All analysis was performed in R, except for the calculation of the confidence intervals in Figures 2.2, 2.4, B.1 and B.3-8, which were computed in Stata. My confidence intervals account for heteroscedasticity and serial correlation (Newey & West, 1987). The lag used in calculating each confidence interval was chosen using an optimal lag selection procedure (Newey & West, 1994).

B.3 Data processing, analysis, and interpretation of specific figures and tables

Figure B.3 information

AIS transponders can be turned off on purpose or can randomly fail to transmit. To account for the latter possibility, I normalized the count of off events for a given vessel type by the hours of vessel presence (i.e. vessel density) for vessels of the same vessel type (see Section B.1 for descriptions of these two datasets). I processed observations of off instances and vessel presence hours into integer bins, summed over all EEZ-sea regions and all days, divided the

number of off instances by the number of vessel hours, and multiplied by 10,000 (to get the number of off instances per 10,000 vessel hours).

There is no significant discontinuity in off events at the EEZ-high seas boundary for unauthorized foreign fishing vessels, nor is there a precise trend in off events on either side of the boundary (Figure B.3a). Additionally, the frequency of off instances is too low to meaningfully alter estimates of the effect of EEZs on fishing effort. Finally, the nighttime lit vessels dataset provides further evidence that AIS transponder manipulation is not significantly biasing my deterrence effect estimates. Vessels in this dataset use bright lights at night to attract catch. If they are fishing, they appear in the data regardless of whether they are fishing inside an EEZ or fishing on the high seas. The similarity of Figure 2.2c (AIS unauthorized foreign fishing) to Figure 2.2b (nighttime lit vessel count) therefore provides additional evidence that AIS transponder manipulation is not driving estimated deterrence effects.

There are several reasons why unauthorized foreign vessels would not strategically turn off their AIS transponders in order to avoid detection. The expected benefit of reduced collision risk (from not turning off transponders) could exceed the expected cost of being caught illegally fishing in another nation's EEZ if the probability of being caught is low. Additionally, enforcement agencies may use monitoring systems other than AIS, such as radar.

Figure B.4 and Table B.4 information

In Figure B.4a-e, I test whether my total deterrence effect estimate in Figure 2.2c is sensitive to excluding the unauthorized foreign fishing effort observations that are closest to an EEZ-high seas boundary. This test is motivated in part by the concern that my deterrence effect estimates would be too large if enforcement inside EEZs increases unauthorized foreign fishing effort just outside EEZs (Ferraro et al., 2018). This scenario would lead us to overestimate the total deterrence effect of EEZs because my measure of unauthorized foreign fishing effort for the control group (unauthorized foreign fishing effort outside EEZs on the high seas) would be higher than the true counterfactual unauthorized foreign fishing effort if EEZs did not exist. On the other hand, my deterrence effect estimates would be too small if unauthorized foreign vessels reduce high seas fishing effort in advance of EEZ boundaries in order to ensure that they do not accidentally fish inside EEZs (e.g., as drifting longline and purse seine vessels seem to do in Figure B.7b,d).

In both of these cases, bias in the total deterrence effect estimate is most likely to occur from unauthorized foreign fishing effort observations that are closest to an EEZ-high seas boundary. By excluding these observations and re-estimating the total deterrence effect, I can get a sense for whether the total deterrence effect estimated reported in Figure 2.2c is too large, too small, or robust to these concerns. This type of robustness check is referred to as a "donut regression discontinuity" (donut RD) (Barreca et al., 2011). I also test in Figure B.4 whether my total deterrence effect estimate in Figure 2.2c is sensitive to my choice of only analyzing fishing effort that occurs within 50 km of an EEZ-high seas boundary.

Figure B.4b-e include unauthorized foreign fishing effort that occurs within 50 km or 100 km of an EEZ-high seas boundary, and exclude observations within 10 km or 25 km of an EEZ-high seas boundary. The range of observations that are included is referred to as the "bandwidth" and the range of observations that are excluded is referred to as the "donut hole". For example, Figure B.4c uses unauthorized foreign fishing effort within 100 km of an EEZ-high seas boundary (bandwidth is 100 km), but drops observations within 10 km of an EEZ-high seas boundary (donut hole is 10 km). I control for a linear trend in distance to an EEZ-high seas boundary instead of a third-order polynomial because donut RDs require extrapolating through the donut hole to the discontinuity cutoff value (see Figure B.4b-e). Figure B.4a replicates Figure 2.2c with a linear trend. When assessing how my various donut RD specifications change the total deterrence effect estimate, I always compare my donut RD estimates to the estimate in Figure B.4a.

Every combination of different bandwidths and donut holes yields deterrence effect estimates that are .3 to 2 percentage points larger than my baseline estimate in Figure B.4a (see Table B.4 for numeric estimates corresponding to Figure B.4a-e). This exercise suggests that the total deterrence effect estimate displayed in Figure 2.2c is not biased by the potential spillover concerns described above.

Figure B.4f displays an additional test for whether enforcement inside EEZs causes spillovers of unauthorized foreign fishing into control regions (high seas regions within 50 km of an EEZ). As discussed above, this type of spillover would make my deterrence effect estimates upward biased. The intuition for the test in Figure B.4f is that EEZs whose control regions have a greater degree of overlap with the control regions of other EEZs should have larger deterrence effects, all else equal, if this type of spillover is causing upward bias in my deterrence effect estimates. The reason that EEZs with more control region overlap would have greater deterrence effect estimates is that their control regions would be receiving enforcement-induced spillovers from other EEZs in addition to own-EEZ spillovers. For example, the control region corresponding to Iceland's EEZ in the Norwegian Sea would be receiving spillovers from other EEZs that surround the high seas of the Norwegian Sea (Norway, Denmark, Greenland, and the Faroe Islands) in addition to receiving own-spillovers (from enforcement of Iceland's EEZ).

For each EEZ-sea region, I calculate the fraction of its control region that is overlapping with the control regions of other EEZ-sea regions (minimum value = 0, 25th percentile = .07, median = .16, 75th percentile = .40, maximum = 2.17). An EEZ-sea region's overlap fraction exceeds 1 when the area of overlap with every other control region is larger than the area of the EEZ-sea region's control region. Following the same procedure used to create Figure 2.4a, I first grouped the 178 EEZ-sea regions with more than zero AIS fishing hours into 20 quantiles according to their control region's overlap fraction. Then I estimated Equation 2.2 (in Section 2.4) via ordinary least squares regression, obtaining a separate deterrence effect for each quantile group. Recall that the dependent variable in this regression is hours of unauthorized foreign fishing per thousand km^2 for a given EEZ-sea region and integer bin.

In Figure B.4f, overlap fraction groups farther to the right on the x-axis contain EEZ-sea regions with larger overlap fractions. If spillovers cause upward bias in my estimates,

deterrence effects should be increasing to the right along the x-axis. In fact, deterrence effects are slightly decreasing in overlap fraction, though the trend is not statistically significant (p-value from regressing overlap fraction group deterrence effect on a constant and a linear trend in overlap fraction group number is .34; N=20). Figure B.4f therefore provides further evidence that my deterrence effect estimates are not biased by potential spillovers.

Figure B.5 information

Some countries, such as China and Taiwan, do not make their EEZ access agreements publicly available. Vessels from these countries are therefore always classified as unauthorized foreign when they are fishing closest to any EEZ other than their home country. As a consequence, I may be underestimating deterrence effects by misclassifying vessels that are actually authorized foreign. This misclassification would lead to underestimated deterrence effects because unlike unauthorized foreign vessels, authorized foreign vessels are more likely to fish just inside EEZs (Figure 2.2d). Figure B.5a plots unauthorized foreign fishing by vessels from (flagged to) countries with at least one public access agreement. Figure B.5b plots unauthorized foreign fishing by vessels from countries with no public access agreements (e.g. Chinese vessels). The deterrence effect in both figures is about 80%, suggesting that incomplete access agreements data is not significantly affecting my results.

Figure B.6 and Table B.3 information

GFW provides two global, daily fishing hours datasets: .01 degree resolution data at the flag state-gear type level (the primary dataset used in this paper) and .1 degree resolution data at the individual vessel level. The latter data contains vessels' MMSI, a unique identifier, which I joined to a third GFW dataset containing estimated vessel gear type, gross tonnage, length, and engine power (Kroodsma et al., 2018). I matched .01 degree resolution fishing observations to .1 degree resolution observations in order to add vessel characteristics to the .01 degree resolution dataset. I uniquely matched 79.4% of .01 degree resolution fishing hours observations to .1 degree resolution fishing hours observations. I used the variables these two datasets have in common to match observations across them: the location, date, gear type, flag state, and quantity of fishing hours. I calculated fishing hours-weighted average vessel characteristics for the .01 degree resolution observations that matched to multiple .1 degree resolution observations. I use the dataset created at this stage to create Table B.3.

For Figure B.6, I then calculated fishing hours-weighted median gross tonnage, length, and engine power for each vessel type and for each gear type. I used these median values to classify fishing hours observations as belonging to above or below median vessels. I then summed fishing hours observations over all EEZ-sea regions and over all days, and divided by the surface area in each integer bin in millions of km^2.

Figure B.6 shows that larger vessels (in terms of gross tonnage) have larger discontinuities at the boundary, suggesting they are more able to choose their fishing locations strategically (e.g. because of superior technology). Larger unauthorized foreign vessels are more able to

"fish the line" just outside EEZs on the high seas, and larger authorized foreign and domestic vessels are more able to avoid competing with unauthorized foreign vessels on the high seas by fishing just inside EEZs. Larger unauthorized foreign vessels also account for a larger proportion of unauthorized fishing inside EEZs. These results are unchanged when vessel length or engine power are used to divide vessels into above and below median size (available upon request).

Figure B.10 information

EEZ-sea regions with fish stocks that move more frequently across their high seas boundaries could have larger deterrence effects if unauthorized foreign vessels are more likely to fish just outside these EEZs (e.g., in order to catch fish as they swim from the EEZ into the high seas). I use two measures of fish mobility to test this hypothesis. First, I compute the fraction of an EEZ-sea region's catch that is from oceanodromous species. Oceanodromous fish are migratory fish that spend their entire life in the ocean. Second, I compute the average ocean surface current direction at the EEZ-high seas boundary for each EEZ-sea region. EEZ-sea regions in which the current typically flows out of the EEZ toward the high seas might have more unauthorized foreign vessels fishing just outside the EEZ on the high seas (and thus have larger deterrence effects). After computing these two values for each EEZ-sea region, I follow the same procedure used to generate Figure 2.4a in order to non-parametrically estimate a relationship between deterrence effects and these two measures of fish mobility.

I computed the fraction of an EEZ-sea region's catch that is from oceanodromous species as follows. First, I downloaded annual, taxon-level catch data for each EEZ-sea region in my analysis from 2012 to 2014 (the most recent year available) from the Sea Around Us using the seaaroundus R package (Chamberlain & Reis, 2017; Pauly & Zeller, 2015). I dropped observations that contained "Miscellaneous" or "fishes not identified" in the "taxon_scientific_name" column (e.g., "Miscellaneous marine crustaceans" and "Marine fishes not identified"). For each EEZ-sea region-taxon pair, I queried FishBase and SeaLifeBase for the taxon's migration patterns using the rfishbase package (Boettiger et al., 2012). Species migration patterns are recorded in the "AnaCat" variable in the Species Table in FishBase and SeaLifeBase and can take the following values: anadromous, catadromous, amphidromous, potamodromous, limnodromous, oceanodromous, non-migratory, and missing. In cases without an initial match between a Sea Around Us taxon name and scientific name(s) in FishBase or SeaLifeBase, I iteratively queried FishBase and SeaLifeBase at higher taxonomic classifications until I found a match. For example, if the Sea Around Us taxon name was "Gadiformes" (an order), I obtained the AnaCat variable of all species in the Gadiformes order. In all cases, I filtered FishBase/SeaLifeBase observations to those in the same FAO region as the EEZ-sea region and dropped FishBase/SeaLifeBase observations that were missing an AnaCat value. If I obtained migration patterns for the same species from both FishBase and SeaLifeBase, I used the migration pattern value from FishBase. I computed the fraction of species that are oceanodromous for EEZ-sea region-taxon pairs that had multiple FishBase/SeaLifeBase matches. For example, I calculated that 71% of

Gadiformes species that are likely present in the Irish part of the North Atlantic Ocean are oceanodromous.

After determining whether each EEZ-sea region-taxon pair is oceanodromous (or the fraction that is oceanodromous), I computed the weighted fraction of an EEZ-sea region's catch that is oceanodromous, using the tons caught of each taxon in the EEZ-sea region between 2012 and 2014 as weights. I thus obtained a value between 0 and 1 for each EEZ-sea region (minimum value = 0, 25th percentile = .70, median = .92, 75th percentile = .99, maximum = 1). I was unable to compute this value for the South Georgian part of the Southern Ocean because all of its Sea Around Us taxa were "Miscellaneous", "fishes not identified", or had missing AnaCat values in FishBase and SeaLifeBase. However, I was able to compute this value for all other EEZ-sea regions in my analysis. I also computed the fraction of an EEZ-sea region's catch that are not non-migratory, but found that this variable had less variation across EEZ-sea regions (minimum value = .29, 25th percentile = .72, median = .99, 75th percentile = .998, maximum = 1).

I computed average ocean surface current direction at each EEZ-sea region's high seas boundary as follows. I downloaded surface current velocity data from 2012 to 2016 from NASA's Earth Space Research group (ESR, 2009). The data contain surface current velocity at the 5-day, .33 degree resolution. For each observation intersecting a given EEZ-sea region's high seas boundary, I calculated whether the current was moving away from the centroid of the EEZ-sea region. I recorded a value of 1 if it was, and recorded a value of 0 otherwise. I then calculated the average current direction over all grid cells and all 5-day periods for each EEZ-sea region. I thus obtained a value between 0 and 1 for each EEZ-sea region (minimum value = .11, 25th percentile = .45, median = .52, 75th percentile = .57, maximum = .85). A value of 0 would indicate that the current is always flowing into the EEZ-sea region at the EEZ-sea region's high seas boundary, and a value of 1 would indicate that the current is always flowing out of the EEZ-sea region at the EEZ-sea region's high seas boundary.

I created Figure B.10a,b using the same procedure I implemented to create Figure 2.4a (see Section 2.4). I first grouped the EEZ-sea regions with more than zero AIS fishing hours into 20 quantiles according to their fraction of catch from oceanodromous species (Figure B.10a) and average surface current direction (Figure B.10b). There are 8 or 9 EEZ-sea regions in each quantile group. Then I estimated Equation 2.2 (in Section 2.4) via ordinary least squares regression, obtaining a separate deterrence effect for each quantile group.

In both parts of Figure B.10, quantile groups farther to the right on the x-axis are expected to contain EEZ-sea regions with fish stocks that move more frequently from EEZs into the high seas. If unauthorized foreign vessels are more likely to locate themselves just outside these EEZs in order to catch fish as they swim from these EEZs into the high seas, then deterrence effects should be increasing to the right along the x-axis. However, neither Figure B.10a nor Figure B.10b exhibit a trend in deterrence effects. p-values from regressing quantile group-specific deterrence effects on a constant and a linear trend in quantile group number are .21 and .89, respectively (N=20). By contrast, deterrence effects clearly increase in average NPP. The p-value from regressing the NPP quantile group-specific deterrence effect estimates in Figure 2.4a on a constant and a linear trend in quantile group number

is .01 (N = 20). The two proxies for fish mobility I have examined in this section seem to be less important for understanding deterrence effect heterogeneity than NPP, a proxy for fishery value (see Sections 2.2 and 2.4).

B.4 The historical origins of 200 nautical mile-wide EEZs

In 1947, Chile became the first nation to declare a 200 nm exclusive zone. The lawyer in charge of finding a legal precedent for this unilateral declaration chose 200 nm to match his imprecise map of a neutrality zone around Chile that was declared by the United States in 1939. The width of the neutrality zone was actually 300 nm (Hollick, 1977). In the ensuing decades, other countries followed Chile's precedent, and the right of coastal nations to a 200 nm EEZ was finally codified at the third UN Conference on the Law of the Sea between 1973 and 1982 (Hannesson, 2013). Nations with fewer than 400 nm of ocean separating them typically divide the available ocean area equally. I only use EEZ boundaries that are 200 nm from shore and border the high seas in my analysis.

This history supports the assumption that is necessary for my regression discontinuity design to be valid (Section B.2), because it suggests that it is very unlikely that unobservable variables that affect fishing change discontinuously at EEZ-high seas boundaries. The 200 nm maximum width for EEZs was not chosen because fishing opportunities change discontinuously at this distance from shore, so it is very likely that discontinuous changes in fishing at EEZ-high seas boundaries are due to the discontinuous change in institutions at these boundaries (EEZs on one side and not the other).

B.5 Theoretical models predicting that more valuable EEZs have larger deterrence effects and more enforcement effort

I develop two theoretical models in this section to show that (Claim 1) EEZs that are more valuable near their high seas boundaries have larger deterrence effects and (Claim 2) countries with EEZs that are more valuable near their high seas boundaries find it in their interest to exert more enforcement effort. First, I demonstrate that my empirical result in Figure 2.4 can be supported by economic theory. Then, I show that my explanation for the empirical result in Figure 2.4, that countries are incentivized to exert more enforcement effort if their EEZs are more valuable, can also be supported by economic theory.

Claim 1: Deterrence effects are increasing in EEZ value

Suppose a representative unauthorized foreign fishing vessel maximizes profit (π) by choosing fishing effort just inside a given EEZ (i), fishing effort just outside the EEZ (o), and fishing effort everywhere else (e). I develop a static model for simplicity and because my empirical analysis is a spatial cross-section. Revenue from fishing just inside or just outside the EEZ is $R(i, o; v)$, where v is a fixed (exogenous) parameter representing the "value" or quality of the fishery near the EEZ boundary. Revenue from fishing effort everywhere else is $M(e)$. Suppose the cost of a unit of fishing effort is c. Then fishing effort costs are linear in total fishing effort and equal $(i + o + e)c$. Finally, fishing opportunities are identical just inside and just outside the EEZ except that the vessel incurs an additional cost $\sigma(i)$ from fishing just inside the EEZ that reflects the probability of being punished for illegal fishing and the magnitude of punishment (e.g. fine level) if punishment occurs. I refer to $\sigma(i)$ as the vessel's expected punishment cost.

Let subscripts denote partial derivatives with respect to a function's argument and let $(\cdot)$ indicate that a function's arguments have been suppressed. I make the following assumptions. First, the vessel's expected punishment cost from illegally fishing just inside the EEZ is increasing and convex ($\sigma_i(i) > 0$ and $\sigma_{ii}(i) > 0$). Second, both revenue functions are increasing and concave in fishing effort ($R_i(\cdot)$, $R_o(\cdot)$, $M_e(e) > 0$, and $R_{ii}(\cdot)$, $R_{oo}(\cdot)$, $M_{ee}(e) < 0$). Third, the marginal increase in revenue from increasing fishing effort just inside or just outside the EEZ is increasing in the value of the fishery near the EEZ boundary ($R_{iv}(\cdot)$, $R_{ov}(\cdot) > 0$). Because fishing revenue opportunities are identical just inside and just outside the EEZ, I assume that these terms are equal ($R_{iv}(\cdot) = R_{ov}(\cdot)$), and also assume that $R_{ii}(\cdot) = R_{oo}(\cdot)$.

The vessel's decision problem is:

$$\max_{i,\, o,\, e} \pi = R(i, o; v) + M(e) - (i + o + e)c - \sigma(i)$$

The vessel's first-order conditions (FOCs) with respect to i, o, and e are:

FOC i: $R_i(\cdot) - c - \sigma_i(i) = 0$

FOC o: $R_o(\cdot) - c = 0$

FOC e: $M_e(e) - c = 0$

The deterrence effect, τ, for a given EEZ is total unauthorized foreign fishing effort just inside the EEZ minus total unauthorized foreign fishing effort just outside the EEZ. Let * indicate the optimized value of a choice parameter (e.g., i^*). The difference in the representative foreign vessel's fishing effort just inside the EEZ and just outside the EEZ is $i^* - o^*$ and is given by the above three first-order conditions. In the context of this model, since unauthorized foreign vessels are identical, $\tau = (i^* - o^*)N$, where N is the number of unauthorized foreign fishing vessels. EEZs that deter unauthorized foreign fishing have $\tau < 0$. Claim 1 is that deterrence effects are increasing (becoming larger negative numbers) as the value of the fishery near the EEZ boundary increases. Mathematically, this claim is $\frac{d\tau}{dv} = (\frac{di^*}{dv} - \frac{do^*}{dv})N < 0$. We show this claim by totally differentiating the three FOCs with

respect to i, o, e, and v, and applying Cramer's Rule to derive $\frac{di^*}{dv}$ and $\frac{do^*}{dv}$.

$$\begin{bmatrix} R_{ii}(\cdot) - \sigma_{ii}(\cdot) & R_{io}(\cdot) & 0 \\ R_{oi}(\cdot) & R_{oo}(\cdot) & 0 \\ 0 & 0 & M_{ee}(\cdot) \end{bmatrix} \begin{bmatrix} di \\ do \\ de \end{bmatrix} = \begin{bmatrix} -R_{iv}(\cdot) \\ -R_{ov}(\cdot) \\ 0 \end{bmatrix} dv$$

Applying Cramer's rule to the above system of equations gives $\frac{di^*}{dv} > 0$ and $\frac{do^*}{dv} > 0$ as long as $R_{oo}(\cdot) < R_{io}(\cdot)$ (equivalently, $R_{ii}(\cdot) < R_{oi}(\cdot)$). This conditions means that increasing fishing effort in the same location causes a larger decrease in marginal revenue than increasing fishing effort in the adjacent location.

Though fishing effort just inside and just outside the EEZ both increase in the value of this fishery v, fishing effort just inside the EEZ increases by a relatively smaller amount. Intuitively, the potential revenue from fishing just inside and just outside the EEZ increases by the same amount, but less fishing effort is allocated to just inside the EEZ because of the risk of being punished for illegally fishing inside the EEZ. To see this mathematically, let A denote the above 3x3 matrix (the left-hand side matrix) and let $det(A)$ denote the determinant of A. Then $\frac{d\tau}{dv} = (\frac{di^*}{dv} - \frac{do^*}{dv})N = \frac{-R_{iv}(\cdot)M_{ee}(\cdot)\sigma_{ii}(\cdot)}{det(A)}N$. Since $R_{iv} > 0$, $M_{ee} < 0$, and $\sigma_{ii}(\cdot) > 0$, the numerator of $\frac{d\tau}{dv}$ is positive. Since $det(A)$ is negative by the second-order condition for a maximum, $\frac{d\tau}{dv} < 0$. Deterrence effects are increasingly large (more negative) as the value of the fishery near the EEZ boundary increases.

Claim 2: Enforcement effort is increasing in fishery value

Now consider a country choosing enforcement effort z to minimize the quantity of unauthorized foreign fishing effort inside its EEZ and the cost of enforcement effort, $c(z)$. Let $I(z; v)$ denote total unauthorized foreign fishing effort inside the country's EEZ, where v represents the exogenous component of the fishery's value. Other variables may affect unauthorized foreign fishing effort inside the EEZ, such as fishing opportunities in other locations, but it is not necessary to model them explicitly in order to support Claim 2. As before, I have developed a static model for simplicity and because my empirical analysis is a spatial cross-section.

I assume that unauthorized foreign fishing effort inside the EEZ is decreasing in enforcement effort ($I_z(z; v) < 0$). I also assume that the marginal decrease in unauthorized foreign fishing effort from increased enforcement effort is increasing (becoming less negative) as fishery value increases ($I_{zv}(z; v) > 0$). Intuitively, this assumption means that additional enforcement effort "buys" less deterrence when the fishery is more valuable because unauthorized foreign vessels are more willing to risk punishment in order to access a more valuable fishery.

The country solves:
$\max_z -I(z; v) - c(z)$
The first-order condition with respect to z is:
$-I_z(z; v) - c_z(z) = 0$

Totally differentiating the first-order condition with respect to z and v and then rearranging terms gives $\frac{dz}{dv} = \frac{-I_{zv}(z;v)}{I_{zz}(z;v)+c_{zz}(z)}$. Since $I_{zv} > 0$, the numerator is negative. The denominator is also negative by the second-order condition for a maximum. Therefore, enforcement effort is increasing in fishery value ($\frac{dz}{dv} > 0$). Intuitively, if fishery value increases, $I(z; v)$ increases, all else equal. But the cost of enforcement effort for the country $c(z)$ has not changed. Enforcement effort increases with fishery value because the marginal benefit of an additional unit of enforcement effort (in terms of a reduction of unauthorized foreign fishing inside the EEZ) increases more than the marginal cost of an additional unit of enforcement effort.

B.6 Supplementary Figures

Figure B.1: No other discontinuities at EEZ-high seas boundaries

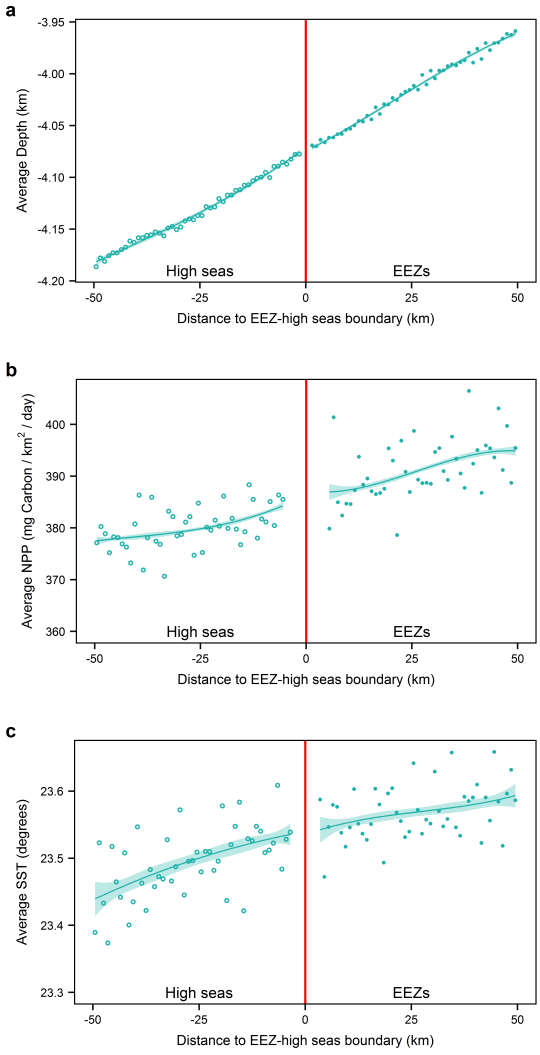

Notes: Average (a) ocean depth, (b) net primary productivity (NPP), and (c) sea surface temperature (SST) with respect to an EEZ-high seas boundary. Grid cells are assigned to the minimum integer bin (over all EEZ-sea regions) that their cell center intersects (see Section 2.4). Weighted average values over all EEZ-sea regions are calculated using grid cell areas (all variables) and the number of days each composite comprises (NPP and SST only) as weights. NPP and SST averages are calculated using data between 2012 and 2016. Points are data. Lines are ordinary least squares third-order polynomial fits in distance to the boundary. 95% confidence intervals (shaded) are estimated using standard errors that account for heteroscedasticity and serial correlation (Newey & West, 1987).

Figure B.2: EEZ-sea regions in analysis

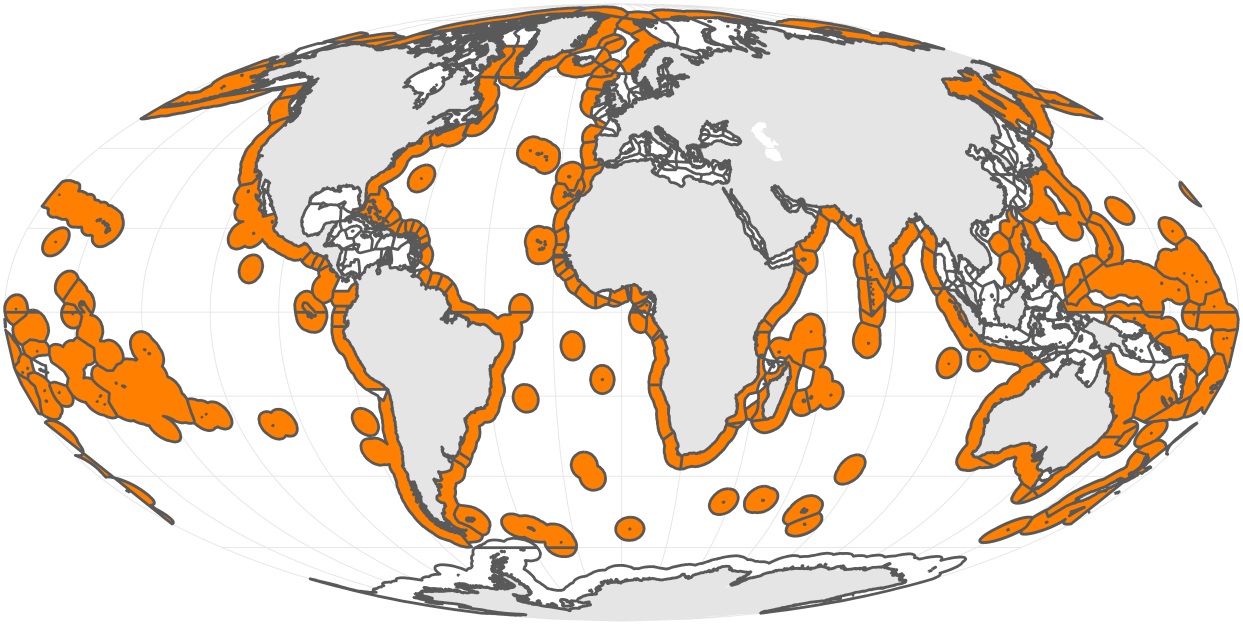

Notes: EEZ-sea regions that are 200 nm wide and border the high seas are filled orange. Note that I have filled the entire area of these EEZ-sea regions for visibility, but only analyze fishing effort that occurs within 50 km of an EEZ-high seas boundary. All other EEZ-sea regions are unfilled. Antarctica is excluded from the analysis because its resources do not belong to a single nation.

Figure B.3: AIS transponder off events by distance to an EEZ-high seas boundary

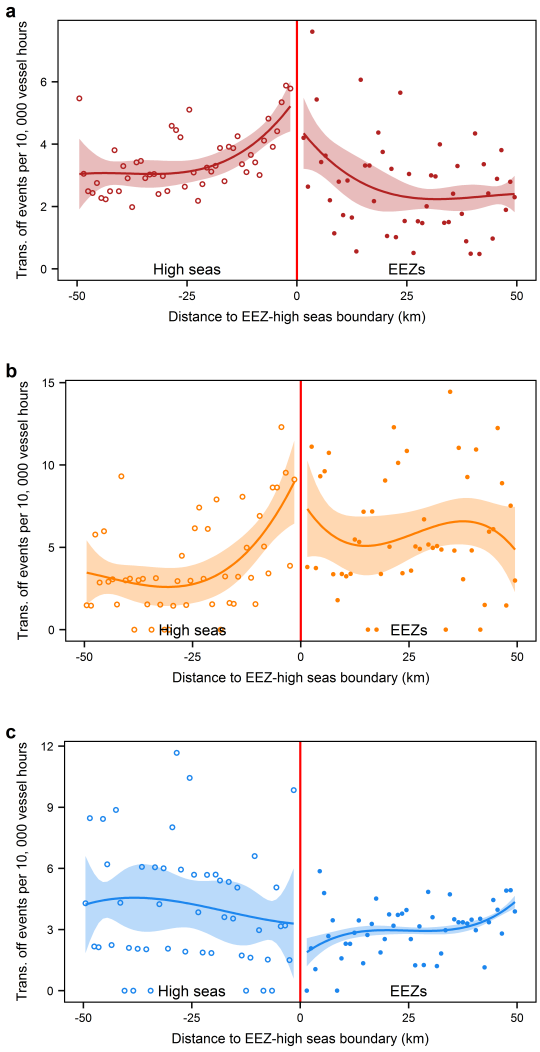

Notes: Off events per 10,000 hours of AIS vessel presence between 2012 and 2016 for (a) unauthorized foreign fishing vessels, (b) authorized foreign fishing vessels, and (c) domestic fishing vessels. See Section B.3 for a discussion of this figure. Points are data. Lines are ordinary least squares third-order polynomial fits in distance to the boundary. 95% confidence intervals (shaded) are estimated using standard errors that account for heteroscedasticity and serial correlation (Newey & West, 1987).

Figure B.4: Robustness of deterrence effect estimates to potential spillovers

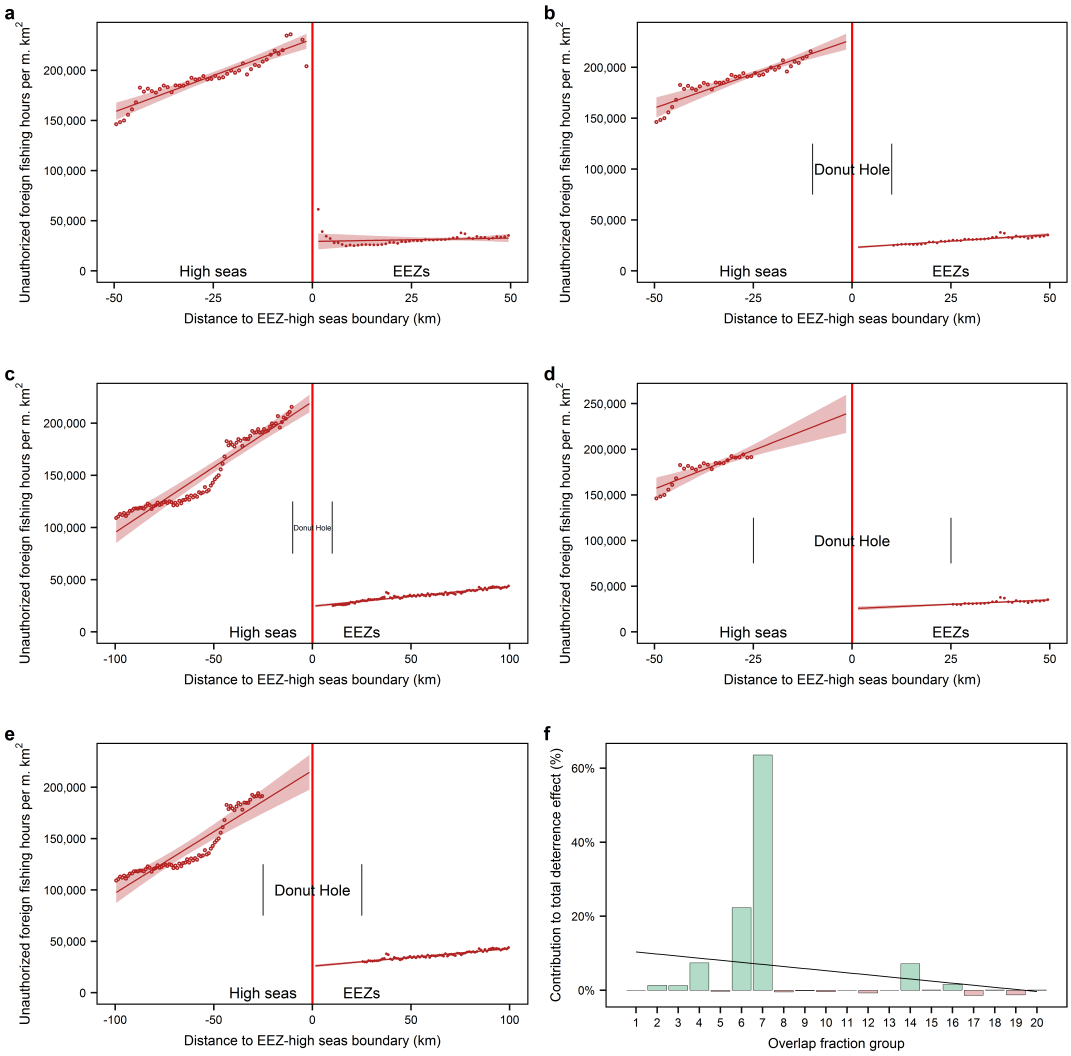

Notes: Deterrence effect estimate using (a) all observations within 50 km of an EEZ-high seas boundary, (b) observations between 10 and 50 km from a boundary, (c) between 10 and 100 km, (d) between 25 and 50 km, and (e) observations between 25 and 100 km from a boundary. See Table B.4 for numerical point estimates corresponding to these figures. Points are data. I control for a linear trend in distance to the boundary instead of a third-order polynomial because higher-order polynomials are unsuitable for extrapolating to the boundary, as is required in a donut RD. 95% confidence intervals (shaded) are estimated using standard errors that account for heteroscedasticity and serial correlation (Newey & West, 1987). (f) Contribution of each overlap fraction group to the total deterrence effect. I estimate a deterrence effect for each overlap fraction group, and divide each group's effect by the sum of all groups' deterrence effects. Overlap fraction groups that contribute a positive percentage (green) deter unauthorized foreign fishing. The black line is a linear trend. See Section B.3 for a discussion of this figure.

Figure B.5: Unauthorized foreign fishing by availability of EEZ access agreements

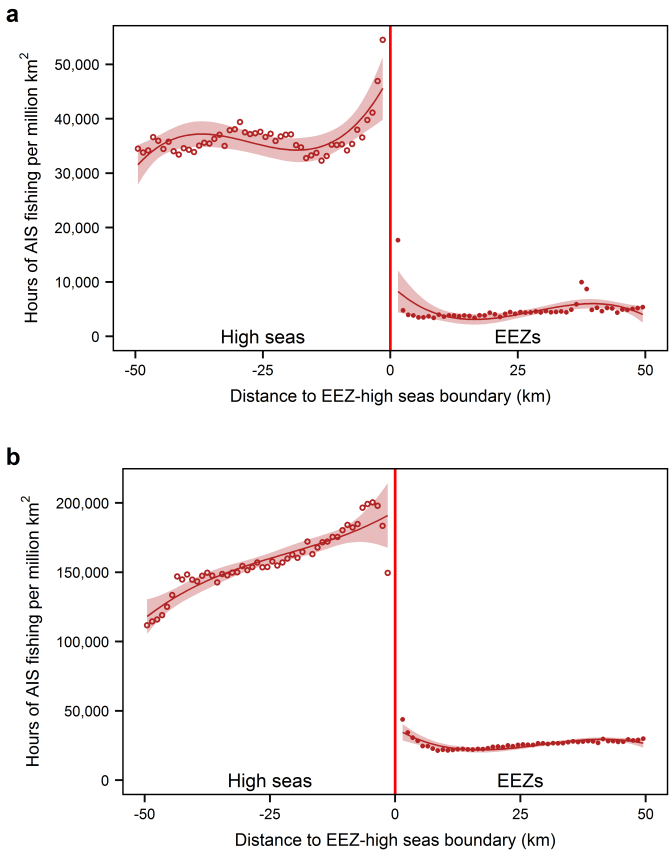

Notes: Unauthorized foreign fishing by vessels from countries that (a) make their access agreements publicly available and (b) do not publish their access agreements. See Section B.3 for a discussion of this figure. Points are data. Lines are ordinary least squares third-order polynomial fits in distance to the boundary. 95% confidence intervals (shaded) are estimated using standard errors that account for heteroscedasticity and serial correlation (Newey & West, 1987).

Figure B.6: Larger fishing vessels have larger discontinuities

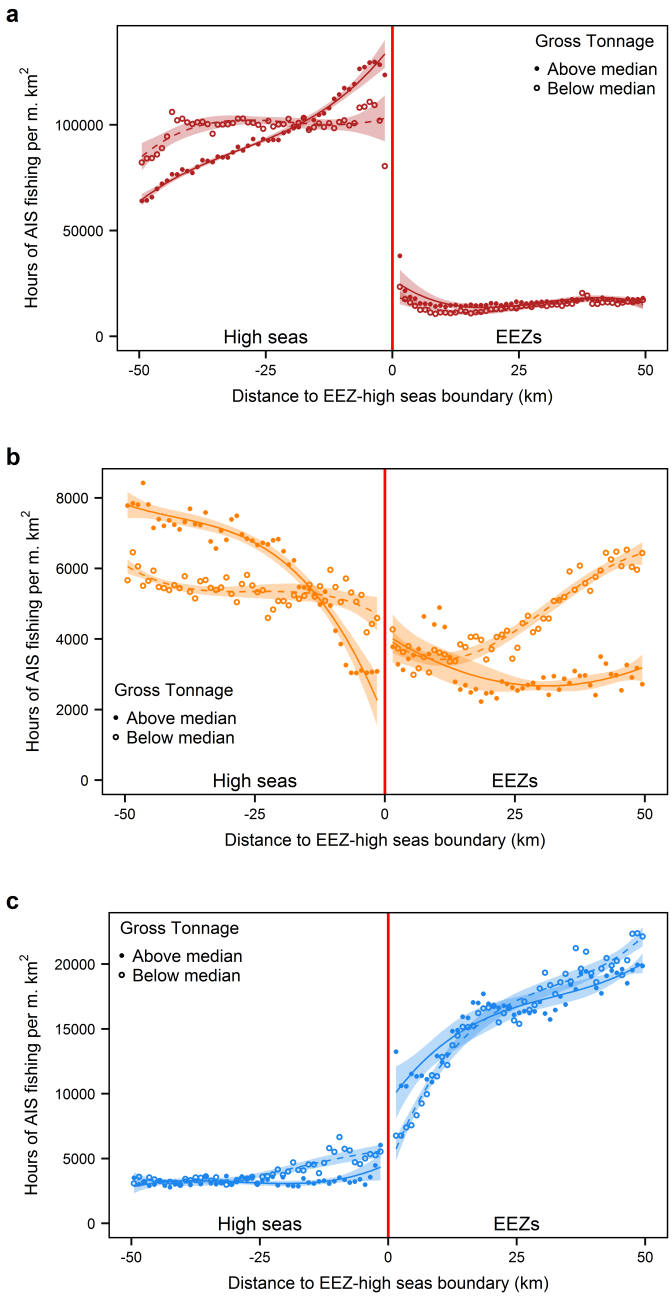

Notes: Fishing by above and below median gross tonnage (a) unauthorized foreign vessels, (b) authorized foreign vessels, and (c) domestic fishing vessels. See Section B.3 for a discussion of this figure. Points are data. Lines are ordinary least squares third-order polynomial fits in distance to the boundary. 95% confidence intervals (shaded) are estimated using standard errors that account for heteroscedasticity and serial correlation (Newey & West, 1987).

Figure B.7: Deterrence effect by gear type

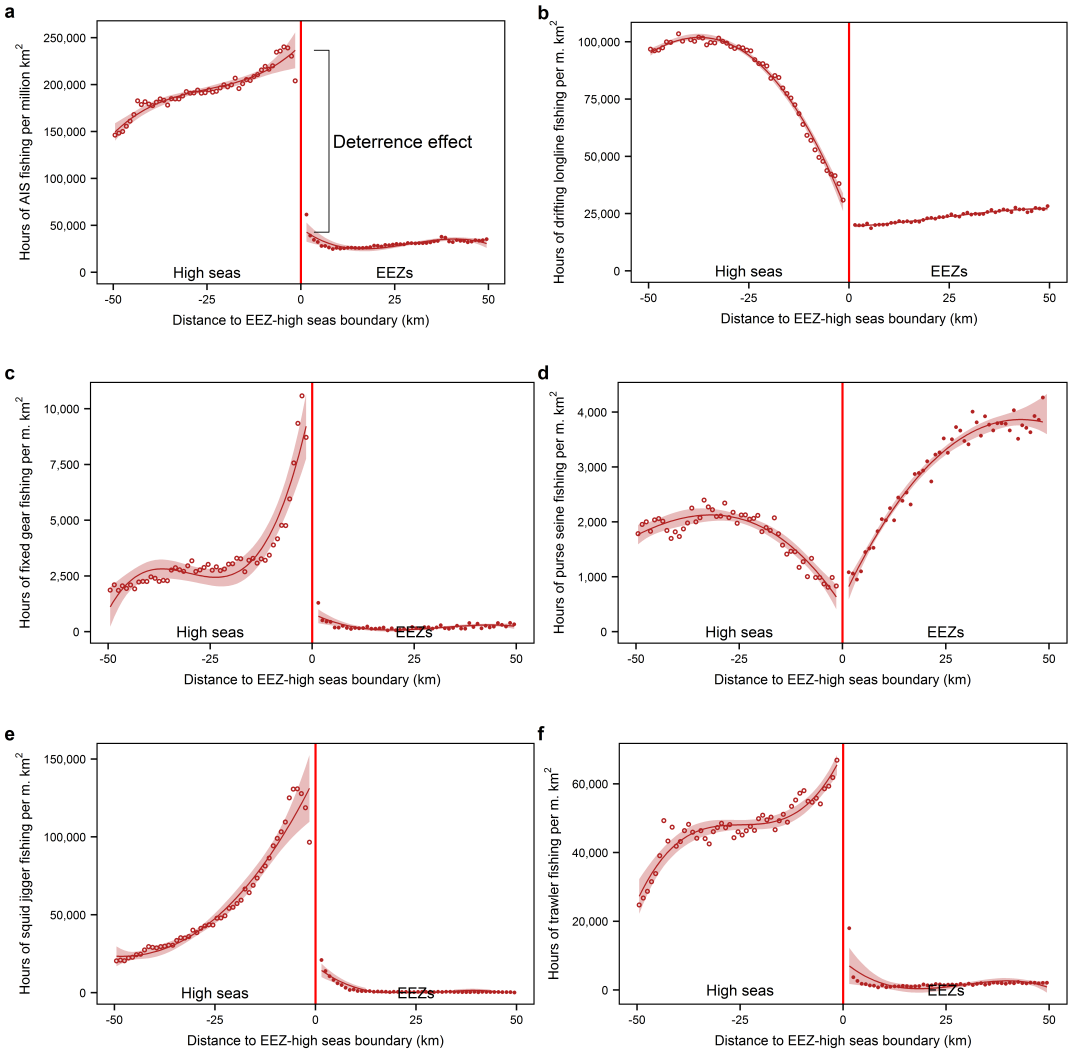

Notes: a, Hours of fishing by unauthorized foreign vessels for all gear types (equivalent to Figure 2.2c; reproduced here for reference). Hours of unauthorized foreign (b) drifting longline fishing, (c) fixed gear fishing, (d) purse seine fishing, (e) squid jigger fishing, and (f) trawler fishing. Points are data. Lines are ordinary least squares third-order polynomial fits in distance to the boundary. 95% confidence intervals (shaded) are estimated using standard errors that account for heteroscedasticity and serial correlation (Newey & West, 1987).

Figure B.8: Unauthorized foreign fishing for the top three flag states (fishing countries) in each gear type

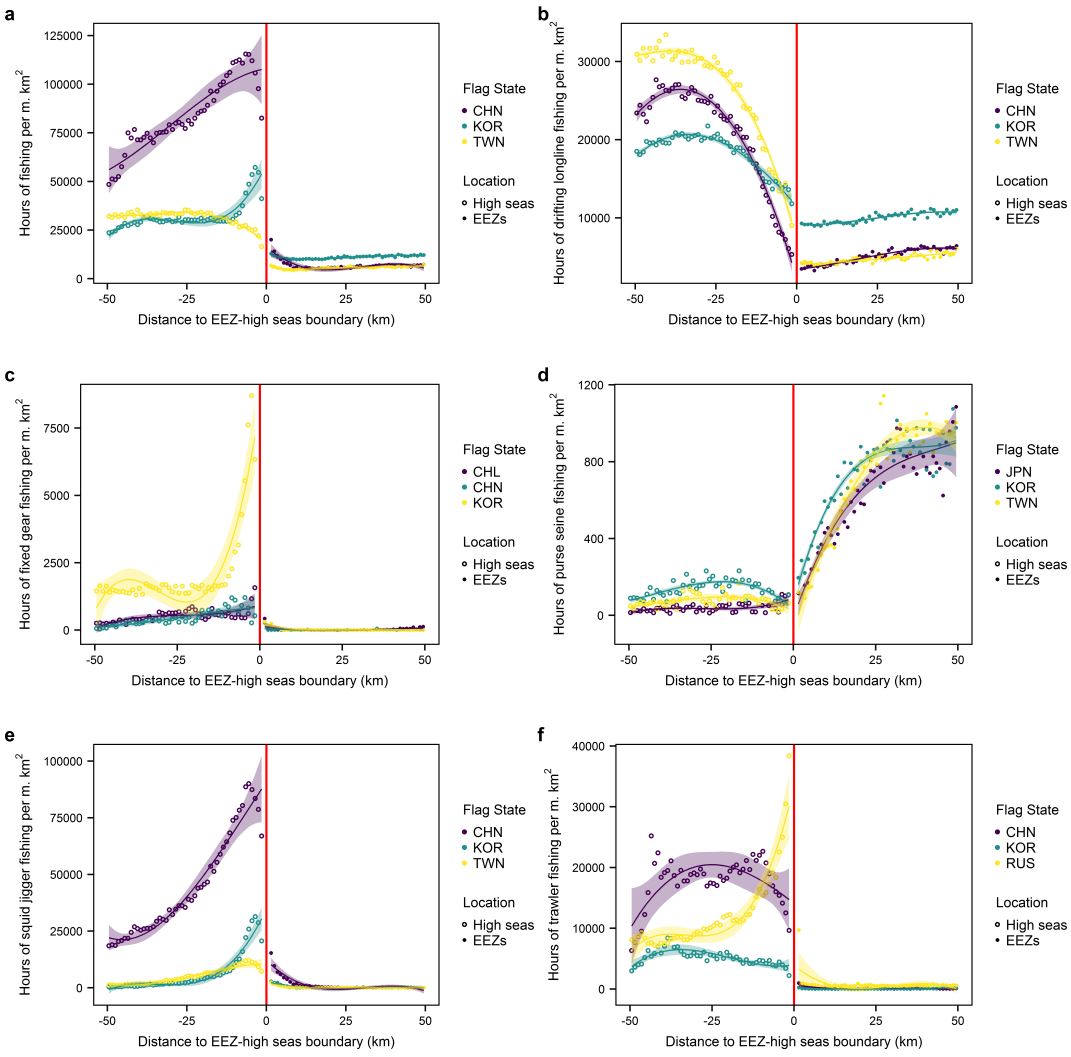

Notes: a, All gear types, (b) drifting longline fishing, (c) fixed gear fishing, (d) purse seine fishing, (e) squid jigger fishing, and (f) trawler fishing. I calculated the top three flag states for each gear type in terms of total hours of unauthorized foreign fishing within 50 km of any EEZ-sea region in my analysis between 2012 and 2016. Points are data. Lines are ordinary least squares third-order polynomial fits in distance to the boundary. 95% confidence intervals (shaded) are estimated using standard errors that account for heteroscedasticity and serial correlation (Newey & West, 1987).

Figure B.9: EEZ-sea regions that do not deter unauthorized foreign fishing

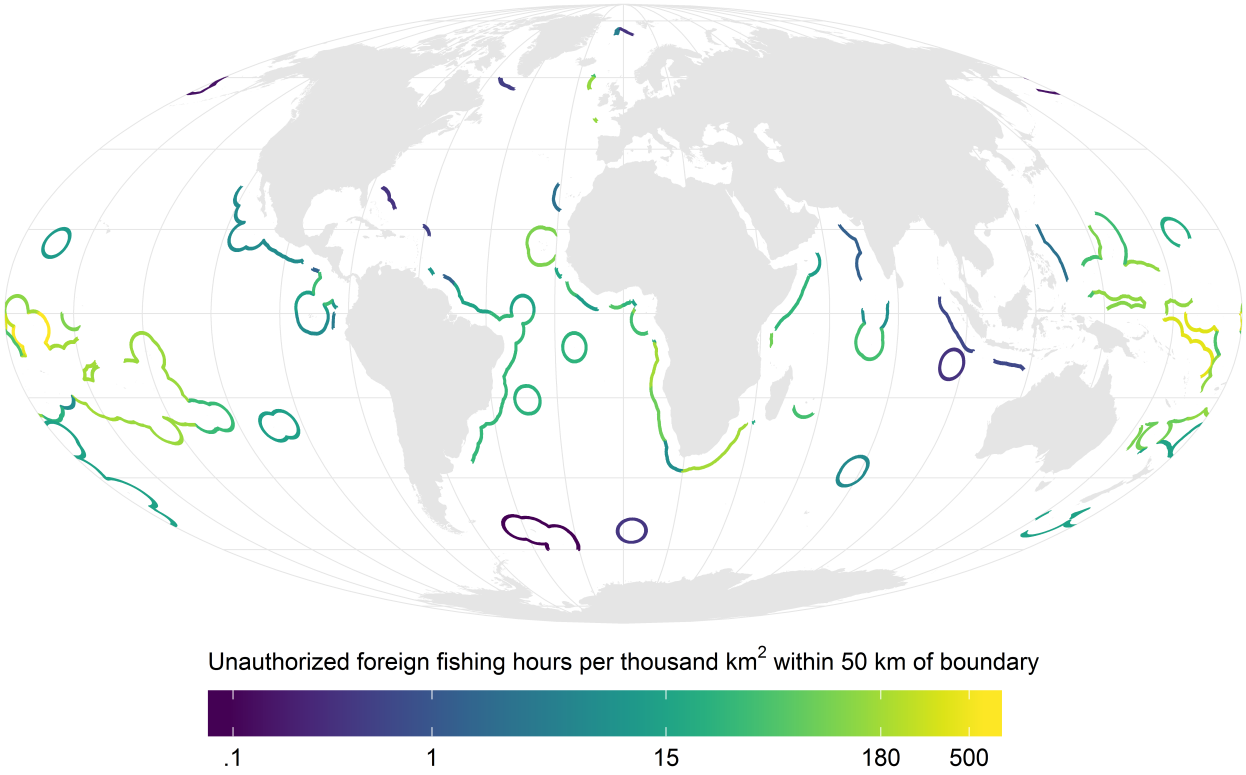

Notes: These 83 EEZ-sea regions have enough unauthorized foreign fishing within 50 km of their high seas boundary to estimate a deterrence effect (more than 10 hours), but they do not deter unauthorized foreign fishing (unauthorized foreign fishing is higher just inside their EEZ than just outside).

Figure B.10: Deterrence effect heterogeneity by fish stock movement patterns

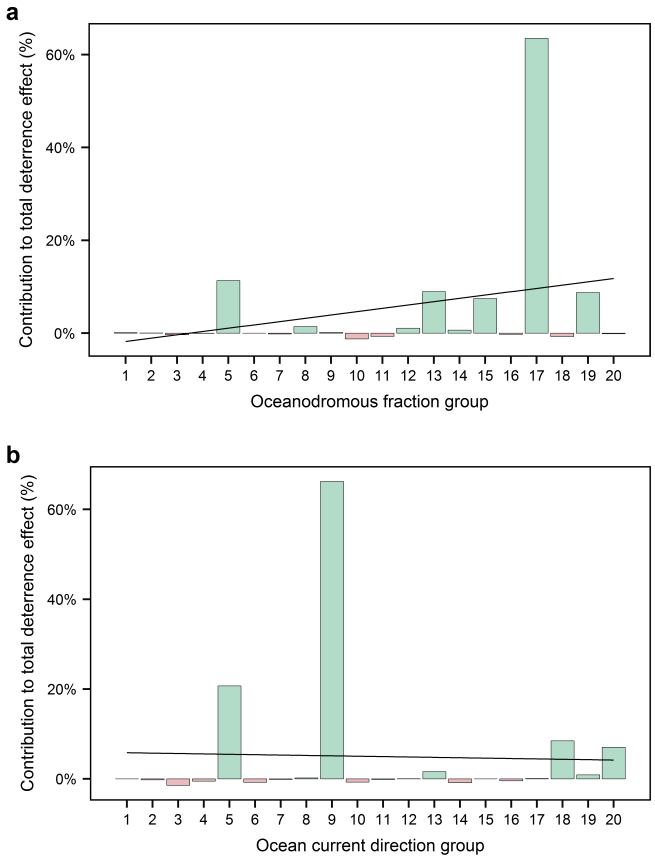

Notes: Contribution of each (a) oceanodromous fraction group and (b) ocean surface current direction group to the total deterrence effect. The creation of these variables is described in Section B.3. I estimate a deterrence effect for each quantile group, and divide each group's effect by the sum of all groups' deterrence effects. Quantile groups that contribute a positive percentage (green) deter unauthorized foreign fishing. The black lines are linear trends.

B.7 Supplementary Tables

Table B.1: Effect of EEZs on fishing effort

	Fig. 2.2a Total AIS (1)	Fig. 2.2b VBD (2)	Fig. 2.2c Unauth. For. (3)	Fig. 2.2d Auth. For. (4)	Fig. 2.2d Domestic (5)
Levels	-190,359	-5,496	-195,197	1,927	2,911
	(23,570)***	(608)***	(20,887)***	(686)***	(2,013)
NW lag	2	6	4	4	7
Logs	-1.37	-1.33	-1.66	0.22	0.36
	(0.21)***	(0.10)***	(0.25)***	(0.09)**	(0.10)***
NW lag	3	8	2	4	4
Percentage	-74.6%	-73.5%	-81.0%	24.8%	43.0%

Notes: This table contains numeric estimates corresponding to Figures 2.2a-d. The "levels" row displays the estimated effect of EEZs on the untransformed dependent variable. The "logs" row displays the estimated effect of EEZs on the natural log of the dependent variable. Newey-West (NW) standard errors are displayed in parentheses (Newey & West, 1987). The optimal NW lag for each regression was chosen using the procedure described in Newey and West (1994). The "percentage" row expresses the effect of EEZs as a percentage difference in fishing just inside EEZs compared to just outside EEZs. This percentage difference uses the estimated effect from the natural log specification and is computed using the formula $100(e^{logeffect} - 1)$. All regressions have 98 observations. ***p < 0.01, **p < 0.05, *p < 0.1.

Table B.2: Gear type composition by vessel type

	Unauthorized Foreign	Authorized Foreign	Domestic
Drifting Longlines	46.9%	58.5%	29.9%
Trawlers	22.8%	16.5%	55.1%
Squid Jiggers	26.2%	0.0%	2.0%
Fixed Gear	1.6%	10.8%	4.9%
Purse Seines	2%	13.9%	3.7%
Other	0.4%	0.2%	4.4%
Total Fishing Hours	3,318,382	276,947	561,728

Notes: Each column lists the percentage of AIS fishing hours between 2012 and 2016 from each gear type for a given vessel type. Only fishing within 50 km of an EEZ-high seas boundary is included in this table.

Table B.3: Mean vessel characteristics by vessel type and gear type

Geartype	Characteristic	Unauthorized Foreign	Authorized Foreign	Domestic
Drifting Longlines				
	Gross Tonnage	379 [251]	264 [133]	311 [339]
	Length (m)	42.8 [12]	33.2 [10.5]	30.9 [11.5]
	Engine Power (kW)	828 [330]	421 [224]	587 [391]
Trawlers				
	Gross Tonnage	2,287 [1,961]	1,926 [2,341]	1,439 [1,318]
	Length (m)	73.2 [17.7]	61.7 [27.6]	57.7 [19.5]
	Engine Power (kW)	2,967 [1,527]	2,194 [1,822]	2,264 [1,465]
Squid Jiggers				
	Gross Tonnage	925 [313]	NA [NA]	596 [220]
	Length (m)	58.7 [6.7]	NA [NA]	53.5 [4.7]
	Engine Power (kW)	1,321 [356]	NA [NA]	1,246 [243]
Fixed Gear				
	Gross Tonnage	697 [255]	297 [221]	456 [310]
	Length (m)	51.2 [6.4]	32.6 [10.6]	38.4 [13.1]
	Engine Power (kW)	1,097 [274]	556 [402]	693 [299]
Purse Seines				
	Gross Tonnage	1,399 [424]	1,355 [566]	1,402 [447]
	Length (m)	69.3 [8.5]	64.6 [15]	64.9 [11.8]
	Engine Power (kW)	2,728 [655]	2,402 [860]	2,757 [815]
Other				
	Gross Tonnage	574 [438]	265 [163]	740 [550]
	Length (m)	51 [15.3]	37.5 [15.1]	45.3 [13.2]
	Engine Power (kW)	1,354 [565]	694 [438]	1,219 [606]
All Geartypes				
	Gross Tonnage	984 [1,226]	694 [1,185]	1,004 [1,137]
	Length (m)	54.6 [17.5]	42.2 [20.6]	48.3 [20.6]
	Engine Power (kW)	1,490 [1,172]	1,005 [1,194]	1,637 [1,386]

Notes: Mean of a characteristic is weighted by AIS fishing hours within 50 km of an EEZ-high seas boundary between 2012 and 2016. Hours-weighted standard deviations displayed in brackets.

Table B.4: Deterrence effects excluding observations closest to an EEZ-high seas boundary and using different bandwidths

	(a)	(b)	(c)	(d)	(e)
Levels	-201,861	-203,693	-195,512	-217,826	-189,830
	(4,223)***	(3,762)***	(3,418)***	(9,819)***	(6,701)***
NW lag	6	6	8	5	7
Logs	-2.11	-2.29	-2.20	-2.29	-2.14
	(0.06)***	(0.02)***	(0.02)***	(0.06)***	(0.04)***
NW lag	6	6	7	5	6
Percentage	-87.9%	-89.9%	-88.9%	-89.9%	-88.2%
Difference		-2.0%	-1.1%	-2.0%	-0.3%
Donut hole	0 km	10 km	10 km	25 km	25 km
Bandwidth	50 km	50 km	100 km	50 km	100 km
Observations	98	80	180	50	150

Notes: This table contains numeric estimates corresponding to Figure B.4a-e. The "levels" row displays the estimated effect of EEZs on hours of unauthorized foreign fishing effort per million km^2. The "logs" row displays the estimated effect of EEZs on the natural log of hours of unauthorized foreign fishing effort per million km^2. Newey-West (NW) standard errors are displayed in parentheses (Newey & West, 1987). The optimal NW lag for each regression was chosen using the procedure described in Newey and West (1994). The "percentage" row expresses the effect of EEZs as a percentage difference in fishing just inside EEZs compared to just outside EEZs. This percentage difference uses the estimated effect from the natural log specification and is computed using the formula $100(e^{logeffect} - 1)$. The "difference" row is the percentage difference minus the percentage difference in Figure B.4a. The "donut hole" row refers to the observations that are excluded from the regression. The "bandwidth" row refers to the data used in the regression. For example, the column (c) regression uses unauthorized foreign fishing effort within 100 km of an EEZ-high seas boundary (bandwidth = 100 km), but excludes observations within 10 km of an EEZ-high seas boundary (donut hole = 10 km). See Section B.3 for additional details and interpretation of these results. ***p < 0.01, **p < 0.05, *p < 0.1.

Appendix C

Armed conflict increases elephant poaching

C.1 Supplementary Figures

Figure C.1: Effect of conflict onset on contemporaneous PIKE, using different battle death thresholds to define conflict onset events

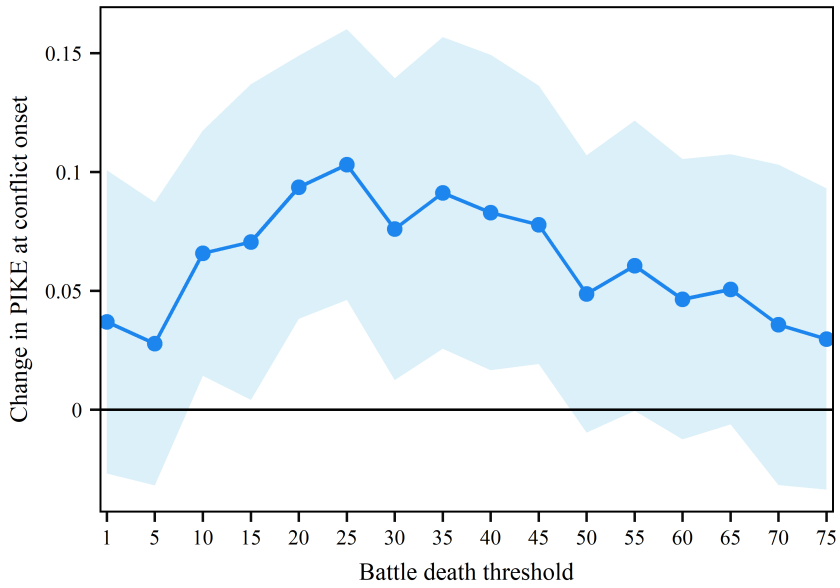

Notes: Each point represents the result of a separate regression. The regressions re-estimate Equation 1, but use the battle death threshold indicated by the x-axis to define onset events. All regressions have 631 observations. Standard errors are estimated by cluster bootstrapping with replacement at the country-level (1,000 replications). 95% confidence intervals are displayed.

Figure C.2: Effect of conflict onset on contemporaneous PIKE, using different buffer distances to connect onset events to MIKE sites.

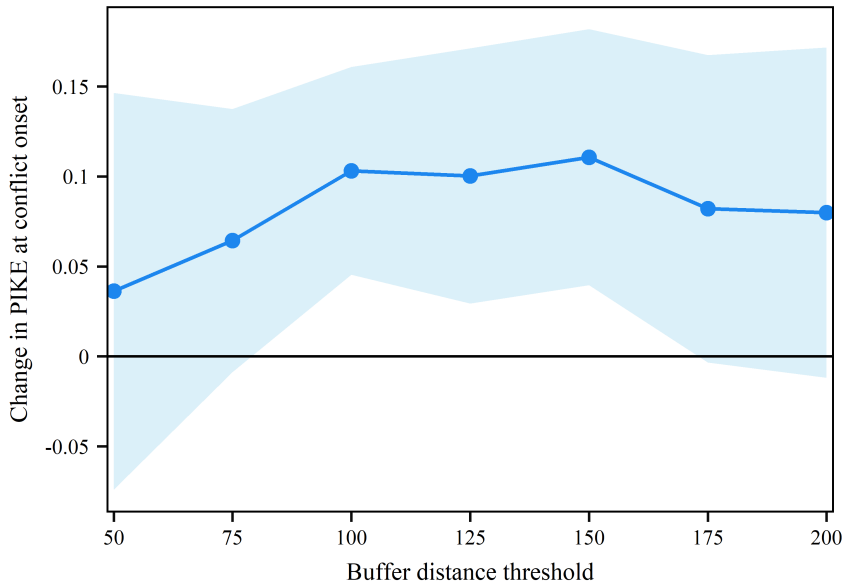

Notes: Each point represents the result of a separate regression. The regressions re-estimate Equation 1, but use the buffer distance indicated by the x-axis to connect onset events to MIKE sites. The third-order polynomials in temperature and precipitation are also recalculated using the new buffer distance. All regressions have 631 observations. Standard errors are estimated by cluster bootstrapping with replacement at the country-level (1,000 replications). 95% confidence intervals are displayed.

Figure C.3: Effect of conflict onset on contemporaneous PIKE, "correcting" for change in probability of detecting poached carcasses at conflict onset.

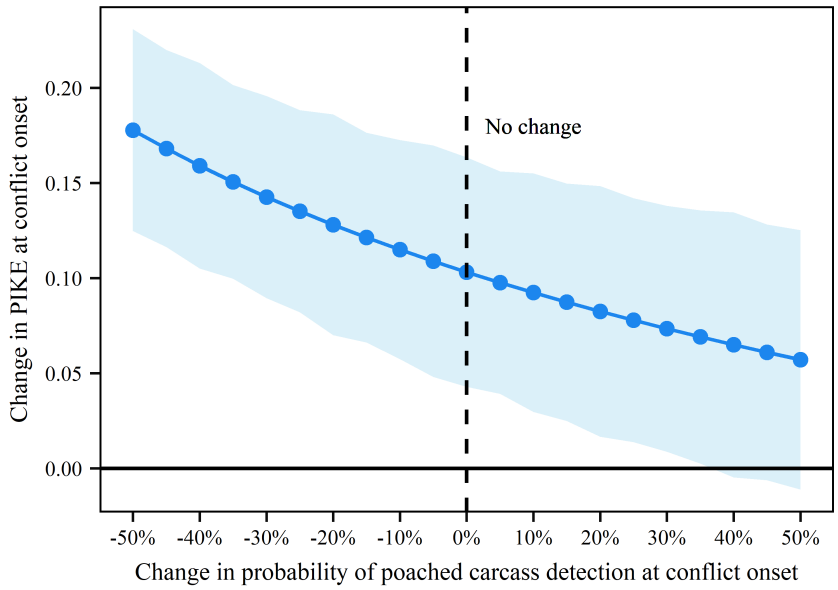

Notes: Each point represents the result of a separate regression. The regressions reproduce the Equation 1 specification, but "correct" for a different change in the probability of poached carcass detection at conflict onset. For example, if I assume that poached carcasses were 20% more likely to be detected at conflict onset, I deflate the observed count of poached carcasses by 20% for all site-years in which conflict onset occurred (divide the count by 1.2). I do not change carcass counts for site-years in which conflict onset does not occur. After "correcting" carcass counts in this manner, I recalculate PIKE and estimate Equation 1. All regressions have 631 observations. Standard errors are estimated by cluster bootstrapping with replacement at the country-level (1,000 replications). 95% confidence intervals are displayed.

Figure C.4: Distribution of residuals from estimating Equation 1.

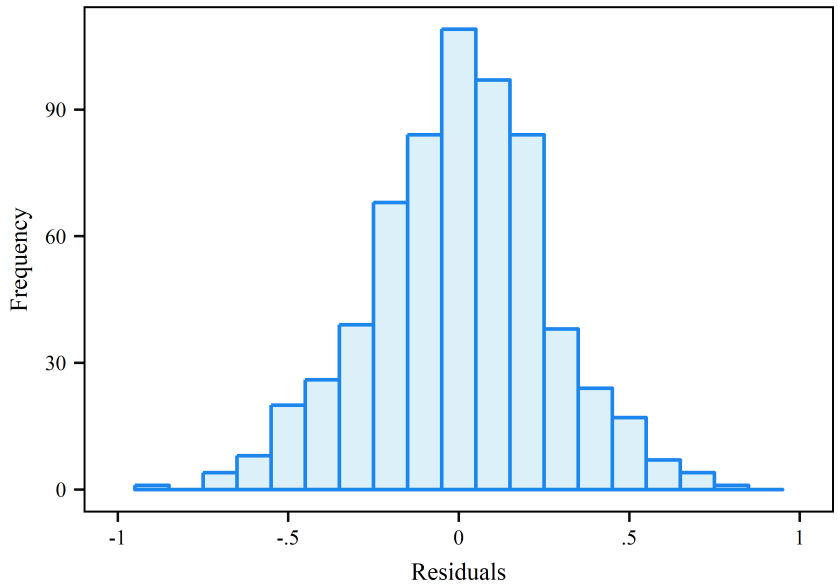

Notes: This figure plots residuals from estimating Equation 1 by ordinary least squares regression. A Shapiro-Wilk test fails to reject the null hypothesis that the residuals are normally distributed (p-value equals .104; N = 631).

Figure C.5: Temporal dynamics of poaching with respect to conflict onset, using illegal carcass count as dependent variable and controlling for natural mortality carcass count.

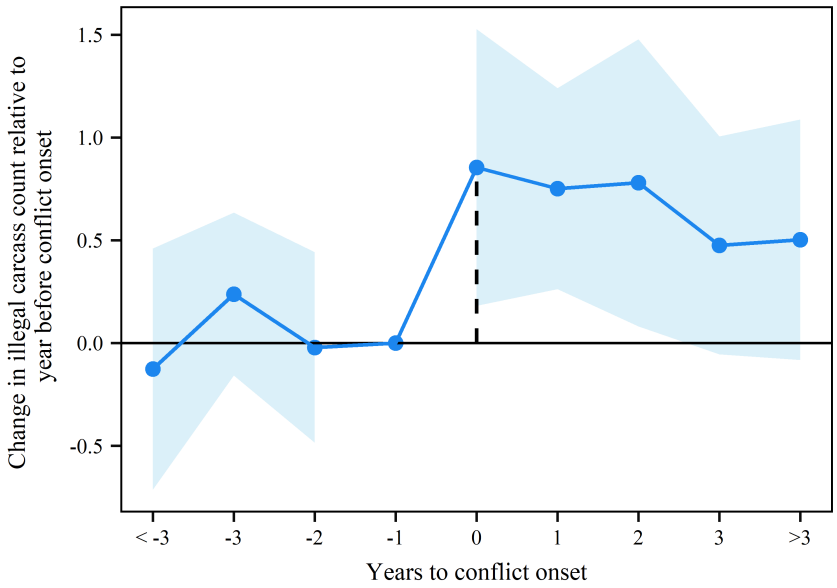

Notes: This figure reproduces the event study displayed in Figure 3.2 in the main text, but estimates a negative binomial regression with illegal carcass count as the dependent variable instead of PIKE, and adds ln(natural mortality count + 1) as a control variable. Coefficients are interpretable in log points. Standard errors are not used in the extrapolation, but are nevertheless displayed in the figure as 95% confidence intervals. In the figure, standard errors are clustered at the country-level and calculated analytically because a number of negative binomial model runs did not converge when attempting the clustered bootstrap.

C.2 Supplementary Tables

Table C.1: Poaching summary statistics, 2002-2014

	N	Mean	Std. Dev.	Min	Median	Max
PIKE	631	0.47	0.39	0	0.475	1
Poached Carcasses	631	11.04	24.94	0	2	225
Non-Poached Carcasses	631	13.01	31.87	0	2	323

Notes: This table summarizes all elephant mortality data reported to the MIKE program for the years 2002-2014, excluding three MIKE sites that only reported data for one year (see Poaching data subsection under Methods).

Table C.2: Characteristics of conflict onset events, by proximity to MIKE sites.

	<100 km	>100 km	p-value
Panel A. Intensity in year of onset			
Battles (median)	8	5	0.016
Battle Deaths (median)	61	55	0.08
Panel B. Type of conflict (%)			
Non-state–Civilians	32.1	17	0.001
Non-state–Non-State	43.1	64.4	0
Non-state–State	16.1	11.9	0.241
State–Civilians	8.8	5.4	0.213
State–State	0	1.3	0.025
Total number of conflict onsets	137	371	

Notes: The unit of observation for this table is a conflict-year. p-values are from a two-sided t-test. Conflicts that satisfy the 25 battle death threshold of conflict onset in multiple years are counted as separate onset events. The 137 conflict onsets within 100 km of MIKE sites contain 112 unique conflicts. Conflict onsets near MIKE sites in years without poaching data are included in this table. Of the 631 MIKE site-years with poaching data, 86 have a conflict onset event (14%).

Table C.3: Relationship between conflict onset and poaching, using different measures of poaching and different estimation procedures.

	(1)	(2)
Conflict Onset	0.221*	0.294*
	(0.115)	(0.153)
Natural Mortality	0.165**	0.254***
	(0.077)	(0.083)

Notes: All regressions control for ln(natural mortality carcasses + 1) in addition to the control variables in Equation 1. The conflict onset coefficient is interpretable in log points. Column 1 is estimated by ordinary least squares and the dependent variable is ln(poached carcasses + 1). Column 2 is estimated by negative binomial regression with a log link function, and the dependent variable is poached carcass count. A negative binomial model was used instead of a Poisson model because of overdispersion in the count of poached carcasses (see Table C.1). All regressions have 631 observations. Standard errors in Column 1 are estimated by cluster bootstrapping with replacement at the country-level (1,000 replications). Standard errors in Column 2 are clustered at the country-level (39 countries) and are calculated analytically because a number of negative binomial model runs did not converge when attempting the clustered bootstrap. ***P $<$ 0.01; **P $<$ 0.05; *P $<$ 0.1

Table C.4: Relationship between PIKE and alternate measures of conflict.

	(1)	(2)	(3)
1{Δ Conflicts}	0.056		
	(0.044)		
1{Δ Battles}		0.081**	
		(0.034)	
1{Δ Battle Deaths}			0.084**
			(0.043)
Obs. w/ intensity change	176	206	214

Notes: Each column re-estimates Equation 1, but replaces the conflict onset indicator with an indicator for change in conflict intensity. Though there are many ways to measure conflict intensity, I use an indicator for change in intensity to maximize statistical power and to facilitate comparison with Table 1 in the main text. Each regression in this table uses a different measure of change in conflict intensity: (1) number of unique conflicts, (2) number of battles, and (3) number of battle deaths. Number of unique conflicts is calculated by considering all battles which occur within 100 km of each MIKE site-year, and counting the number of unique conflicts these battles represent (defined by having unique actor pairs). Conflicts do not need to be "active" (more than 25 battle deaths) to be included. The indicator for change in number of unique conflicts equals 1 if the number of unique conflicts occurring near a given site is different this year compared to last year, and equals 0 otherwise. The indicators for change in the number of battles and battle deaths are defined similarly. All regressions have 631 observations. The final row in this table lists the number of observations for which the change in intensity indicator equals 1. Standard errors are estimated by cluster bootstrapping with replacement at the country-level (1,000 replications). ***P < 0.01; **P < 0.05; *P < 0.1

Table C.5: Effect of conflict onset on contemporaneous poaching, 2002-2017.

	Site and year fixed effects	With site trends	With country-by-year fixed effects
Conflict onset	0.099**	0.045	0.100**
	(0.039)	(0.030)	(0.046)
R-squared	0.553	0.677	0.841

Notes: This table replicates Table 1 using poaching data between 2002 and 2017. The regressions in this table do not control for temperature or precipitation because the weather dataset used in this paper is only available until 2014. Coefficients represent the effect of conflict onset on contemporaneous poaching, where poaching is measured by PIKE. All regressions are estimated by ordinary least squares with 779 observations, and include MIKE site fixed effects and year fixed effects. Column 2 adds MIKE site-specific trends to the base specification. Column 3 adds country-by-year fixed effects to the base specification (which subsume the year fixed effects). The MIKE data used in estimating the effects displayed in this table was downloaded on October 28, 2018 from https://fusiontables.google.com/DataSource?docid=1juiqNCOUwqperYcoq_uCWaZ5lEs8t09hfRry_I37&usp=drive_open#rows:id=4. The UCDP conflict data used in estimating the effects displayed in this table was downloaded on October 28, 2018 from http://ucdp.uu.se/downloads/ged/ged181-RData.zip. Clustered standard errors at the country-level are displayed in parentheses and are estimated by bootstrapping with replacement at the country-level (1,000 replications). ***P $<$ 0.01; **P $<$ 0.05; *P $<$ 0.1.

Table C.6: Non-relationship between natural mortality and conflict onset.

	(1)	(2)
Conflict onset	-0.085	-0.120
	(0.098)	(0.157)

Notes: All regressions include the same regressors that are used in Equation 1. The conflict onset coefficient is interpretable in log points. Column 1 is estimated by ordinary least squares and the dependent variable is ln(natural mortality count + 1). Column 2 is estimated by negative binomial regression with a log link function, and the dependent variable is natural mortality count. A negative binomial model was used instead of a Poisson model because of overdispersion in the count of natural mortality carcasses (see Table C.1). All regressions have 631 observations. Standard errors in Column 1 are estimated by cluster bootstrapping with replacement at the country-level (1,000 replications). Standard errors in Column 2 are clustered at the country-level (39 countries) and are calculated analytically because a number of negative binomial model runs did not converge when attempting the clustered bootstrap. ***P $<$ 0.01; **P $<$ 0.05; *P $<$ 0.1